Exploring DNA polymerases towards their size limits in processing modified nucleotides

Dissertation zur Erlangung des

akademischen Grades eines Doktors der

Naturwissenschaften (Dr.rer.nat.)

vorgelegt von

Moritz Welter

an der

Universität Konstanz

Mathematisch-Naturwissenschaftliche Sektion

Fachbereich Chemie

Konstanz, 2019

Konstanzer Online-Publikations-System (KOPS)
URL: http://nbn-resolving.de/urn:nbn:de:bsz:352-2-1vsssa7un2d9i2

Tag der mündlichen Prüfung: 28. Juni 2019

1. Referent: Prof. Dr. Andreas Marx

2. Referent: Prof. Dr. Jörg Hartig

This work was prepared from November 2013 till June 2018 in the group of Prof. Andreas Marx (Chair of Organic and Cellular Chemistry) at the University of Konstanz. The work was supported by the Konstanz Research School Chemical Biology.

Parts of this work were published in:

I D. Verga, **M. Welter**, A. L. Steck, et al., DNA Polymerase-Catalyzed Incorporation of Nucleotides Modified with a G-Quadruplex-Derived DNAzyme, *Chemical Communications* **2015**, *51*, 7379-7381.

II D. Verga, **M. Welter**, A. Marx, Sequence Selective Naked-Eye Detection of DNA Harnessing Extension of Oligonucleotide-Modified Nucleotides, *Bioorganic & Medicinal Chemistry Letters* **2016**, *26*, 841-844.

III **M. Welter**, D. Verga, A. Marx, Sequence-Specific Incorporation of Enzyme-Nucleotide Chimera by DNA Polymerases, *Angewandte Chemie International Edition* **2016**, *55*, 10131-10135.

IV J. Balintova, **M. Welter**, A. Marx, Antibody-Nucleotide Conjugate as a Substrate for DNA Polymerases, *Chemical Science* **2018**, *9*, 7122-7125.

V **M. Welter**, A. Marx, Preparation and Application of Enzyme-Nucleotide Conjugates, *Current Protocols in Chemical Biology* **2018**, *10*, 49-71.

VI A. Marx, **M. Welter**, J. Balintová, WO/2017/097973, **2017**.

Danksagung

Zunächst möchte ich mich bei Prof. Dr. Andreas Marx für die Möglichkeit bedanken, dieses interessante und anfangs etwas experimentelle Thema in seiner Arbeitsgruppe bearbeiten zu dürfen. Ich danke dir für das entspannte, kollegiale Betreuungsverhältnis, bei dem ich über die Jahre jederzeit mit meinen Problemen zu dir kommen konnte und immer wieder den Schubs in die richtige Richtung bekommen habe, der zur Überwindung mancher Probleme nötig war.

Prof. Dr. Hartig und Prof. Dr. Scheffner möchte ich für die Übernahme des Zweitgutachten und des Prüfungsvorsitzes danken. Zudem möchte ich mich für ihren Input im Rahmen meines Thesiskomitees bedanken, aus dem einige wertvolle Ideen entstanden sind.

Generell gilt mein Dank selbstverständlich allen ehemaligen und aktuellen Mitgliedern der AG Marx für die großartige Arbeitsatmosphäre, die Hilfsbereitschaft aller und die unvergesslichen Abenteuer bei Feiern und Ausflügen. Im Folgenden möchte ich noch einige Leute hervorheben:

„Die alte Garde“ mit Stephan Hacker, Daniel Schneider, Holger Bußkamp und Janina von Watzdorf, die mir gerade in der Anfangszeit im Labor immer mit Rat und Tat beiseite standen.

Daniela Verga und Jana Balintova möchte ich für die gute Zusammenarbeit auf diesem Thema danken.

Alle festangestellten Mitarbeiter der AG, welche die Gruppe durch ihre Arbeit zusammenhalten und uns Doktoranden im Laboralltag viel Arbeit abnehmen.

Meine Boxnachbarn aus der „Box 2“: Kim Leitner, Martin Mex und Daniel Hammler. Ihr habt über die Jahre nicht nur wissenschaftlich oft geholfen, sondern auch häufig die Stimmung gerettet, wenn mal wieder nichts geklappt hat.

Joos Aschenbrenner, Kathrin Götz und allen Mitgliedern der 11Uhr-Mensa-Truppe möchte ich für viele lustige Diskussionen danken, beim Mittagessen sowie im Labor.

Alexander Finke und Simon Kienle möchte ich zudem für das Korrekturlesen meiner Arbeit danken.

Und natürlich alle Freunde und Kollegen, die sich hier nicht namentlich wiederfinden.

Ein besonderer Dank gilt meinen Eltern, deren Zuspruch und Förderung jeglicher Art mir ein sorgenfreies Studium ermöglicht haben.

Zum Abschluss möchte ich noch Sabine danken, die mich die gesamte Zeit meiner Promotion begleitet und unterstützt hat.

Table of Contents

List of Figures

List of Tables

List of Abbreviations

µl	microliter
µM	micromolar
2'OMe	methylated 2'-OH group of a NTP
5mC	cytosine methylated at the *C*5 position
A	adenine
Å	Ångström (10^{-10} m)
APS	ammonium persulfate
bp	base pairs
BRAF	v-Raf murine sarcoma viral oncogene homolog B
BSA	bovine serum albumin
C	Cytosine
cDNA	complementary DNA
cfDNA	cell free tumor DNA
Cq	termed quantitation cycle
d	doublet
DBCO	dibenzocyclooctyne
dd	doublet of doublet
DIPEA	*N*,*N*-diisopropylethylamine
DMF	dimethylformamide
DNA	deoxyribonucleic acid
dNTP	any deoxynucleoside triphosphate
dPAGE	denaturing polyacrylamide gel electrophoresis
dsDNA	double stranded DNA
$dT^{n\mathit{HRP}}TP$	HRP-conjugated dTTP with n indicating the linker length
E. coli	*Escherichia coli*
ELISA	enzyme-linked immunosorbent assay
eq	equivalents
ESI-MS	electrospray ionization mass spectrometry
et al.	et alia
G	Guanine
HeLa	Henrietta Lacks cervical cancers cells
HRP	horseradish peroxdiase
Hz	Hertz
IEX-FPLC	anion exchange fast protein liquid chromatography
IEX-HPLC	anion exchange high pressure liquid chromatography
KF	*Klenow Fragment*
KF exo$^-$	DNA polymerase I Klenow Fragment 3'->5' exonuclease deficient
LAMP	loop-mediated isothermal amplification
LC-MS	liquid chromatography coupled mass spectrometry
LNA	locked nucleic acid
LOD	(lower) limit of detection
m	multiplet
M	molar

m/z	mass-to-charge ratio
m^6A	adenine methylated at the *N*6 position
malHRP	maleimide activated HRP
mg	milligram
min	minute
miRNA	micro RNA
ml	milliliter
MQ	Milli-Q ultrapure water
mRNA	messenger RNA
NHS	N-hydroxysuccinimide
nt	nucleotide(s)
NTP	any nucleoside triphosphate
OH	hydroxyl group
ovn	overnight
p	quintet
PBS	phosphate buffered saline
PCR	polymerase chain reaction
PDB	protein data bank
PEG	polyethylene glycol
PEx	primer extension
POC	point of care
PP	Pyrophosphate
ppm	parts per million
q	quartet
RNA	Ribonucleic acid
RP-HPLC	reversed phase high pressure liquid chromatography
rpm	revolutions per minute
RT	reverse transcription
rt	room temperature
s	singlet
s	second
SDS-PAGE	sodium dodecyl sulfate–polyacrylamide gel electrophoresis
SNP	singe nucleotide polymorphism
ssDNA	single stranded DNA
T	thymine
t	triplet
TdT	Terminal deoxynucleotidyl transferase
TEMED	Tetramethylethylenediamine
TFA	trifluoroacetamido-
tRNA	transfer RNA

1– Introduction

1.1 – The Nucleic Acids: DNA and RNA

1.1.1 – The discovery of DNA, its purpose and its structure

Shortly after Georg Mendel published his famous rules of inheritance in 1866[1], the swiss physician Friedrich Miescher first described a new chemical substance found in the nuclei of leucocytes isolated from surgical bandages in 1869. An elemental analysis of the substance he, based on its origin within the cell, named "nuclein", showed that in contrast to the already known proteins, it contained a substantial amount of phosphorous.[2] Over the following decades, nuclein was thoroughly studied leading to the identification of its chemical building blocks[3-6], its organization in chromatin/chromosomes and its acid-like behavior, which awarded it the name "nucleic acid".[7-8] Almost 60 years after Mieschers publication, experiments on *Streptococcus pneumonia* by Frederick Griffith suggested that the inheritance principles described by Mendel are based on a "transforming factor" present in the cells.[9] In 1944, Oswald Avery and co-workers identified nuclein, by then called deoxyribonucleic acid (DNA), as the transforming factor Griffith had described.[10] However, as many researchers thought only proteins would be specific enough to account for the plethora of information that has to be inherited, it took another several years, until the experiments of Erwin Chargaff in 1949 and Alfred Hershey and Martha Chase in 1952 helped to establish the sole role of DNA as the carrier of genetic information in higher organisms.[11-12] Yet, a major puzzle piece required for a more profound understanding of how DNA carries this information was still missing: the structure. This changed in 1953 when James Watson and Francis Crick published an article in *Nature*, based on X-ray data by Rosalind Franklin, Raymond Gosling and Maurice Wilkins, proposing the model of a right-handed double helix.[13-17]

1.1.2 – Properties of DNA

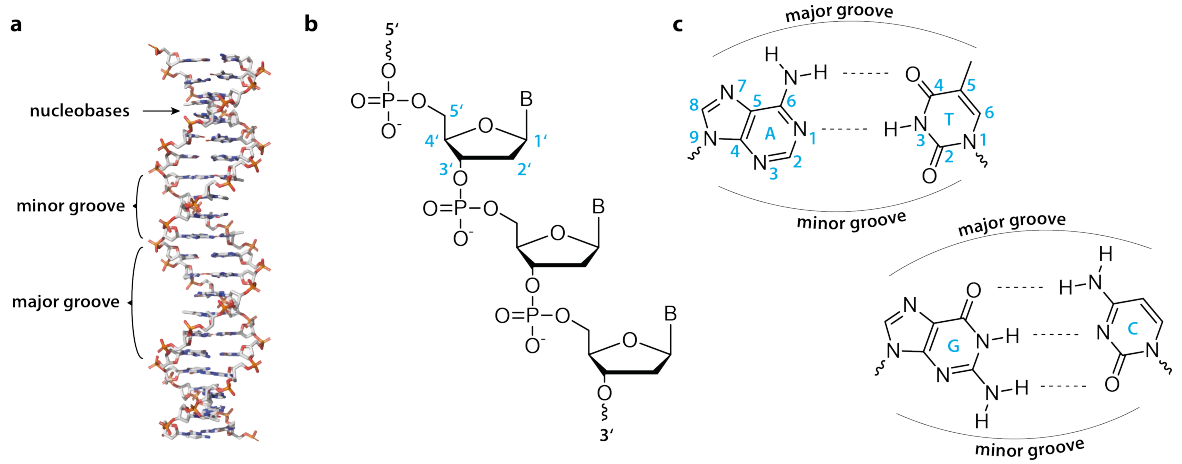

Figure 1: The structure of DNA. a) Structure of the B-form of DNA that is found under physiological conditions. The deoxyribose-phosphate backbone on the outside of the anti-parallel double helix (silver/orange/red) encompasses a major and a minor groove. The nucleobases are faced towards the helix axis on the inside. b) Primary structure of the DNA. The nucleoside monophosphates are connected via phosphodiester bonds between their 3'- and the 5'-hydroxyl group of the next nucleotide. Thus, a DNA strand has an orientation accordingly denoted by 5' and 3' end. The nomenclature used for the individual positions of the deoxyribose moiety is given in blue. B= Base c) Base pairing inside the double helix. Each purine base (**A**denine, **G**uanine) exclusively pairs with its corresponding pyrimidine base (**T**hymine, **C**ytosine) via hydrogen bonding. The nomenclature used for individual atoms/positions of the purine (A, G) and pyrimidine bases (T, C) is given in blue on the A:T base pair exemplarily.

Today we know that the B-form Watson and Crick described in 1953 is the most abundant DNA form under physiological conditions (*Figure 1a*). It comprises two anti-parallel strands of deoxyribonucleotides in which one of the four nucleobases (**A**denine, **G**uanine, **T**hymine, **C**ytosine) is connected to the anomeric carbon of a 2' deoxyribose sugar moiety via a *N*-glycosydic bond (*Figure 1b, c*). Among each other, the nucleotides are connected by a 3', 5' phosphodiester bond resulting in the distinction of the 5' and the 3' end of a DNA strand. The nucleobases face towards the inside of the helix where two nucleotides respectively form a base pair (bp) through hydrogen bonding at their "Watson-Crick-Face" (*Figure 1c*).[18] In accordance with Chargaff's prediction, adenine pairs with thymine and guanine pairs with cytosine.[19]

In the B-helix, one turn stretches 33.2 Å and is comprised of 10.4 bp. On the outside, the deoxyribose-phosphate backbone entails the formation of a narrow, deep minor and a shallow, broad major groove (Figure *1a*).[20] Thus, access for DNA binding proteins is more facile in the major groove allowing them to bind to a DNA sequence specifically.

Several more DNA helix types and structures that have been identified so far depend on specific sequence contexts or exist only under harsh conditions. For example, the left-handed Z-DNA was observed during supercoiling, a state that is associated with transcriptional control in which the DNA double helix is over- or under wound.[21-22] The A-form DNA is in contrast mostly found under dehydrating

conditions.[23] Other types are mostly of theoretical nature as they solely exist under biologically not relevant *in vitro*-conditions.[24] However, the role of different helix types in the cell is still subject of ongoing studies.

1.1.3 – Properties of RNA

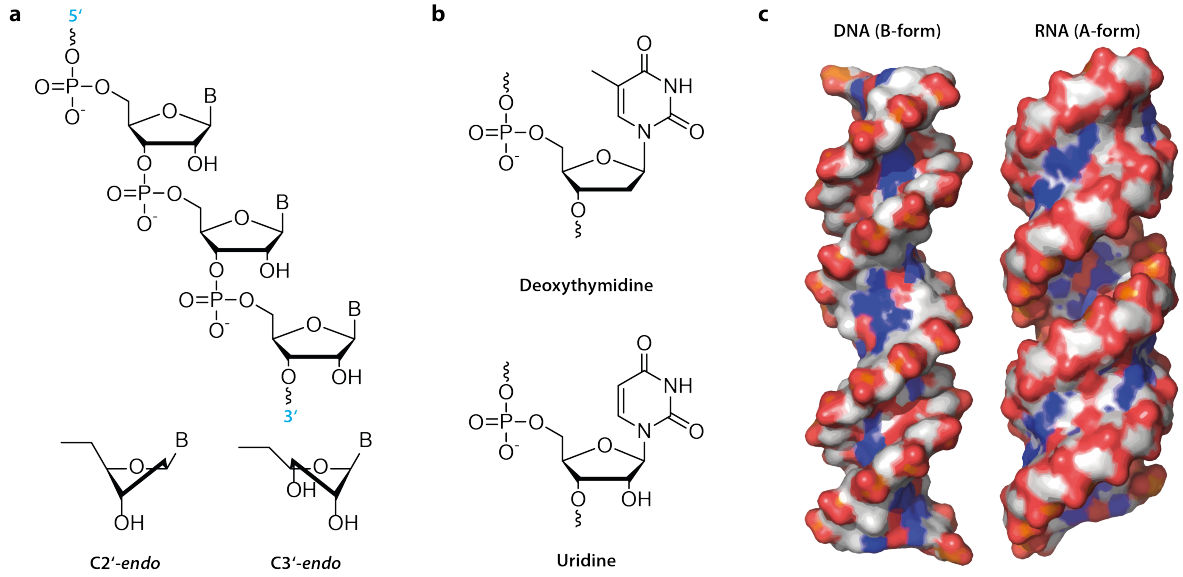

Figure 2: Structural differences between DNA and RNA. a) Primary structure of RNA. The 2'-OH group of the ribose leads to the preferred adaption of a C3'-endo pucker and thus an A-form helix. In DNA, the deoxyribose preferably adapts a C2'-endo pucker, facilitating the B-form helix. b) Comparison of the DNA nucleotide thymidine and its RNA equivalent uridine. c) Surface view of the two most common helix forms under physiological conditions for DNA (B-form) and RNA (A-form).

Twenty years before P. Levene determined 2'-deoxyribose as the sugar constituting DNA ("thymus nucleic acid") in 1929, he already found ribose to be the sugar moiety in another nucleic acid which was, at that time, referred to as 'yeast nucleic acid' (Figure *2a*).[4, 25] At that time many researchers considered yeast nucleic acid to be the plant equivalent to DNA. In 1933, however, J. Brachet found it to be localized mostly in in the cytoplasm of eukaryotic cells while DNA is exclusively found in the nucleus.[26-27] Based on several publications since then, Crick proposed his famous dogma of molecular biology in which DNA is the universal carrier of the genetic information in higher organisms. The sequence information is transcribed into RNA transferring it to the cytoplasm, where ultimately each base triplet is translated into a distinct amino acid.[28] Apart from the sugar moiety, the only other chemical difference of RNA compared to DNA is the replacement of thymine with uracil (Figure *2b*). However, these two seemingly minor differences result in substantial chemical and biological differences that explain why DNA is the carrier of the genetic information.

First, RNA degrades fast under alkaline conditions due to the possibility of an intramolecular attack of a deprotonated 2' hydroxyl group on the 3' phosphodiester. The presence of the 2' hydroxyl group secondly favors the adaption of 3'-endo conformation on the ribose compared to the 2'-endo conformation observed for deoxyribose (Figure *2a*). In contrast to DNA, double-stranded RNA therefore adopts an A-form with a less accessible major groove and significantly higher stiffness impeding the accessibility by binders and the organization into chromatin and ultimately chromosomes (Figure *2c*).[29] Thirdly, spontaneous deamination of cytosine directly yields uracil and therefore poses a high risk for mutagenesis in RNA.[30]

Hence, DNA became the genetic "storage molecule" in higher organisms, while RNAs evolved higher versatility. Apart from being the information carrier (messenger RNA or mRNA), transfer RNAs (tRNA) and ribosomal RNAs (rRNA) serve as specific mediators and catalysts in protein biogenesis, small RNA can determine other RNAs fate (miRNA) and several other RNAs are involved in diverse cellular processes like signaling.[31]

1.2 – DNA Polymerases

1.2.1 – Structure of DNA polymerases

The ability to duplicate genetic information is a premise for the growth of an organism and the continuity of life in general. For this task, specific enzymes have evolved: the DNA polymerases. The first of these enzyme to be discovered was DNA polymerase I from *E. coli* which was isolated by A. Kornberg and colleagues in 1956.[32-33] Today, 7 DNA polymerase families (A, B, C, D, X, Y, RT) are distinguished based on sequence similarity and structure. They share a general structure resembling a right hand in which three subdomains are distinguished: the palm domain, the finger domain and the thumb domain. The palm domain contains the residues responsible for catalysis, while the thumb and finger domains help to bind and position the processed DNA and nucleotides (Figure *3a*).[34-35]

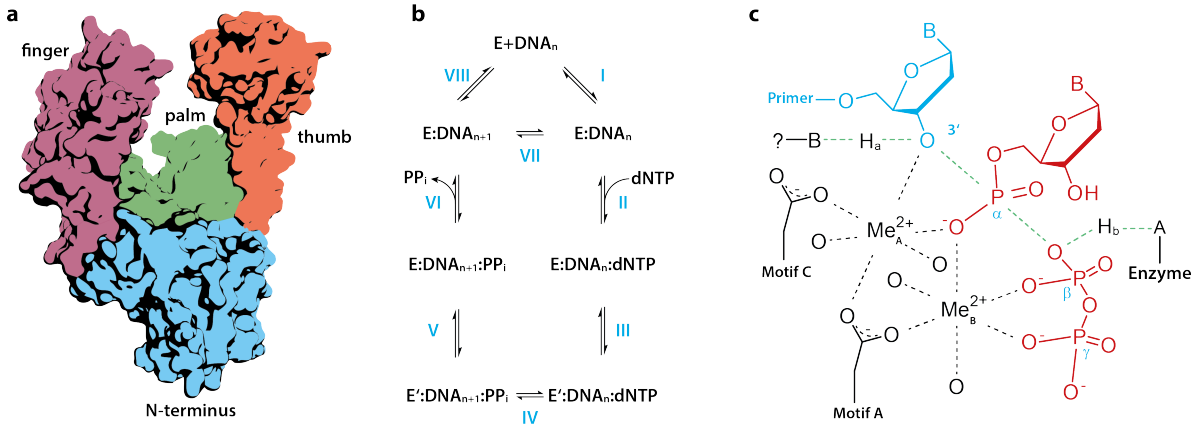

Figure 3: Structure and mechanism of DNA polymerases.Right-hand structure of *KlenTaq* DNA polymerase (PDB: 1KTQ[36]) with the finger domain, thumb domain and the palm domain that contains the catalytic center. b) Steps of the nucleoside triphosphate incorporation. I: Enzyme (E) and the primer-template complex (DNA) form the binary complex. II: Binding of a nucleoside triphosphate leads to the formation of a ternary complex. III: A conformational change in the enzyme tightens the ternary complex and aligns the participants for catalysis. IV: The nucleotide is incorporated. V: Another conformational change loosens the ternary complex. VI: Pyrophosphate is released. VII: Processivity of DNA polymerases. A new catalytic cycle begins without the DNA polymerase leaving the DNA strand. VIII: The DNA polymerase dissociates from the DNA strand.[37] c) Two metal ion catalysis mechanism in the active site. The attack of the 3' hydroxyl group of the primer on the α-phosphate is facilitated by metal ions A and B and a base. Metal ion B in combination with several amino acid side chains of the enzyme coordinate the leaving pyrophosphate.[38]

Shortly after the DNA structure was solved, a debate about the mechanism of DNA replication arose. The orientation of the bases towards the "safe" inside of the helix led many researchers to believe that a new DNA helix is manufactured next the original double-stranded helix. This mechanism was referred to as "conservative replication". However, this mechanism would require the enzyme conducting replication to independently transfer the sequence information from an intact DNA strand to a newly synthesized one. In 1958, Meselson and Stahl showed that isotopes fed to *E. coli* were distributed evenly in the DNA of the successive generations, thus proving that the mechanism of DNA replication is in fact

semi-conservative. Hence, this meant that the double strand is split during replication into single-stranded entities which provide the sequence information or 'template' for the synthesis of a new, complementary strand.[39]

DNA polymerases responsible for the replication of DNA are mostly members of the families A and B. As in general, with the exception of an X-family member called the terminal deoxynucleotidyl transferase (TdT)[40-41], DNA polymerases are unable to start the synthesis *de novo*, they require a short RNA or DNA fragment to first bind to the parental DNA strand so that its 3'-OH group can serve as the starting point for the synthesis. These short DNA fragments are referred to as 'primers'. The primer-template pair (DNA_n) is then bound by the DNA polymerase (E) in a binary complex (E:DNA) with the 3'-hydroxyl terminus of the primer resting in the active site of the enzyme (Figure *3b*, I).[37] Subsequently, the finger domain facilitates the binding of a dNTP, resulting in a ternary complex (II, E:DNA_n:dNTP, "open conformation"). A conformational change within the polymerase tightens the ternary complex and thus arranges all reagents in the correct positions necessary for catalysis (III, "closed conformation").

The attack of the 3' hydroxyl group of the primer on the α-phosphate of the dNTP is facilitated by two divalent metal ions (Figure *3*c, Me_A, Me_B) that are coordinated by two well-conserved aspartic acid residues in the DNA polymerase. They serve as a lewis acid to lower the energy barrier presented by the negative charge on the α-phosphate and thus enable the attack of the hydroxyl group. One of the metal ions additionally stabilizes the pyrophosphate leaving group.[38] A third metal ion was observed in the active site of DNA polymerases in several crystal structures. Its importance and role in catalysis is however heavily debated.[42]

Following the addition of the nucleotide monophosphate (IV), the enzyme-DNA complex returns to a relaxed state (V) and the pyrophosphate is released (VI). Ultimately, the DNA polymerase slides along the primer-template pair to shift the new 3' end into the active site of the polymerase (VII). Thus, multiple nucleotides can be incorporated without the enzyme leaving the primer-template complex (VIII). With this unique skill called 'processivity', DNA polymerases were shown to incorporate up to several hundred nucleotides per second *in vivo*.

1.2.2 – DNA polymerases as drivers of evolution

As mentioned before, the main task of DNA polymerases is to maintain the genetic information across generations. However, to allow a gradual evolution and thus organisms to adapt to changing environmental conditions, the genetic information at the same time also has to be allowed to slowly change

across generations. In living cells, apart from large-scale transformations such as translocations, insertions and deletions, this is in part accomplished by mutagenesis induced via DNA damages such as depurination and deamination of cytosine which can cause the DNA polymerase to misread the template sequence in replication.[30] Additionally, a small, intrinsic error-rate is observed in replicative DNA polymerases.[43-44] This mutability has to be carefully balanced as excessive flexibility of the genome also increases the occurrence of pathogenic mutations. Therefore, DNA damage within cells is restored by a set of repair mechanisms in which representatives of the DNA polymerase families X and Y are involved in order to confine the amount of errors replicative DNA polymerases have to face. Misincorporations made during replication can furthermore be corrected by the 3'-5' exonuclease activity found in some DNA polymerases. In this process called 'proof-reading', mispaired nucleotides are removed by the DNA polymerase itself directly following their undesired incorporation and the correct nucleotide is inserted instead. Thus, reported error rates for common DNA polymerase show approximately one misincorporation every 10^5 to 10^7 incorporations.[34, 43]

1.2.3 – DNA polymerases in biotechnology

DNA polymerases have evolved over millions of years leading to a myriad of different enzymes with varying properties. With the ability to isolate these enzymes from cells and organisms, these properties can be harnessed for biotechnological applications. The introduction of the polymerase chain reaction (PCR) in the 1980s by K. Mullis, for example, enabled researchers to utilize the native replication machinery *in vitro*, allowing the amplification of DNA fragments at will.[45-46] In PCR, the DNA sequence of interest is targeted by two specific primers that anneal to the respective DNA strands of the original sequence and are elongated by the DNA polymerase under consumption of added dNTPs. The technique demands a temperature gradient program in order to separate the newly synthesized double stranded DNA at high temperatures and allow the annealing and prolongation of a new primer at lower temperatures in each cycle. PCRs therefore are conducted in special machines called thermocyclers that automatically run the required temperature cycles. Since most DNA polymerases which were accessible at the time PCR was introduced are denatured at the high temperatures used for strand separation, the polymerase had to be re-added for each replication step. The discovery of thermostable enzymes such as the *Taq* DNA polymerase in the thermophilic bacterium *Thermus aquaticus*[47] and the KOD DNA polymerase in the archaea *Thermococcus kodakaraensis*[48] greatly simplified the procedure as they survive the denaturation step and hence no interaction with the reaction solution during the amplification is necessary anymore.[49]

Beside these enzymes, other natural DNA polymerases demonstrate increased fidelity, faster processing, a greater tolerance for buffer compositions and/or the ability to displace double-stranded DNA encountered during replication (strand displacement), which allows amplification at a constant temperature (referred to as 'isothermal').[34, 50-52] As this cuts out the need for thermocyclers, isothermal DNA amplification is of huge interest to reduce the requirements of nucleic acid amplification assays. A very popular method employing strand displacement DNA polymerases is the loop-mediated isothermal amplification (LAMP), which uses a set of four primers that generate self-primed hairpin loops.[53] LAMP provides a rapid amplification of target sequences and, in some cases, has been shown to be more sensitive than PCR.[54-55]

Taken together, DNA polymerases for almost every conceivable application can be isolated from natural sources. With the employment of synthetic evolution strategies as error-prone PCR and site directed mutagenesis, however, researchers are nowadays able to improve and adapt the natural enzyme scaffolds for particular applications yielding new, unique enzymes.[56-57] N. Blatter and co-workers e.g. generated a derivative of the N-truncated Klenow fragment of the *Taq* DNA polymerase, '*Klentaq',* in which four amino acid exchanges (L459M, S515R, I638F and M747K) enabled the polymerase to synthesize DNA strands on the basis of RNA templates.[58] This ability was hitherto only found in specialized reverse transcriptases.

Apart from the use of 'tailor-made' enzymes, the scope of DNA polymerase catalyzed reactions in biotechnological applications can additionally be expanded by the application of modified nucleotides that interfere with the replication process at distinct sites of interest or functionalize the synthesized DNA.

1.3 – Modified Nucleotides

1.3.1 – Natural DNA and RNA modifications

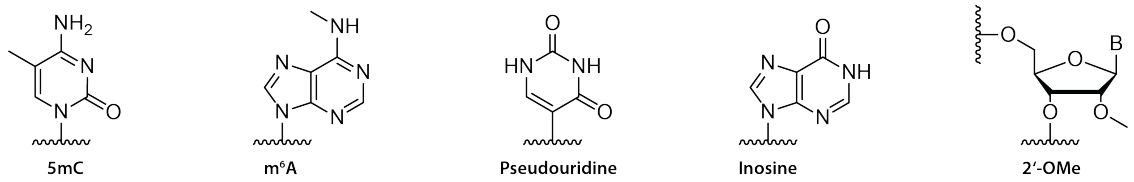

Figure 4: A selection of natural modifications found in DNA and/or RNA. 5mC is the most abundant epigenetic marker in the DNA of higher eukaryotes. m^{6}A is the predominant DNA modification in prokaryotic DNA as well as a major RNA modification in eukaryotic RNA. Pseudouridine and Inosine are crucial modifications for tRNA function.

Beside the "standard" set of nucleotides found in RNA and DNA, a myriad of different natural modifications on the nucleobases and (deoxy)ribose moieties of these nucleotides have been reported over the last decades (Figure *4*).[59] Next to hydroxyl-[60], formyl-[61] and carboxy-[62] groups, isomeric forms[63] and alternative purine derivatives[64], they especially include methylations on the nucleobase and ribose moiety.[65-68]

In DNA *i.e.* modifications on the nucleobase can alter the chromatin structure and hence the accessibility of genes for transcription, which is crucial for the controlled expression of distinct proteins required over time.[69] Since they thus account for a regulatory information on top of the sequence information comprised by the nucleotide succession, these modifications are accordingly referred to as 'epigenetics'.[70] Between the domains of life, the type and levels of epigenetic markers can drastically vary. In higher eukaryotes *e.g.* 5-methylcytosine (5mC) is the most abundant modification while in prokaryotes N^6-methyladenosine (m^{6}A) is the most abundant DNA modification.[65-66, 71]

In RNA, modifications can occur on the nucleobase as well as on the 2'-hydroxyl group of the ribose moiety (Figure *4*, 2'-OMe). Since RNA, in addition, does not have to store the genetic information, the sequence can be heavily processed after transcription. This even includes the incorporation of non-canonical bases such as the isomeric pseudouridine and the purine derivative inosine that are crucial for the function of tRNAs. The field of RNA modifications is thus much larger than DNA modifications accounting for the versatility observed among RNAs. In analogy to epigenetics, the research field of RNA modifications is termed 'epitranscriptomics'.[59]

As in DNA, their occurrence and levels varies between organisms. m^{6}A, which is the most abundant DNA modification in prokaryotes *e.g.*, is among the most abundant RNA modifications in higher eukaryotes.[72] It is among others found in mRNAs, tRNAs and rRNAs and thus is involved in key processes

such as RNA location[73], splicing[74] and translation[75]. Studies furthermore indicate that m^6A might be linked to RNA degradation.[76]

Another key RNA modification in higher eukaryotes is the methylation on the 2'-hydroxyl group of the ribose moiety which is especially observed in rRNAs (Figure *4*).[67] It is proposed that the methylation facilitates rRNA folding and hence is essential for correct ribosome function.[77-79]

For many DNA and RNA modifications, their role within the cell is not sufficiently understood. While pull-down assays and deletion experiments can help to identify binding partners and can indicate the effect of a modification, the location of a distinct epigenetic marker can be critical for its role. However, the low abundance of the corresponding nucleic acids combined with the loss of the epigenetic/epitranscriptomic information in amplification assays impedes the direct study of these modifications. Techniques that allow the site specific sensing of epigenetic markers in nucleic acids are therefore strongly demanded by the scientific community. So far, countless approaches have been published including bisulfite sequencing that allows site-specific detection of 5mC in laborious comparative experiments.[80] However, no approach that allows a fast, simple and cost effective sensing of epigenetic markers has prevailed so far.[81]

1.3.2 – Synthetic DNA and RNA modifications

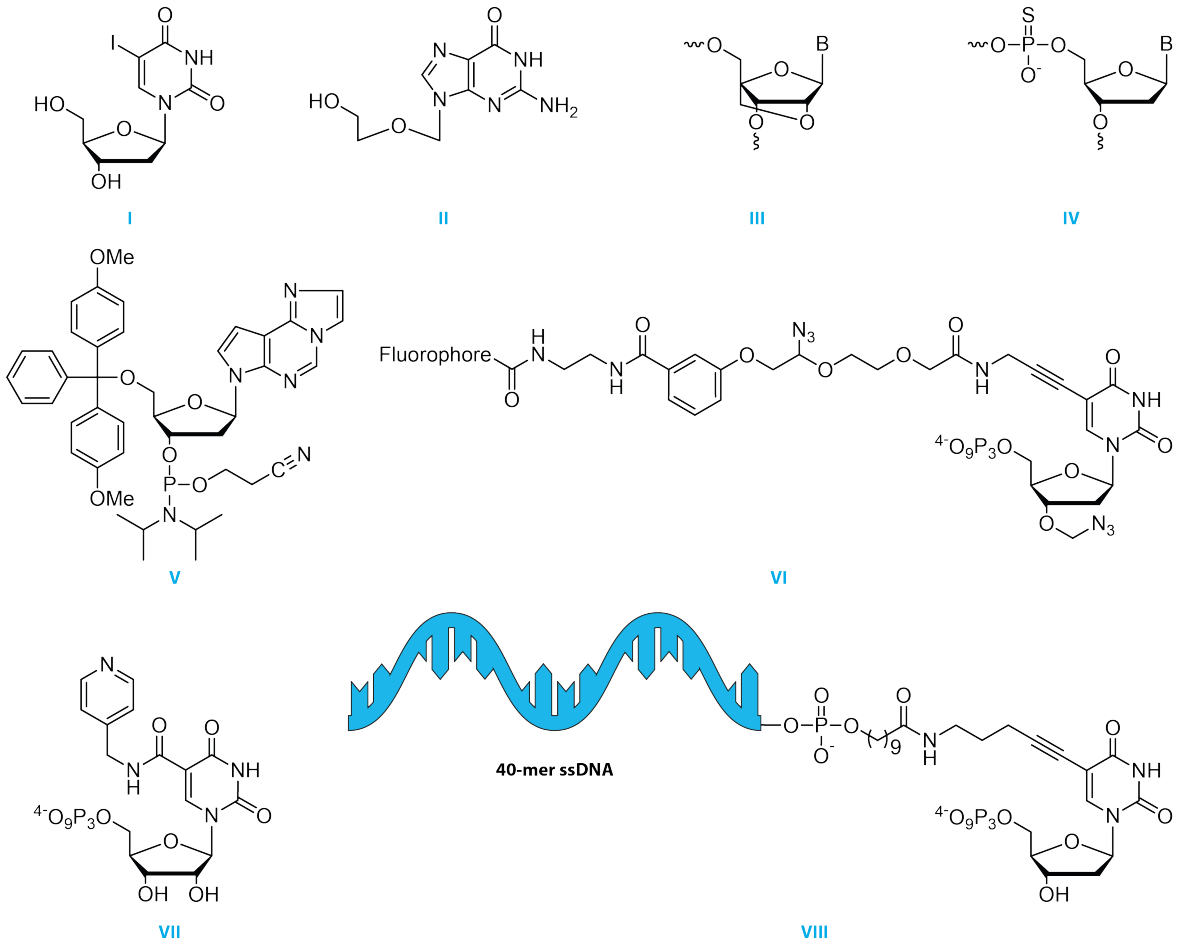

Figure 5: A selection of synthetic nucleotide derivatives. I: Idoxuridine[82], II: Aciclovir, III: Locked nucleic acids (LNA), IV: Phosphothioate linked dNMP, V: Fluorescent adenine derivative phosphoramidite building block for solid phase synthesis[83], VI: dTTP derivative used in Illumina sequencing[84], VII: Uridine derivative used in RNA aptamer catalyzed Diels-Alder reactions[85], VIII: dTTP derivative connected to a 40-mer ssDNA sequence[86]. Structures VI-VIII have been enzymatically introduced into oligonucleotides.

With the help of synthetic organic chemistry, nucleosides and nucleotides can be modified beyond the scope of their natural alterations. Starting in the 1960s, synthetic nucleoside analogues such as Idoxuridine (Figure 5, I) and Aciclovir (II) were used in the therapy of viral infections and cancer.[82, 87-88] These analogues are metabolized by the cell similarly to their natural counterparts, but later on interfere with substantial cellular processes like replication, thus inhibiting the progeny of a virus or cell. Today, synthetically modified nucleosides and nucleotides do not only play important roles in medicine, but also help to study and influence the behavior of crucial cell components and processes. Especially in the context of nucleic acids they now are valuable tools in daily laboratory practice.[84, 89]

For example, substitution of natural buildings blocks for ribose modified ones such as in locked nucleic acids (LNA, III) can increase the stability of the oligonucleotide against elevated temperatures and degrading enzymes as well as the hybridization properties which make them well-suited candidates for

antisense based therapeutics.[90-91] Modifications of the phosphate chain, like the substitution of one none-bridging oxygen with sulphur (IV) can help to generate nuclease resistant linkages in oligonucleotides.[92] Moreover, base-modified nucleotides constitute a wider field of tools including even the creation of non-natural, orthogonal base pairs.[93-94]

In general, modified oligonucleotides can be synthesized in three different ways. The first one is the solid phase synthesis. In the most commonly used version of solid phase synthesis, the posphoramidite method, protected nucleoside phosporamidite building blocks (Figure *5*, V) are added stepwise to the 5' end of each other.[95-96] Following each addition, the phosphorous(III)-species is oxidized and unreacted 5' hydroxyl groups are capped in order to prevent frameshifts. After its synthesis, the oligonucleotide is cleaved from the solid phase and deprotected. Solid phase synthesis has been employed for the preparation of oligonucleotides for several decades as it is robust, scalable and provides some flexibility in terms of modifications. However, the particular chemistry used during the individual steps of the synthesis sets certain restrains to the nature of possible modifications. The difficulty to synthesize longer oligonucleotides due to imperfect coupling yields and the laborious preparation and purification of the nucleic acids additionally limit the applicability of solid phase synthesis.[93]

Besides the solid-phase synthesis of modified oligonucleotides, nucleic acids in general can be semi-synthetically modified by chemical reagents and enzymes.[97-99] Since the nucleobases share very similar functional groups, the selective modification of a particular base is challenging and the scope of this approach is limited to few modification strategies with a high risk of incomplete modification and side-reactions.[97]

Opposed to the (semi-)synthetic generation of oligonucleotides is the enzymatic synthesis. Here, the modified nucleotides serve as substrates for DNA or RNA polymerases and are thus incorporated into a nascent DNA or RNA strand by the natural machinery (Figure *5*, VI-VIII).[93, 100-102] This enables the facile generation of long nucleic acids and by harnessing the template dependency and fidelity of replicative polymerases allows the sequence specific incorporation of modifications. However, nucleic acid polymerases have evolved over billions of years to incorporate the natural bases with high selectivity.[103-105] Nucleotide modifications hence have to meet certain criteria to serve as a substrate for these polymerases:

A large number of nucleotide structures has been reported for the enzymatic synthesis of modified nucleic acids.[106] In these studies, modifications on the phosphate chain and the sugar moiety were mostly

poorly accepted by the DNA polymerases, resulting in low incorporation rates.[107-108] Modification on the base, however, were well tolerated by the enzyme, with the position and nature of the modification having a crucial impact on the processing by the polymerase. Modifications attached to the C5/C6-site of pyrimidine and the C8/C7 positions of (deaza-)purine bases (also referred to as the 'Hoogsten face') were favored as they do not interfere with the Watson-Crick base pairing which is needed for complementary base pairing. In the double-stranded helix, these modifications point away from the inside of the helix towards the major groove in which steric restrains are looser than in the minor groove where, e.g. modifications on the 2 position of purines are oriented to. Comparative studies have demonstrated that the C5 position of pyrimidines and the C7 positions of deazapurines are the preferred modification sites as nucleotides bearing additional groups on these positions are accepted best by common DNA polymerases of the A and B-family such as *KlenTaq* and KOD.[109-113]

Compared to the other methods, the enzymatic modification of DNA thus offers the simplest and most versatile approach for the generation of modified nucleic acids.

1.3.3 – Structural basis for the processing of modified nucleotides

In contrast to the elucidation of the best modification site, the reason why these modified nucleotides are still accepted even by high-fidelity DNA polymerases was elusive for many years. Yet, understanding the mechanism of the incorporation of these nucleotides would enable researchers to adapt the modifications and predict the likelihood for a successful incorporation.

Crystallographic studies by Obeid *et al.* and Bergen *et al.* gave first insights into how A-family DNA polymerases process modified nucleotides.[114-115] They found that the acceptance of the C5 position of pyrimidines and the C7 position of deazapurines relies on the presence of cavities that connect the active center of the A-family DNA polymerase *KlenTaq* with the outside of the enzyme. The flexible linker on a C5 modified dTTP analogue (Figure *6a*, the same linker was used for the ssDNA conjugated nucleotide in Figure *5*, VIII) protruded into a cavity above the O-helix formed by side chain of R587 and the O-helix residues L657, M658, R660, A661 and T664 (Figure *6b*). The linker itself contained an amide bond that was stabilized by the amino acid side chains of R600 and T664. The same linker on C7 deaza-dATP analogues (Figure *6c*), in contrast, protruded into a different cavity between Arg587, the O-helix (R659, R660, K663) and the palm domain (N610, Q820, and K831). The amide bond was here shown to interact with K663 and R660 of *KlenTaq* DNA polymerase.

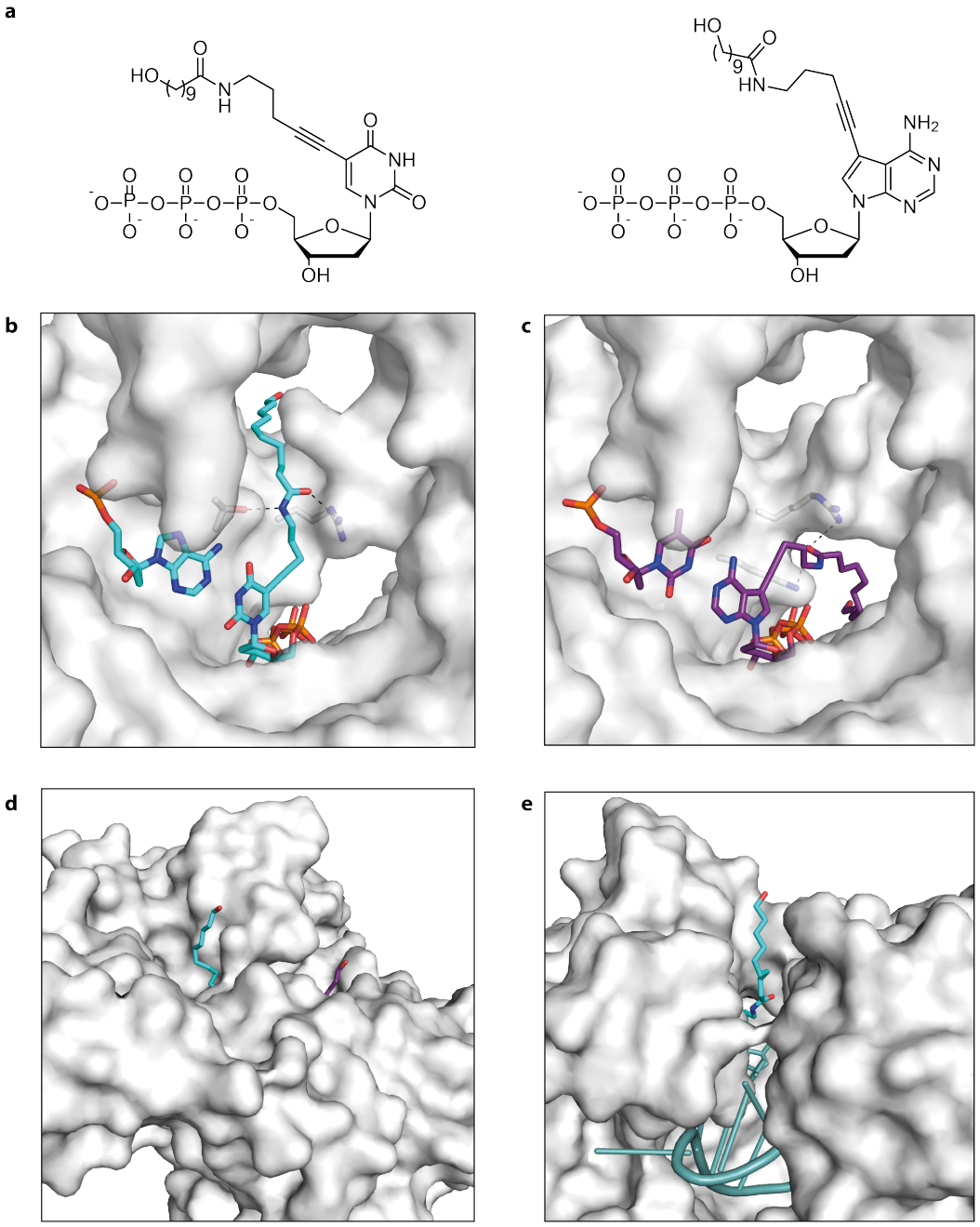

Figure 6: Crystal structures of *KlenTaq* DNA polymerase with synthetically modified nucleotides. a) Structures of a dTTP (left) and dATP (right) derivative modified with a C_{10} ω-hydroxyalkyl linker on their C5 and C7 deaza position. b) A dTTP derivative modified with flexible C_{10} ω-hydroxyalkyl linker in the active site of the DNA polymerase. The linker is stabilized via hydrogen bonding of its amide bond with T664 and R660 amino acid side chains of the enzyme. c) A dATP analogue bearing the same linker on its C7-deaza position. The linker protrudes into a different cavity and is stabilized by K663 and R660. d) Surface view of *KlenTaq* DNA polymerase with the C_{10} ω-hydroxyalkyl linker of the dTTP and the dATP analogue sticking out of the enzyme. e) View from the side of the enzyme showing the cavity encompassing the linker. Images were created using PDB 4DFK and 4DF4.[114]

In both cases, the presence of the linker chain led to only slight perturbance of the DNA polymerase structure by shifting the position of R660. The interaction of the linker with amino acid side chains of the enzyme via hydrogen bonding was shown to increase the acceptance of the modified nucleotide by the DNA polymerase and in some cases even resulted in higher incorporation rates than observed for

the natural substrate. As the active site and R660, as a member of the B-motif, are highly conserved in bacterial DNA polymerases, a similar mechanism is assumed for the incorporation of modified nucleotides in other prokaryotic DNA polymerases. In addition, studies on the archaeal DNA polymerases KOD and 9°N revealed an even stronger tendency to incorporate modified nucleotides for B-family polymerases.[116-118] The reason for this behavior is not yet fully understood, but a recent publication by Kropp *et al.* presenting structural data for KOD DNA polymerase in closed ternary complexes indicates that the active site of B-family DNA polymerases offers more space and interactions for the accommodation of nucleotide modifications.[110, 119]

If the linker attached to the modified nucleotide is long enough, it can span the whole diameter of the cavity and thus place an attached cargo on the outside of the ternary complex (Figure *6d* and *e*). This circumstance enables the incorporation of 'cargos' significantly larger than the small functional groups and long, thin chains as e.g. polyethylene glycol (PEG) that have been reported previously.[120] Several groups have taken advantage of this fact with the biggest 'cargo' attached being a 40-mer single-stranded DNA attached to the C5 position of dTTP (Figure *5*, VIII).[86] The spatial scope of nucleotide modifications, however, is not yet fully studied. In 2013, Sørensen and co-workers have reported that TdT is able to catalyze the incorporation of macromolecule-conjugated nucleotides to the 3' end of a single-stranded DNA indicating that nucleotide modifications with drastically increased size might be relevant in the enzymatic synthesis of modified DNA.[121-122] Since TdT is the only DNA polymerase able to synthesize DNA strands without any template, the incorporation of nucleotides proceeds randomly with several dNTPs being incorporated successively. This establishes TdTs role during the V(D)J recombination in immune cells, where it plays a crucial role in providing the genetic flexibility to produce the plethora of immunoglobulins and T-cell receptors required to deal with the myriad of antigens faced during lifetime.[41] However, as the structure and mode of catalysis of TdT show substantial differences to other DNA polymerases, it is unclear whether these results can be transferred to template-dependent DNA polymerases.[122-124] TdT has previously been shown to be promiscuous in dNTP processing, probably explained by wide crevices allowing dNTPs to diffuse directly into the active site of the polymerase and the lacking need for precise Watson-Crick base pairing.[121, 125] Replicative DNA polymerases, in contrast, demonstrate accurate, template dependent selection of the complimentary dNTP with only small crevices being found in the ternary complex.[114, 119] Modifications being as bulky as a complete protein might therefore perturb the complex and thus the enzymatic activity.

1.3.4 – Nucleic acid diagnostics

The role of nucleic acids as the sole carriers of genetic information make them a prime target for the detection, identification and differentiation of individuals and organisms. Since typically only small amounts of DNA or RNA are obtainable for testing, the sensitivity of nucleic acid based assays is critical for the success of any method. With the development of amplification technologies like PCR in 1983, researchers were able to amplify low amounts of DNA and thus enable nucleic acid testing based on trace amounts of genetic material.[46] A well-known example for the employment of PCR in the analysis of small nucleic acid residues is forensic DNA profiling developed by A. Jeffreys 1984, which is routinely used in criminal prosecution.[126]

In the present biochemical and medicinal practice, PCR is an indispensable technique as well and its development was thus awarded with the Nobel Prize in chemistry in 1993. Several variations of the PCR platform today allow the analysis of distinct properties of the target sequence.

Due to the template dependency of the used DNA polymerases, the appearance of a PCR product can confirm the presence of a particular target sequence. The use of helix intercalating dyes additionally allows monitoring the amplification in 'real time' when utilizing thermocyclers equipped with fluorescence detectors. Analysis of the amplification curves can be used further to quantify the amount of the target sequence in the sample and with the employment of reverse transcriptases, the PCR platform enables the generation of complementary DNA (cDNA) based on RNA targets.[127-128] Small, even single nucleotide mutations can be detected with the help of allele-specific primers that only allow efficient amplification if a canonical base pairing on the 3' end of the primer is met.[129] In addition to these, many more adaptions and variations of PCR have been applied over the years and still new methods are reported e.g. for sensing epigenetic markers with synthetically evolved DNA polymerases.[81, 130]

While the information gained via PCR based methods is mostly indirect or limited to distinct areas of the template sequence, gene sequencing offers the direct elucidation of the base succession in DNA samples.[131] The emergence of modern sequencing platforms has lowered the cost per run and time effort needed for sequencing and thus made sequencing available for a broader audience in research and medicine.[84, 132] Comparison of chemically treated DNA samples can moreover help to locate epigenetic markers in the sequence such as 5mC.[80]

Next to PCR assays and sequencing, nucleic acids can be detected in the form of 'simple' hybridization assays in which the target is detected by its annealing to a solid phase immobilized complementary sequence, often in form of arrays.[133] This method is, among others, used to simultaneously monitor the level of multiple nucleic acids e.g. for gene expression analysis.[134]

The techniques described above are only the most commonly used in nucleic acid diagnostics. Since this field is of major interest in research and medicine, the demand for cheaper, easier and more sensitive or accurate methods drives the development of new technologies. Recently, point-of-care testing (POC testing) is gaining popularity, as the idea connected to it points out several fundamental drawbacks of diagnostic methods applied today.[135]

The necessity for costly equipment and trained personnel to conduct the experiments limit the execution of the tests to specialized laboratories. Testing is hence both costly and time consuming which in urgent cases can have serious health implications for the patient. Furthermore, in resource poor environments, where infectious diseases repeatedly become epidemic, specialized laboratories and trained personnel are lacking due to financial and infrastructural cutbacks. Therefore, researchers, doctors and pharmaceutical companies are looking for diagnostics assays that can be quickly conducted by un- or low skilled operators in close proximity (preferentially even at the bedside) of the patients ('point of care'). The methods should rely on little to no machinery and give clear, explicit readouts such as a color signal. Present examples of such POC devices include drug & pregnancy tests or blood glucose meters but POC devices for the analysis of nucleic acids are still scarce due to the specificity and sensitivity needed.[135-138]

To avoid the necessity of thermocycling, many of the amplification based POC devices rely on isothermal techniques utilizing DNA polymerases with strand displacement activity or the double strand separating activity of helicases.[50, 139-140] Since these enzymes are inhibited by typical components of bodily fluids, a nucleic acid purification step is placed upstream of the actual assay.[141-142] With the help of microfluidic devices, purification and amplification can be thereby achieved in one small device the size of a bank card with reasonable cost.[143] The prevalence of smartphones might also facilitate the development of new assays since they come equipped with various sensors that can be used for sensitive readouts.[144-145]

Despite the progress made in recent years, no 'all-in-one' device for nucleic acid testing that meets all the criteria raised for POC has been approved for diagnostic market so far.[138]

2 – Aim of this Work

Modified nucleotides play a key role in many biotechnological techniques. Here, especially the employment in DNA polymerase catalyzed reactions offers great potential as it combines the naturally evolved properties of DNA polymerases with the attributes of the nucleotide modification. Numerous modifications have been reported in DNA polymerase based approaches among which, for example, nucleotides with cleavable fluorescent dyes form the basis of modern sequencing techniques.

While the modifications cover a broad range of functionalities and purposes, their size mostly only covers the range of small molecules. The prospect of the modified nucleotide having to fit into the active site of the DNA polymerase in the tightly bound ternary complex renders the successful employment of larger modifications unlikely. However, several publications have reported crystal structures showing that DNA polymerases are equipped with channels, that could encompass the modifications and thus allow modified nucleotides to be processed. Based on these publications, it was hypothesized that if the 'cargo' is connected to the nucleotide via a long, flexible linker, which is able to bridge the distance from the active site of the DNA polymerase to the outside surrounding through this channel, the' cargo' would not interfere with the processing of the nucleotide and thus would allow macromolecular modifications to be incorporated into the nascent primer strand. Earlier work within our group has shown that this theory holds true for small DNA sequences which already represent a considerable increase in size to the natural nucleoside triphosphates.

In this work, the size limitations of nucleotide modifications should be studied by attaching macromolecules such as a whole enzyme, which are typically several orders of magnitude larger than the small oligonucleotide-modifications used in previous studies. The generated nucleotide-macromolecule conjugates should be employed in DNA polymerase catalyzed primer extension reactions where the macromolecule should serve as a reporter that provides a simple readout to whether the nucleotide was incorporated or not and thus about the presence and genotype of a certain template sequence. Finally, the assay should be set up to meet the criteria raised by point-of-care testing (POC) in which the diagnostics of pathogenic biomarkers is fulfilled without complex machinery or trained personnel e.g. in resource-poor environments.

3 – Results and Discussion

3.1 – Synthesis of Thiol-modified dTTP-Analogs

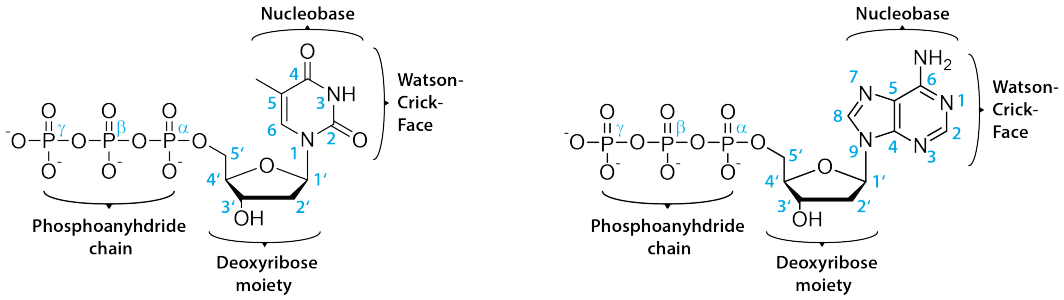

Figure 7: Composition and nomenclature of pyrimidine and purine deoxynucleotides on the examples of dTTP (left) and dATP (right).

The three distinctive moieties of deoxynucleotides, namely phosphoanhydride chain, deoxyribose and nucleobase, offer plenty of opportunity for modification and functionalization. Besides the phosphoanhydride chain and deoxyribose moiety, modifications on the nucleobase are of particular interest in biotechnological applications. Here, the position of the modification has to be carefully considered. For example, alterations on the Watson-Crick-Face of the nucleobase are less favorable in DNA polymerase-based approaches as they possibly disturb base pairing and hence nucleotide processing. Moreover, this could lead to severe cutbacks as helix perturbation or loss of sequence specificity (*Figure 7*). Therefore, a functionalization at the C5 or C6 position of pyrimidines and the C7 or C8 position of purines is clearly favored as the attached modification, is, upon incorporation, embedded in the major groove of the DNA helix. The ability of DNA polymerases to readily process such modified nucleoside triphosphates has been shown numerous times. Among the nucleotides used in these experiments, those modified at the C7 position of deazapurines and the C5 position of pyrimidines have proven to be accepted best by DNA polymerases.[93, 106, 110] Since crystal structures reported by Bergen *et al.* suggest that a linker on the C5 position of pyrimidines extends further from the surface of the enzyme and is easier accessible than the same linker on the C7 deaza positions of purine bases (see *Figure 6*), a C5 modified thymidine derivative was chosen as the basis for the synthesis for this study.[114]

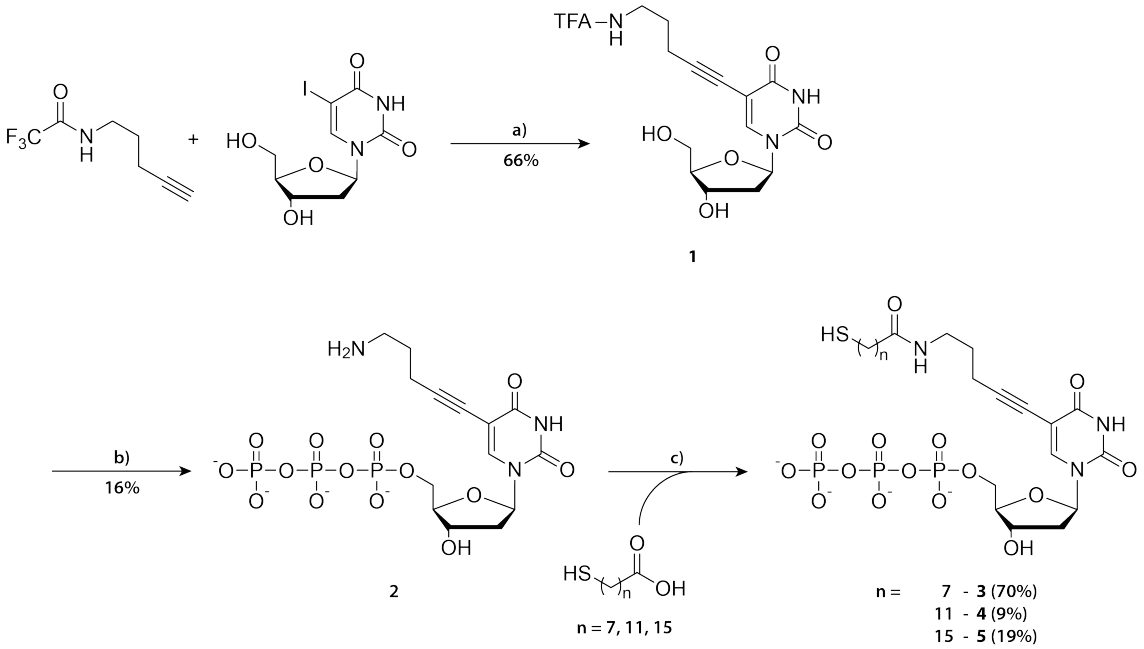

Figure 8: Synthetic strategy for the synthesis of thiol modified dTTP derivatives. a) DMF, $Pd(PPh_3)_4$, CuI, Et_3N, 12 h, rt; b) $POCl_3$, proton sponge, TMP, 1 h, 0 °C; then $(Bu_3NH^+)_2H_2P_2O_7^{2-}$, *n*$Bu_3N$, DMF, 30 min, rt; 50 mM TEAB, 30 min, rt; after IEX-FPLC: aq. 10% NH_4OH solution, 3 h; c) ω-modified mercaptocarbonis acid, DMF, HATU, DIPEA, rt, ovn.

The synthetic route was adapted from prior publications, starting with a Sonogashira cross coupling reaction of 5-iodo-2'-deoxyuridine with 5-trifluoroacetamidopentyne yielding 66% of the trifluoroacetamido (TFA)-protected, amino-functionalized nucleoside **1** (*Figure 8a*).[86, 146-147] The nucleoside was then converted into its corresponding 5'-triphosphate following the synthetic route described by Kovács and Ötvös (*Figure 8b*).[148] In detail, the nucleoside was first mono-phosphorylated with phosphoryl chloride in trimethylphosphate at low temperatures. Next, tributylamine and bis-(tributylammonium)-pyrophosphate were added simultaneously to the activated monophosphate species to convert it into the corresponding triphosphate. The reaction was subsequently quenched and the desired nucleotide was purified by anion exchange-fast protein liquid chromatography (IEX-FPLC). Following this, the lyophilized nucleotide was dissolved and stirred in 10% ammonia solution to remove the TFA protecting group at the C5 linker. The deprotected nucleotide was then purified by reverse phase HPLC (RP-HPLC) followed by repeated lyophilization, which yielded 16% of compound **2**.

In order to conjugate the synthesized nucleotides to their macromolecular 'cargo', the amino-moiety should be functionalized by amide chemistry using ω-modified alkylcarboxylinkers. Studies on crystal structures suggested that the amide bond can interact with amino acid side chains Thr664 and Arg660 in *KlenTaq* DNA polymerase via hydrogen bonds which might stabilize the enzyme-substrate complex and improve nucleotide processing.[114] Considering the broad commercial availability of maleimide-activated enzymes, a thiol group should be introduced to the nucleotide. Additionally, three different

lengths of the ω-thiol linkers ranging from an C7 to a C15 chain should be used during synthesis in order to study the impact of the linker length on processing (*Figure 8c*).

Introduction of the linkers was first envisioned as previously reported by activation of the linker with *N*-hydroxysuccinimide (NHS) in slightly basic sodium carbonate buffer.[86] However, no product was obtained in several attempts leading to the trial of a variety of different amide bond forming reagents. Ultimately, the solid phase peptide coupling reagent (1-[bis(dimethylamino)methylene]-1H-1,2,3-triazolo[4,5-b]pyridinium 3-oxid hexafluorophosphate (HATU)[149] was found to provide access to the thiol-modified nucleotides in sufficient yields. In detail, the ω-thiol carboxylic acid and the nucleotide were first separately treated with a slight excess of DIPEA in dry DMF. Then, HATU was added to the linker to form the activated carboxylic acid intermediate followed by slowly merging both solutions. The yields obtained varied significantly among the different linkers. Up to 70% were achieved for **3** while the employment of 16-mercaptohexadecanoic acid led to a low yield of only 19% **5**. This can partially be explained by the increasing detergent-like properties of the compounds with the expanded hydrophobic alkyl chain that can impede RP-HPLC purification by perturbing the retention times and thus leading to disrupted peaks. In contrast, the poorest yields were obtained for **4** (9%). Due to the product containg the HATU counter-ion hexafluorophosphate (PF_6^-) an additional ion exchange-HPLC (IEX-HPLC) purification had to performed. After the additional purification steps, the protons near the thiol-group were shifted to higher ppm, indicating that the nucleotide hat undergone an unknown side reaction.

In conclusion, C5 thiol-functionalized dTTP analogues could be synthesized starting from 5-iodo-2'-deoxyuridine in three steps. The crucial formation of the amide bond was achieved without any protecting groups, allowing a facile and direct access to the modified nucleoside triphosphates. Purification of the thusly synthesized compounds is partially impaired by the detergent-like properties of the compounds with longer alkyl chains resulting in disrupted HPLC peaks, which might become problematic when studying even longer linker lengths. Yields for the intermediate linker length were lower than for the other two analogues, at least partially owed to the co-elution of PF_6^- in RP-HPLC, which made additional purification steps necessary. After purification, protons near the thiol were shifted, indicating a side reaction of this nucleotide.

3.2 – Conjugation and Purification of Enzyme-Nucleotide Chimeras

In a first approach, the modified nucleotides should be conjugated to an enzyme that is able to catalyze to a colorigenic reaction. This enzymatic reaction should be used to visualize the incorporation of the nucleotide into a DNA strand by the naked eye. A broad variety of enzymes suited for this purpose is available as such reporters are frequently employed in biochemical assays e.g. in ELISA. Among these, Horseradish Peroxidase (HRP) is one of the most commonly used enzmyes.[150-151] HRP is a glycosylated plant peroxidase that comprises up to 15 isoenzymes with differing amino acid chains and glycosylation patterns that award them distinct physical and chemical properties.[152] The most used and best studied isoform of HRP is C1A, a 44 kDa isoform comprising a 34 kDa amino acid chain and 11 kDa of *N*-glycoslyation. HRP is known for its high turnover, broad substrate scope and a profound robustness against harsh environmental conditions which make it an ideal reporter enzyme. Notably, HRP isoforms were reported to tolerate temperatures up to 70°C for several minutes and even chaotropic reagents as urea in high concentrations.[153-155] The enzyme can be inhibited by high phosphate concentrations, some divalent transition metal cations and small anions as cyanide and azide, which tightly bind to the heme group that is crucial for catalysis.[156]

For this study, commercially available maleimide-activated HRP (malHRP) from Sigma Aldrich was used. It is randomly activated at its lysine residues by reacting the enzyme with maleimidocaproic acid N-hydroxysuccinimide ester. HRP isoforms typically contain between five to 14 lysine residues, therefore malHRP from Sigma Aldrich is specified to contain a maximum of three maleimide groups per protein.[157]

To achieve the conjugation to the nucleotide, the lyophilized enzyme was first solubilized in a PBS conjugation buffer. However, concentration determination with $\lambda = 280$ nm was not applicable as the manufacturer was unable to give any detailed information about the isoform of HRP which is being sold. The concentration of the enzyme solution was therefore measured at $\lambda = 403$ nm corresponding to the absorption of the heme group.[158] After the incubation with 5 eq. of **3**-**5** overnight, a simple centrifugal concentration was conducted to remove the excess nucleotide (*Figure 9a*).

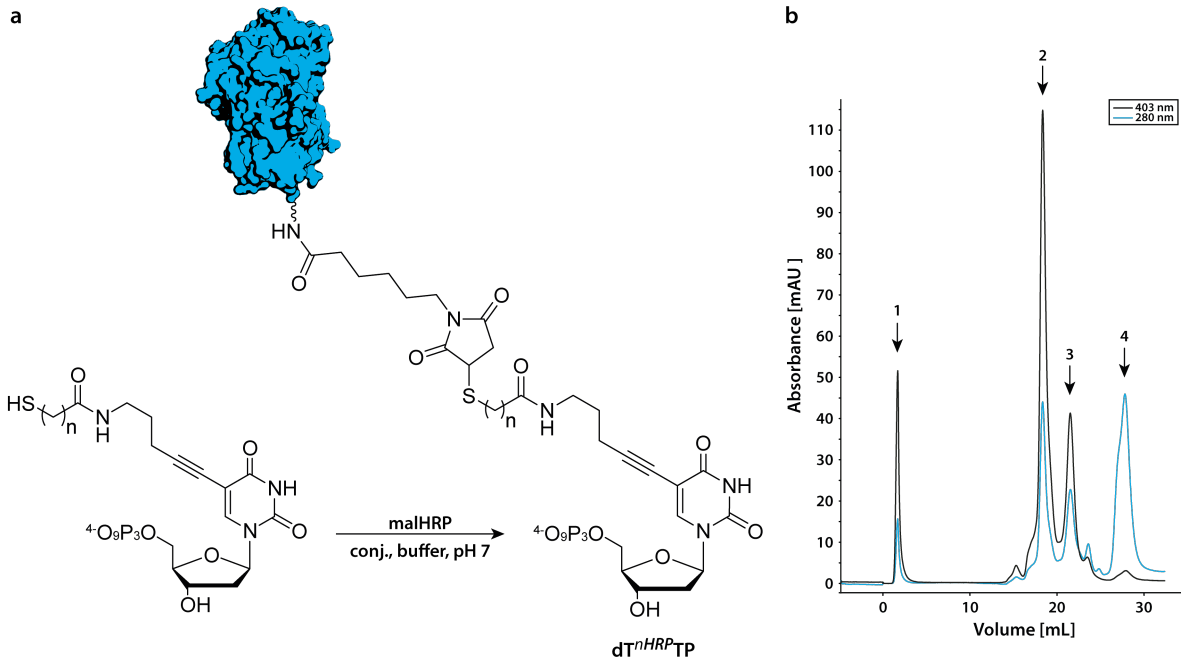

Figure 9: Synthesis of nucleotide-malHRP conjugates. a) Michael addition of the thiol-functionalized nucleotides **3**-**5** with the maleimide-activated HRP in PBS buffer overnight.FPLC run of conjugation reaction with malHRP and compound **5** on an anion exchange chromatography column. A gradient running from 20 mM Tris pH 9 to 1 M NaCl in 20 mM Tris pH 9 in 1 h on a 1 ml HiTrap Q Sepharose column was applied. Peaks were detected at 403 nm (absorption of the heme group) and 280 nm (absorption of proteins and the nucleotide): 1) unconjugated malHRP, 2) mono conjugate, 3) putative double-conjugate, 4) excess nucleotide 5.

To confirm conjugation as well as to further investigate the site of conjugation and to determine which isoform was used, digestion experiments were performed. For this, conjugated and unconjugated enzyme were treated with Pronase protease mixture or Proteinase K and subjected to analytical RP-HPLC. The obtained fractions were analyzed by NanoLC-MS at the Proteomic Facility (University of Konstanz), but due to the complex nature of the samples, no fragments could be assigned to any HRP isoform. Only traces of unconjugated nucleotide could be detected, necessitating a more thorough purification.

Due to the strong anionic charge on the nucleotide under slightly basic conditions, it was reasoned that anion exchange FPLC might allow the isolation of conjugate from excess triphosphate and unconjugated enzyme. Chromatography of the reaction mixture on a anion-exchange column yielded several peaks (*Figure 9b*). The pooled fractions were concentrated and subjected to ESI-MS measurement.

In comparison to unconjugated malHRP (peak 1, 43370 Da), peak 2 demonstrated a shift in mass of +822 Da that can be assigned to the corresponding nucleotide **5** (calcd. 819 Da) within the range of error (*Figure 10*). The successful conjugation is further corroborated by the appearance of peaks at approx. -

80 and -160 m/z of the main peak that can be explained by the loss of phosphate groups on the phosphoanhydride chain as commonly observed for nucleoside triphosphates during ESI-MS measurements.[159] Peak 3 putatively contained malHRP that is conjugated with two nucleotides. Due to the small yields, however, no signal was obtained in ESI-MS for this fraction. Excess nucleoside triphosphate was found in peak 4 at high eluent concentrations.

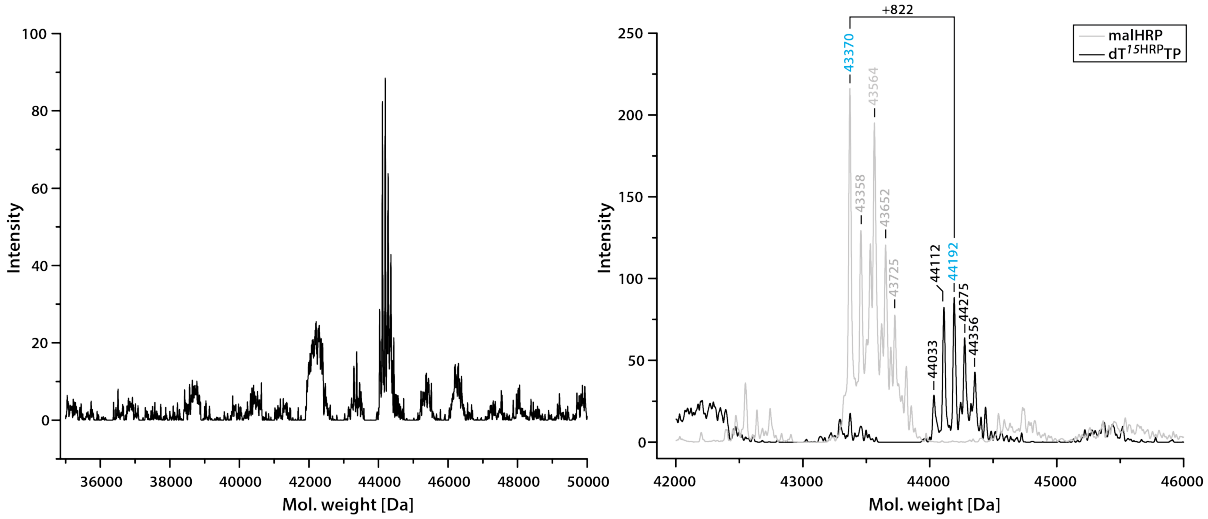

Figure 10: ESI-MS measurement in positive mode exemplarily shown for dT^{15HRP}TP. The deconvoluted peak pattern around the expected m/z for malHRP is shown on the left. In detail analysis compared to the unconjugated malHRP (grey, 43370 Da) is shown on the right. The mass shift observed is +822, calculated weight of compound **5** is 819. Peaks at 44112 Da (-80) and 44033 Da (-159) are caused by the loss of the γ and β phosphate group during ionization.

Conjugation of compounds **3** and **5** to malHRP typically yielded around 30-50% of the mono-conjugated enzymes dT^{7HRP}TP and dT^{15HRP}TP. Conjugation of the nucleotide bearing the intermediate thiol linker (**4**), however, continuously led to poor yields most likely caused by thiol being blocked by the side reaction. All further experiments were thus exclusively carried out with dT^{7HRP}TP and dT^{15HRP}TP.

In summary, thiol-modified dTTP derivatives **3**-**5** were successfully conjugated to malHRP. The conjugation took place at ambient conditions and due to the retardation caused by the triphosphate chain, mono-labeled conjugate was easily purified from excess nucleotide, unlabeled and multiply labeled enzyme by IEX-FPLC. The conjugation could be verified by ESI-MS measurements for all three conjugates, but the conjugation of the intermediate nucleotide resulted in poorer yields compared to the other nucleotides and was therefore discontinued after several attempts.

3.3 – Primer Extension Experiments employing Enzyme-Nucleotide-Chimeras

In the past, a wide selection of modifications has been attached to nucleotides and it has been shown that common DNA polymerases are still capable to process many of these nucleotides. These include dyes[84], spin-[160] and affinity labels[161], nucleosides[162] and oligonucleotides[86]. However, compared to the size of a glycosylated 44 kDa enzyme, these modifications have been rather small. Sørensen and co-workers have reported that a terminal deoxynucleotidyl transferase (TdT) is able to attach nucleotide-enzyme conjugates to the 3' end of oligonucleotides.[121] This reaction, however, proceeds randomly without any sequence specificity or template dependency found in reactions catalyzed by replicative DNA polymerases.

It was reasoned that, given the knowledge that the active site of DNA polymerases such as the *KlenTaq* DNA polymerase is connected to the outside of the enzyme via a tunnel, the DNA polymerase might be able to process nucleoside triphosphates with large modifications if they are connected to the nucleotide with a large, flexible linker that allows the 'cargo' to be placed outside of the enzyme.[114] If that linker is long enough, the size of the 'cargo' should have no influence on the processing of the triphosphate. Therefore, the two conjugates that only differ in linker length were employed to assess the influence the length of the linker has on the incorporation into a DNA strand by a polymerase.

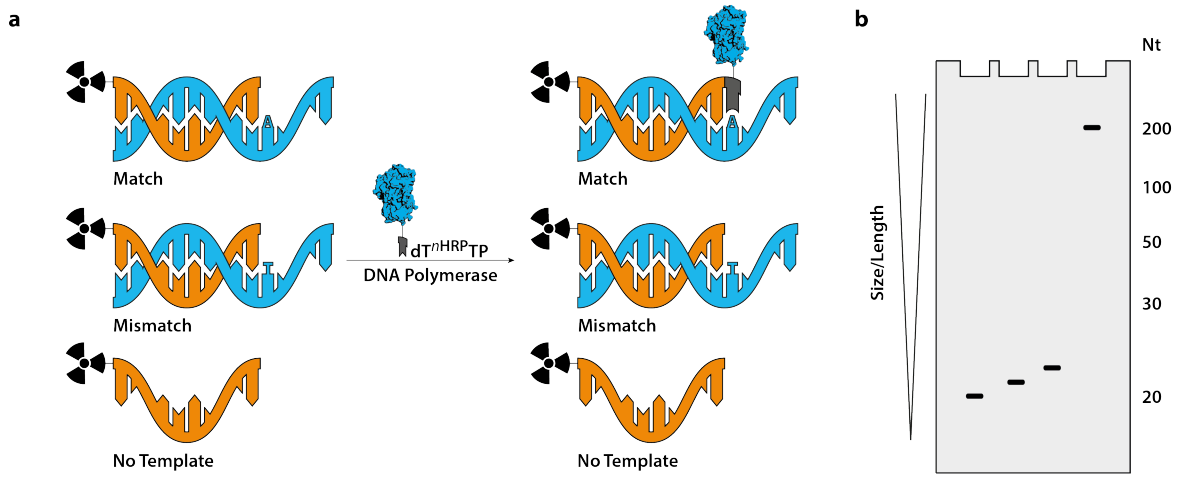

Figure 11: Schematic representation of a PEx experiment. a) A 5' ^{32}P-labeled primer (orange) is paired with a template. After the addition of a DNA polymerase and the (modified) nucleotide, the primer is elongated (matched template). If the template is missing (no template) or the base pairing at the incorporation site is non-canonical, no incorporation is observed. b) Scheme of a dPAGE with samples of differing lengths/sizes. Oligonucleotides of higher length will migrate slower in the gel compared to shorter oligonucleotides. When compared to the unextended primer, the incorporation of a single nucleotide can be visualized.

First, primer extension (PEx) experiments were carried out to see whether the conjugates can be processed by DNA polymerases at all. In these experiments, a 5'-labeled primer was incubated with a template sequence, a DNA polymerase and nucleoside triphosphates (*Figure 11a*). Due to the selectivity of DNA polymerases, the primer should only be extended if the nucleotide, that is cognate to the base given in the template sequence at the 3' end of the primer (match), is present in the reaction mixture. If the template is missing or the base pairing at the incorporation site is incorrect, no incorporation should take place (mismatched/no template). The extension of the primer can then be visualized by autoradiography of a denaturing polyacrylamide gel (dPAGE) where the radioactive 5'-label of the primer is used as readout (*Figure 11b*). Due to the increase in size, extended primers will migrate slower in these gels, roughly proportional to the size or number of the attached nucleoside monophosphates.[86] As the size increase here is quite drastic with the conjugate being several orders of magnitude larger than the natural substrates (approx. 43,000 $Å^3$ vs. 400 $Å^3$), a drastically slower migrating band was expected (*Figure 12a*).

The sequence context of the template used in these experiments is based on the B type raf kinase (BRAF) T1796A point mutation, which is strongly associated with carcinogenesis[163]. Starting, the 5'-radioactively-labeled primer and template were first aligned at elevated temperatures, after which *KlenTaq* DNA polymerase was added to the mixture. The reaction was started at 55°C by the addition of the respective nucleotide (*Figure 12c*). Samples were taken after certain time points by quenching an aliquot of the reaction in a stopping solution and afterwards analyzed by dPAGE and autoradiography.

Compared to natural dTTP (*Figure 12c*, 1) and the unconjugated thiol-modified nucleotide (2 and 3), a drastically slower migrating band was observed when either one of the HRP-nucleotide conjugates was employed in the PEx reaction (4 and 5). This on the one hand proved that the nucleotide is conjugated to the enzyme, and on the other hand demonstrates, that *KlenTaq* DNA polymerase is able to process this enzyme-nucleotide chimera despite of its huge size. As both linkers led to a considerable amount of incorporation, a C8 linker was sufficient to place the 'cargo' outside of the enzyme. On the other hand, incorporation of the C15-linked nucleotide-enzyme chimera resulted in a higher degree of turnover as seen by the primer consumption. For $dT^{15HRP}TP$, a second band was observed migrating even slower than the one corresponding to a conjugate incorporation. This band corresponds to a second incorporation, causing a T:G mispairing due to the lack of exonuclease activity of *KlenTaq* DNA polymerase.[164-165]

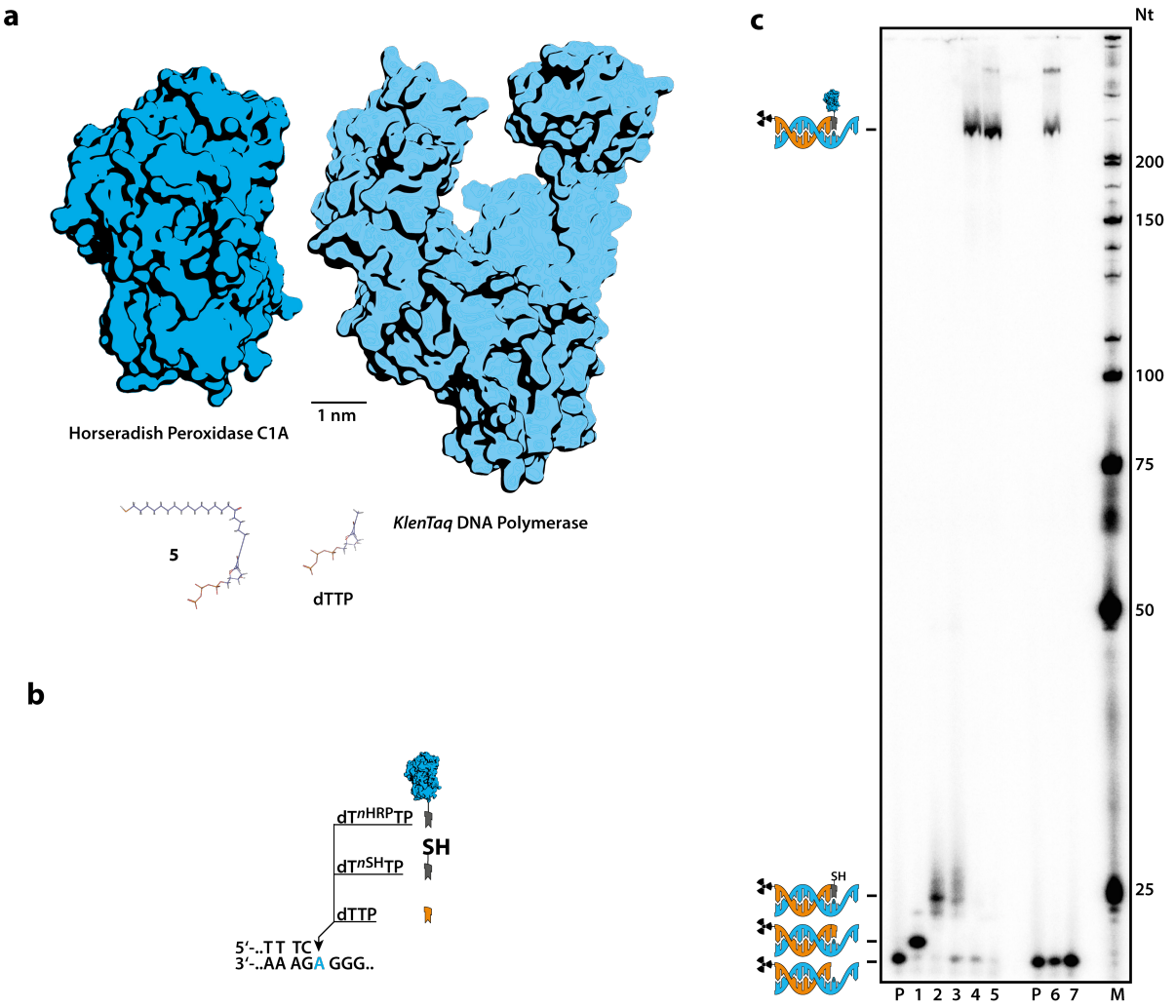

Figure 12: PEx experiments using the HRP conjugates. a) *KlenTaq* DNA Polymerase (PDB: 1KTQ[36]), HRP C1A (PDB: 1HCH[166], without glycosylation), natural dTTP and compound **5** drawn in scale.b) Scheme of the primer/template sequence around the incorporation site and the employed nucleotides.b) dPAGE analysis of a PEx experiment employing the conjugates (1-5) with *KlenTaq* DNA polymerase and on RNA templates with RT-*KTq* DNA polymerase (6-7); **P:** Primer, **1:** natural dTTP, **2:** Compound **3**, **3:** Compound **5**, **4:** dT^{7HRP}TP, **5:** dT^{15HRP}TP, **6:** dT^{15HRP}TP (RNA template), **7:** no template.

In addition to DNA templates, RNA templates have been applied in PEx experiments in order to further broaden the application scope of the conjugates. Blatter *et al.* reported a mutant of the *KlenTaq* DNA polymerase that exhibits reverse transcriptase activity on RNA templates.[58] Employment of this RT-DNA polymerase on an RNA version of the BRAF template with dT^{15HRP}TP led to the same migration shift observed for the wild type *KlenTaq* DNA polymerase, demonstrating that the system established can also be used on RNA sequences (*Figure 12c*, 6).

To further evaluate the difference the linker has on the incorporation efficiency, competition experiments were performed (*Figure 13a*). Here, the conjugates were mixed in distinct ratios with natural dTTP and employed in PEx reactions on the BRAF sequence context as before. After dPAGE analysis and visualization by autoradiography, the band intensities were analyzed compared and plotted in order

to extrapolate at which ratio an equal amount of incorporation can be observed. This experiment can be used as an indication on how well the modified nucleotides are processed by the DNA polymerase.[114] With *KlenTaq* DNA polymerase, these experiments resulted in an approx. 33/1 ratio (dT$^{n\text{HRP}}$TP /dTTP) ratio for dT$^{7\text{HRP}}$TP and a 6/1 ratio for dT$^{15\text{HRP}}$TP (*Figure 13a* and *b*). This demonstrates that while both conjugates were efficiently processed by the DNA polymerase, the longer linker facilitates the incorporation of the nucleotide, possibly by removing spatial constraints between the polymerase and the cargo. Furthermore, being processed only 6-fold worse than the natural nucleoside triphosphate, which is one of the substrates the DNA polymerases has evolved over millions of years to process, was surprisingly good considering the size difference between the two triphosphates.

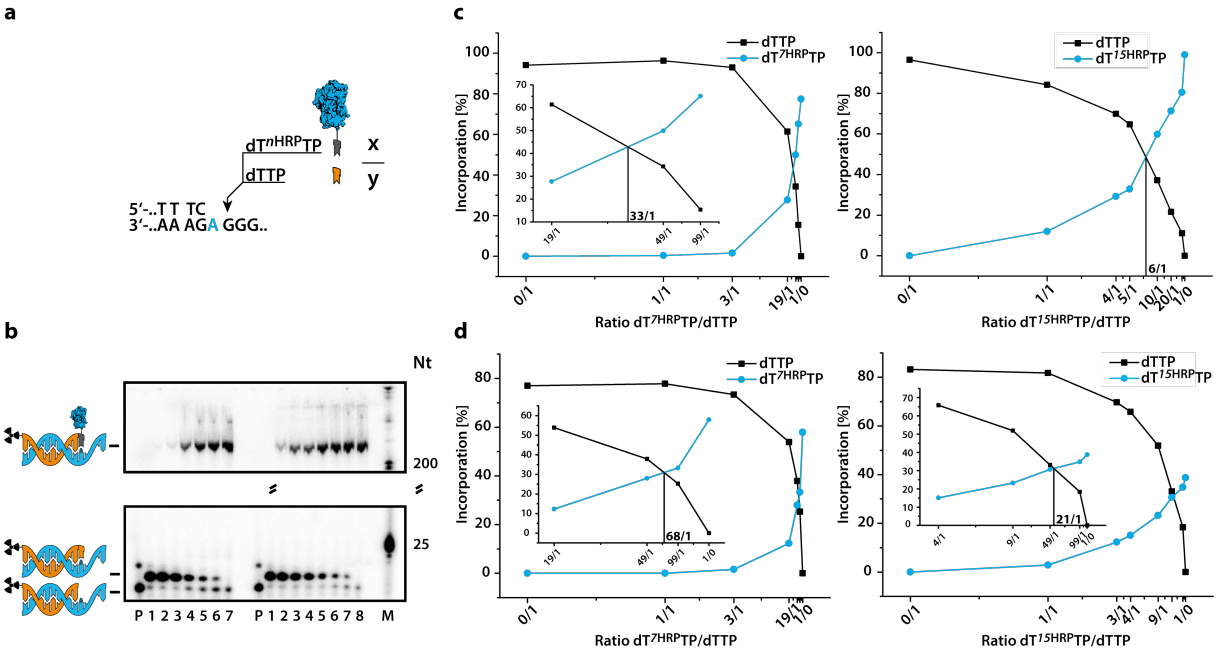

Figure 13: Competition experiments with natural dTTP and the conjugates. a) Partial sequence of the BRAF context used. Natural dTTP and one of the conjugates are employed in PEx experiments in distinctive ratios to determine at which ratio both are incorporated to an equal extent. b) Autoradiography of the competition experiment. dT$^{7\text{HRP}}$TP (left): **1**: 0/1, **2**: 1/1, **3**: 3/1, **4**: 19/1, **5**: 49/1, **6**: 99/1 and **7**: 1/0. dT$^{15\text{HRP}}$TP: **1**: 0/1, **2**: 1/1, **3**: 3/1, **4**: 4/1, **5**: 9/1, **6**: 19/1, **7**: 99/1 and **8**: 1/0. Samples were quenched after 3 min and run on a 9% denaturating gel. Incorporation values were measured by the band intensity of the autoradiograph. c) Plotted results and extrapolation for *KlenTaq* DNA polymerase; d) Plotted results and extrapolation for KF exo$^-$ DNA polymerase.

Competition assays were also carried out in presence of *DNA polymerase I Klenow Fragment 3'-5' exo$^-$* (*KF exo$^-$* DNA polymerase), another bacterial A-family DNA polymerase, yielding ratios of 68/1 for dT$^{7\text{HRP}}$TP and 21/1 for dT$^{15\text{HRP}}$TP, confirming the trend seen for *KlenTaq* DNA polymerase (*Figure 13d*). The inferior processing observed for *KF exo$^-$* DNA polymerase could be explained by enhanced struc-

tural conflicts between the enzyme and the modified nucleotide and the decreased conformational dynamics as a result of the assay being conducted at 37°C as opposed to 55°C with *KlenTaq* DNA polymerase.

As in the initial PEx experiments a second band, which was considered to be caused by a T:G mismatch due to misincorporation of the DNA polymerase, was observed, the possibility of a multiple incorporation of the conjugates should be investigated. The ability of *KlenTaq* DNA polymerase to incorporate nucleotides following a C5-modified dTTP was studied recently with the comparably more rigid 1,4-diethynylbenzene modification. Conformational adaptions of both enzyme and modified nucleotide were necessary while the nucleotide moved upstream but did not compromise the enzymatic activity of the DNA polymerase.[167]

For this, DNA templates encoding for either a consecutive or an iterative incorporation of the conjugates were used (*Figure 14a*). First, dT^{7HRP}TP and dT^{15HRP}TP were employed in PEx reactions with a template containing 11 consecutive As. The reaction was carried out as before, but samples were analyzed by 12.5% SDS-PAGE to allow a better resolution of the higher molecular weight part of the gel (*Figure 14b*). Here, the occurrence of split bands was observed. The shift of the slower migrating band when the 11A template (47 nt) was used compared to the prior BRAF template (37 nt) indicates, that this second band represents the duplex of primer with template in this, regarding oligonucleotides, non-denaturing gel. Employment of dT^{7HRP}TP led to no multiple incorporation of the conjugate as seen before in the lack of misincorporation. Employment of dT^{15HRP}TP however resulted in up to a triple incorporation. Hence, the shorter linker of dT^{7HRP}TP does not allow the DNA polymerase to slide along the nucleic acid chain or reattach at the +1 position for further incorporations. The longer linker of dT^{15HRP}TP on the other hand seems to provide the flexibility that allows for a multiple incorporation. Samples of a successful multiple incorporation of dT^{15HRP}TP were also run on dPAGE for comparison (*Figure 14c*, left). Here, even a fourth band emerged.

dT^{15HRP}TP was subsequently also used in PEx experiments with a template that encodes for a total of 13 iterative incorporations of the conjugate with three natural nucleotides spanning between each incorporation site (*Figure 14c*, right). This experiment was performed in the presence and absence of the other dNTPs. Without any of the other dNTPs, a monoincorporation was observed with a slight degree of misincorporation (*Figure 14c*, middle). These results were in accordance with those obtained from the previous experiments. The addition of the dNTPs led to a multiple incorporation with up to four observable incorporations (*Figure 14c*,). Here, the use of dPAGE and autoradiography limits the readout

as a less dense polyacrylamide gel would lead to diffuse bands and handling problems. Therefore, the number of conjugate incorporations could be higher than what was disclosed by the gel.

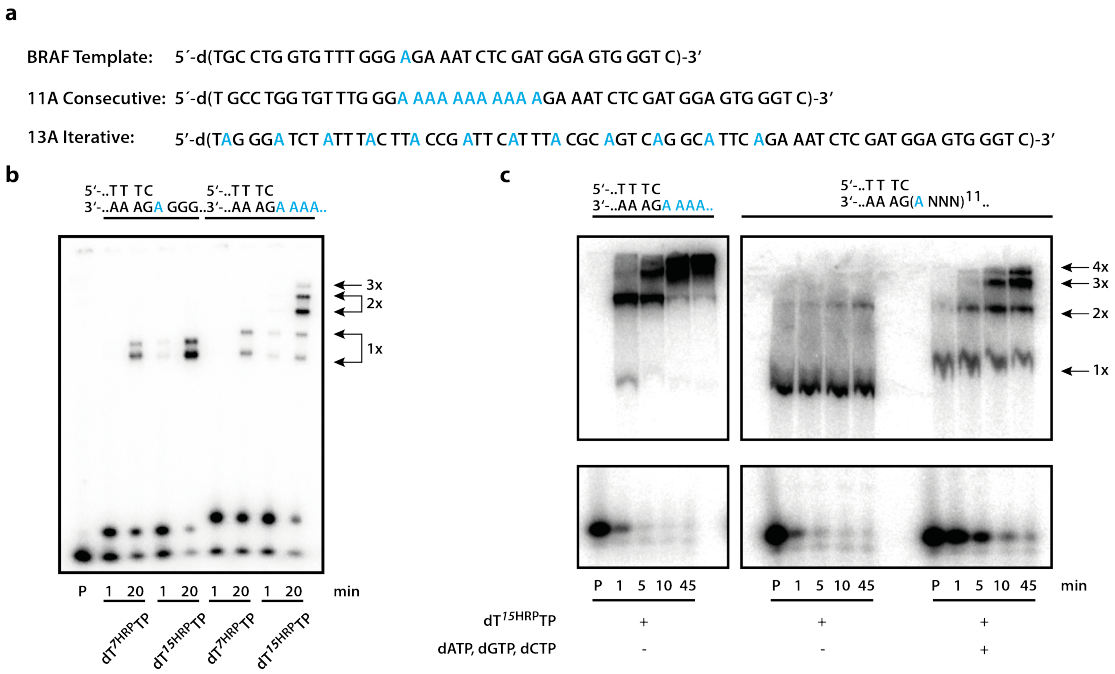

Figure 14: PEx experiments with the conjugates with either a single or a multiple incorporation site. a) Sequence comparison between the BRAF template used in the PEx experiments before and the templates encoding for a consecutive incorporation (11A) and iterative incorporation (13A). b) Autoradiography of a 12.5% SDS-PAGE with samples of PEx reaction employing either the BRAF template (left) or the consecutive multi-incorporation template 11A (right). c) Autogradiography of a 9% dPAGE gel with samples of multi-incorporation.

In total, despite their size, dTTP-HRP conjugates are accepted well as substrates by common DNA polymerases. Incorporation of the nucleotides into a primer strand led to observable, large shifts in migration in dPAGE, confirming the covalent attachment of the enzyme to the primer strand. The use of DNA polymerases with reverse transcriptase activity also allowed the incorporation of the conjugates on the basis of RNA templates. Assays employing the conjugate and natural dTTP in a competitive reaction showed that the conjugates are processed between 6- (dT^{15HRP}TP with *KlenTaq* DNA polymerase) and 68-times (dT^{7HRP}TP with *KF exo*$^-$ DNA polymerase) worse than their natural counterpart. The lower ability of the DNA polymerase to incorporate dT^{7HRP}TP was also confirmed in multiple incorporation experiments, where no multiple incorporation of the shorter conjugates was observed while the application of dT^{15HRP}TP led to up to four incorporations within the limitations of the readout. Concluding, especially the larger conjugate, dT^{15HRP}TP is readily accepted by DNA polymerases and is therefore suitable for the use in applications based on DNA polymerase catalyzed reactions.

3.4 – Primer Extension Experiments with dT^{15HRP}TP on Solid Phase

Based on the results obtained in solution, a PEx experiment was envisioned which would make use of the attached peroxidase to evaluate the incorporation of the nucleotide via a colorigenic reaction. For this, the primer would be immobilized on a solid phase (*Figure 15*).[168-169] Similar to the primer extension reaction in solution, the template dependency and sequence specificity of the DNA polymerase will only allow the immobilized primer to be prolonged, if a template is present and base pairing following the 3' end of primer strand matches the employed nucleotide. If both criteria are fulfilled, the nucleoside triphosphate is incorporated as its corresponding monophosphate and any modification attached to the triphosphate is thus covalently bound to the solid support. Consequently, after washing away all unbound conjugates and the addition of the colorigenic substrate, a color formation should only be observed in those samples in which the aforementioned requirements are met.

This test could be hence used to either detect are certain template sequence, e.g. pathogenic DNA or RNA, or to determine the genotype of a particular DNA or RNA sequence of interest, e.g. for SNP genotyping. As there is no need for expensive equipment like thermocyclers or fluorescence readers, this test would meet the demands of point-of-care devices which enable clinical diagnostics in resource-poor environments.[135-137]

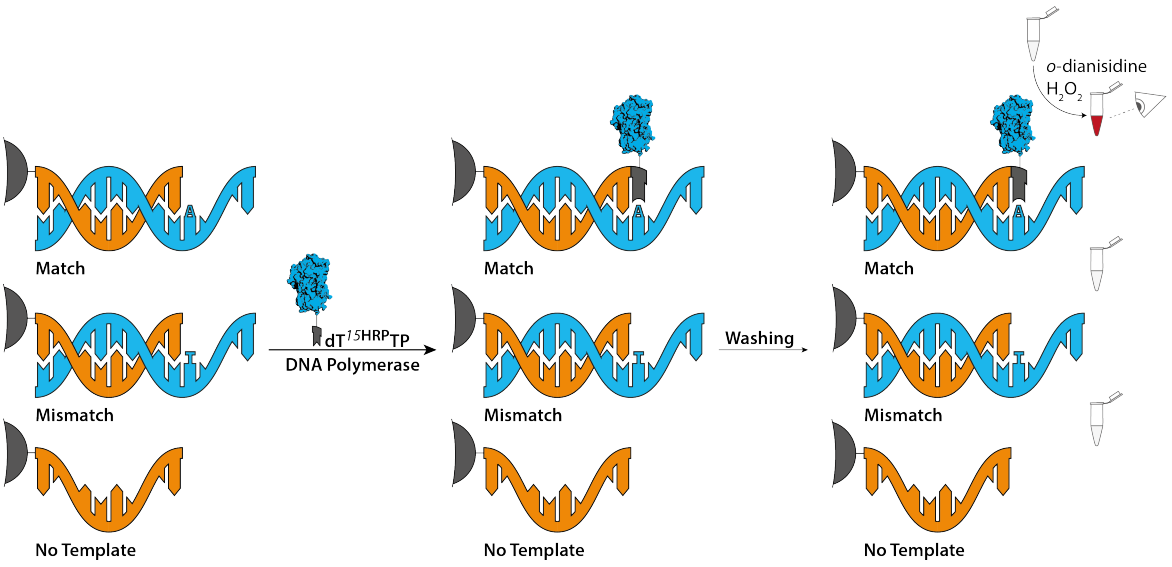

Figure 15: Schematic representation of the PEx assay with immobilized primers. The 5'-biotinylated primers are immobilized on streptavidin coated sepharose beads. After the primer extension reaction with dT^{15HRP}TP, all unbound reagents are removed by filtration and a colorigenic peroxidase substrate solution is added. If the conjugate was incorporated into the primer strand, the peroxidase will convert the colorigenic substrate and a staining of the solution can be observed.

To ensure quantitative removal of the primer extension reaction mixture, streptavidin-coated sepharose beads were chosen as solid phase as they allow fast and quantitative removal of the supernatant by filtration. The beads were first washed several times to remove the azide-containing storage buffer to prevent potential deactivation of the peroxidase by blockage of the heme group and then coated with a biotinylated version of the BRAF primer used in the PEx experiments in solution. Following an incubation with biotin to block remaining streptavidin sites, primer extension was carried out either in presence of a template containing an A opposite the 3'-end of the primer (matched), a template containing a T opposite the incorporation site (mismatched) or no template (blank). In these experiments, only dT^{15HRP}TP was used as it proved to be better processed than dT^{7HRP}TP in the competition and multiple incorporation experiments.

After the primer extension reaction, the beads were transferred into a spin column and the supernatant was removed by filtration in several washing steps. The beads were subsequently transferred back to PCR tubes and a detection solution containing hydrogen peroxide and the peroxidase substrate *o*-dianisidine, a colorless solid that upon oxidation displays a brownish color (*Figure 16a*).[170] A rapid color change was observed when 10 pmol of the matched template were present in the PEx reaction mixture while only minor staining was observed for the unmatched and blank sample (*Figure 16b*). A distinguishable color formation was even noticeable for only 10 fmol of the matched template. Thus, these assays allow a rapid detection of a template sequence with strong discrimination between the matched and the mismatched template as reported for *KlenTaq* DNA polymerase.[165] However, the slight color change - especially in the blank sample where misincorporation is excluded – indicated an unspecific binding of the conjugate to the beads. Several attempts have been undertaken to reduce the amount of unspecific binding, which increased with longer incubation times and higher concentrations of dT^{15HRP}TP on the solid phase. Addition of bovine serum albumin (BSA) or betaine to the blocking buffer did not decrease unspecific binding but in contrary did strongly influence handling of the beads by enhanced adhesion to the reaction tubes and was thus skipped. Also, the screening of several washing procedures and buffers did not yield any significant improvements. Therefore, the reaction times had to be limited to a maximum of 10 min and the colorigenic reaction was quenched after 1 min by the addition of 10 N sulfuric acid, which not only stops the reaction, but also shifts the absorption maximum of o-dianisidine towards λ = 520 nm.[171]

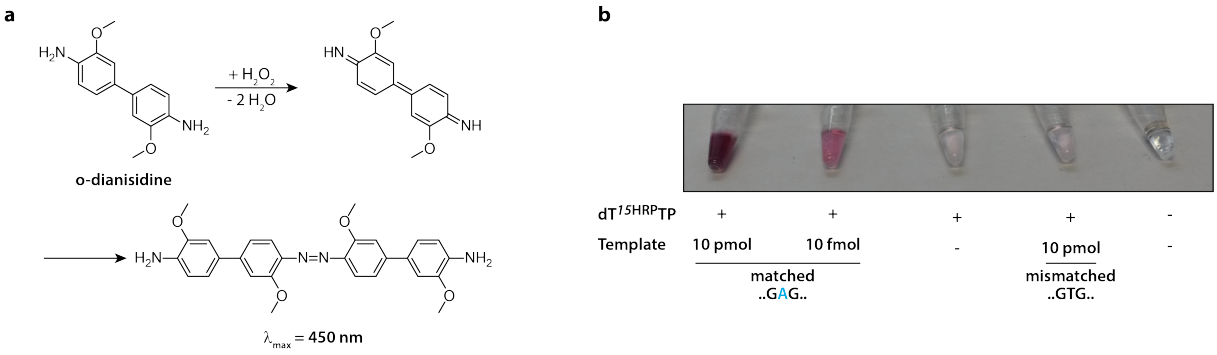

Figure 16: Result of a „naked eye"-assay with dT^{15HRP}TP on streptavidin coated beads. a) Oxidation of o-dianisidine as done by the peroxidase in the presence of hydrogen peroxide. The absorption maximum at λ = 450 nm is shifted to λ = 520 nm in low pH conditions.[170-171] b) Result of a PEx experiment as described in *Figure 15* with dT^{15HRP}TP on streptavidin-coated sepharose beads with either a matched template, no template or a mismatched template.

Subsequently, the lower limit of detection (LOD) was evaluated via a dilution series of the matched DNA template against a blank control and the mismatched template at both a low and a high concentration. These experiments were carried out using *KlenTaq* DNA polymerase (*Figure 17*, left) and *KF exo*$^-$ DNA polymerase, which would theoretically even render heating unnecessary for the procedure due to its activity at temperatures around body heat (*Figure 17*, middle).[172] For both DNA polymerases, an ultimate detection limit of 1 fmol was observed by absorbance measurement and a reliable detection limit by naked eye of around 5 fmol matched template. Discrimination against the unmatched template proved to be sufficient at around a factor of 10-fold, allowing the genotyping of DNA sample.

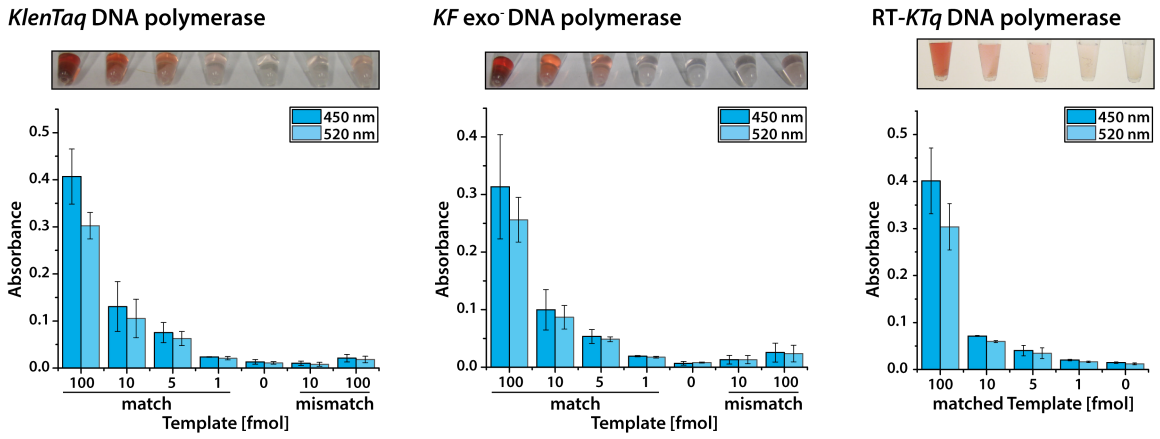

Figure 17: Evaluation of the LOD of the "naked eye" detection assay. The assay was performed on a DNA (*KlenTaq* / *KF exo*$^-$ DNA poymerase) or RNA version (RT-*KTq* DNA poymerase) of the BRAF template employing the indicated amounts of BRAF template. n=3

The lower limit of detection was also determined for the BRAF RNA template with RT-*KTq* DNA polymerase yielding a similar LOD of 5 fmol by naked eye and 1 fmol by absorption (*Figure 17*, right).

In order to demonstrate the feasibility in diagnostic applications, the assay was also carried out with RT-*KTq* DNA polymerase and a primer targeting *E. coli* 16S rRNA (*Figure 18a*).[173] The assay allowed a detection of 0.125 µg of an *E. coli* rRNA Mix containing 16s and 23s rRNA, which equals approx. 90 fmol of 16S rRNA. As a test for selectivity, an excess of human total brain RNA extract was added to a reaction mixture containing 0.5 µg of *E. coli* rRNA (*Figure 18b*).

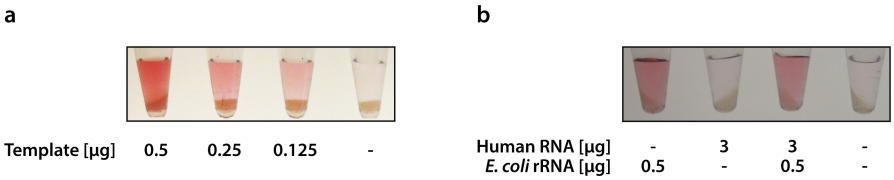

Figure 18: Detection of *E. coli* rRNA by the naked eye. a) Assay performed with a dilution series of E. Coli rRNA mix in order to evaluate the LOD on a biological relevant RNA target. b) Assay with 0.5 µg *E. Coli* rRNA in the presence of human total brain RNA extract as a test for selectivity of the approach.

The assay allowed the detection of bacterial rRNA reliably in the presence of a six-fold excess of human RNA, illustrating the selectivity of the approach. The slightly higher detection limit here is mainly caused by a lack of optimization of the assay. Due to the excess amount of other nucleic acids present in the reaction mixture, the DNA polymerase is continuously bound by competing sequences and therefore extends the intended target at a slower rate than on an isolated template sequence. Thus, longer incubation times or higher DNA polymerases concentration could yield a sensitivity as obtained above.

While the LOD is considerably good for an assay with a naked eye-based readout, it is still far too high for diagnostic applications. For example, the viral load of Ebola RNA in acute infections ranges from approx. 10 zmol to 100 amol RNA copies per ml serum.[174] For Malaria, around 11 amol/ml of *P. falciparum* 18S rRNA is found on average in blood samples.[175] However, copy numbers in early or latent infection and other common blood stream infections are estimated to typically be around 10^3-10^4 genomic copies/ml.[176] The copy number can be increased using high copy nucleic acids such as the rRNA, but will remain in the attomolar to sub-attomolar range.[177-178]

In the case of genotyping, e.g. for the allele-specific diagnosis of cancer driving mutations such as in BRAF, the amount of cell free cancer DNA (cfDNA) was reported to be 500 and 3500 copies/ml plasma, far below the sensitivity of this assay.[179]

Theoretically, the solid-phase based primer used in this setup would allow to extract a target sequence from diluted samples. Conducting the annealing step in higher volumes such as 1 ml was, however, not tested and would also be impracticable due to time consumption and handling issues. The lower limit

of detection is thus still at least 1000-fold too high for the detection of relevant amounts of pathogenic RNA in early stages of an infection.

In order to improve the sensitivity, two major issues would have to be addressed:

First, only one HRP conjugate is incorporated per template. As seen in dPAGE analysis of PEx reactions with the conjugates, a multiple incorporation, even in directly adjacent sites, is possible. This would lead to a linear increase in readout signal with every additional incorporation. To test this hypothesis, the template encoding for 11 consecutive incorporations (11A) was employed in a PEx assay on the solid phase (*Figure 19a*).

An obvious increase of absorbance was observed for the 11A template which suggests a multiple incorporation. With approx. 60%, the gain is, however, lower than the expected linear increase for the up to quadruple incorporation seen in the experiments in solution. This can be at least partially explained by the shorter incubation times and the hindered accessibility of the primer on the solid support leading to a lower degree of multiple incorporation.

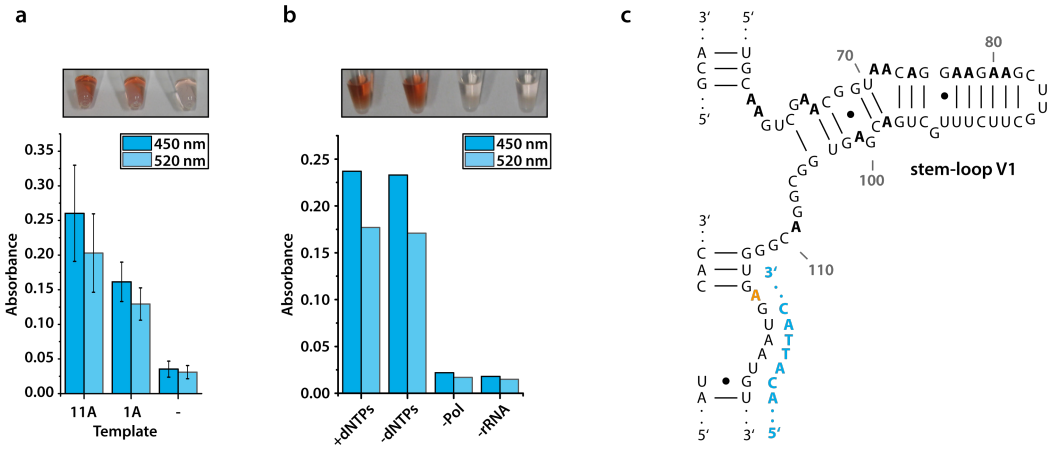

Figure 19: Multiple incorporation of the conjugates in the naked eye detection assay on solid support. a) Multiple incorporation with *KlenTaq* DNA polymerase on the DNA template encoding for eleven consecutive incorporations compared to a template with one possible incorporation (1A) and a non-template control, n=3 b) Detection of 0.2 µg of *E. coli* 16S rRNA in the presence or absence of the remaining dNTPs with RT-*KTq* DNA polymerase. The assay was conducted two times under varying conditions, the depiction is exemplary. c) Sequence context around the stem-loop V1 region adjacent to the primer binding site (orange). The first conjugate is incorporated opposite the A marked in blue at position 116 of the 16S rRNA (adapted from Yarza *et al.* [180]).

To test whether this can be transferred onto the biological relevant target of *E. coli* 16S rRNA, a PEx reaction as seen in *Figure 18* was spiked with the deoxynucleotides dA, dG and dC to allow the incorporation of multiple conjugates opposite the remaining 31 As downstream of the incorporation site (*Figure*

19b). No clear change in absorbance was observed in this case. This might be caused by the presence of the stem-loop V1, which is situated only 12 nucleobases downstream of the primer binding site (*Figure 19c*).[180] Within these 12 bases, only one A is found at position 109, located three nucleotides upstream of the loop. As no denaturation step is possible on the beads and the DNA polymerase has no significant strand displacement activity[181], the stem-loop presumably perturbs DNA polymerase binding and activity in close proximity, resulting in an inability to incorporate additional conjugates. The assay as it stands is thus limited to single-stranded DNA or RNA targets.

Second, unspecific binding of the peroxidase to the sepharose prohibits longer incubation times. Therefore, the PEx reaction as well as the peroxidase reaction have to be kept short to reduce background staining. Horseradish Peroxidase is often used as a reporter in ELISA assays. There, developing times of up to 30 mins are stated, allowing a much more sensitive detection of the peroxidase compared to the 1 min incubation applied in the experiments here.[182] LODs published for colorimetric readouts of HRP-based ELISA assays are in the low attomolar range, indicating, that by removing the unspecific binding, the assay sensitivity could be improved 1000-fold.[183] This is supported by recent work, where antibody-linked nucleotides are used in a primer extension reaction on a similar setup. Similar to ELISA assays, the incorporated antibody is then detected via a secondary antibody-HRP conjugate. This way, unspecific binding of HRP to the beads could be greatly reduced and the detection limit was thus lowered 100-fold to 10 amol.[184]

Last, unspecific binding could also be overcome by using an inert solid support. Accordingly, NHS-activated Tentagel, NHS-activated agarose, glycidyl-activated glass beads, Neutravidin beads and streptavidin-coated 8-well strips have been employed in the assay above. However, none of these solid supports led to any significant improvement over the streptavidin-coated sepharose beads used before. No further improvements could be made with respect to the unspecific binding issue.

The proficiency of PEx and PCR based approaches greatly rely on the properties of the employed DNA polymerase. Detection and genotyping thereby are based on the template dependency and the sequence selectivity found in replicative DNA polymerases. However, additional properties of DNA polymerases can be harnessed. For example, J. Aschenbrenner and co-workers were able to show that on RNA templates RT-*KTq* DNA polymerase shows significantly different incorporation behaviors opposite As methylated in position 6 (m^6A) or 2'O (2'-OMeA).[81, 185] This enabled a direct sensing of methylation sites by RT-PCR. Due to the insights obtained into the crucial role of epigenetic markers over the past years, methods for the rapid and direct sensing of these markers are strongly required.

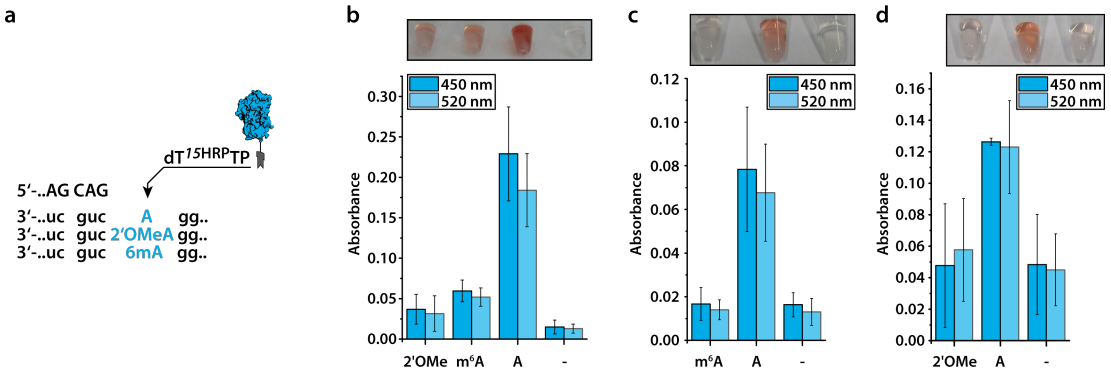

Figure 20: Detection of epigenetic markers in RNA samples. a) Sequence context of the incorporations in a DNA primer on synthetic RNA templates b) detection of 2'OMeA and m^{6}A in synthetic RNA templates with RT-*KTq* DNA polymerase. n=2 c) Detection of m^{6}A in 18S rRNA in human RNA extracts from HeLa cells. Unmethylated template was generated by *in vitro*-transcription of a PCR-amplified copy of the gene and concentration was adjusted to the 18S rRNA content of the extracted RNA. n=3, d) Detection of 2'OMeA in HeLa cell extract. n=3.

It was hypothesized that the assay possibly can be used to visualize the difference of a single methyl group on the template by the naked eye. RT-*KTq* DNA polymerase was first employed in mono-incorporation experiments on synthetic RNA templates presenting either A, 2'OMeA or m^{6}A at the incorporation site (*Figure 20a*). Clear differences were observed with a 3.8-fold discrimination of the A template over the m^{6}A template and a 6.2-fold discrimination over the 2'OMeA template, clearly demonstrating, that the assay indeed can be used to discriminate a single methyl group by the naked eye.

Next, the epigenetic markers should be detected in biological relevant samples. Therefore, human total RNA was extracted from HeLa cells using the Direct-zol™ RNA MiniPrep Kit. Primers were designed to match the known methylation sites 2'OMeA in position 468[186] and m^{6}A in position 1832[187] of the human 18S rRNA. Unmethylated controls, generated via *in vitro*-transcription of a PCR-amplified DNA template of the 18S rRNA sequence, were kindly provided by J. Aschenbrenner. The 18S rRNA content of both methylated and unmethylated rRNA was adjusted by band intensity in GelRed-stained agarose gels.[185] With a discrimination of 4.7-fold for m^{6}A and 2.6-fold for 2'OMeA, the assay resulted in a clear difference in staining between the methylated and the unmethylated template in both cases (*Figure 20b-d*).

Taken together, the ability of DNA polymerases to incorporate the conjugates in PEx reactions on both DNA and RNA targets can be utilized to detect and genotype target sequences in a naked-eye based assay with primers immobilized on a solid phase. The assay allows the detection of as little as 1 fmol of the target sequence in under an hour with (theoretically) no need for complex machinery as *i.e.* thermocyclers. While experiments with 16S rRNA from *E. coli* demonstrated that the assay works in biologically

relevant settings, the lower limit of detection (LOD) is too high for the assay to be used in actual clinical diagnostic. The LOD could be substantially decreased if two key issues of the assay could be overcome. First, a multiple incorporation of conjugates was shown to be possible on synthetic targets, but failed to be advantageous in 16S rRNA experiments. As this most likely could be solved with a more meticulous primer design, this issue should be addressable. Multiple incorporation is, however, also restricted by the incubation time, which itself is limited by the second key issue of the assay: unspecific binding. The permanent background staining caused by unspecific binding of the conjugates to the sepharose beads confines the incubation times at high temperatures (like 55°C for *KlenTaq* DNA polymerase). Changes in the assay procedure and the washing protocols improved the issue, but did not completely eliminate it. Substitution of the solid phase with various other surface materials and immobilization functionalities did also not result in a decrease of unspecific binding.

In addition to detection and genotyping, DNA polymerases with supplementary discrimination properties allow further applications of the conjugate as demonstrated in the detection of epigenetic markers by naked eye. Here, employing RT-*KTq* DNA polymerase with RNA extracts yielded a strong discrimination between methylated and unmethylated sites in the target sequence, allowing a rapid and easy detection of methylation sites in human total RNA samples.

3.5 – PEx Reactions with Glass Slide-immobilized dATP

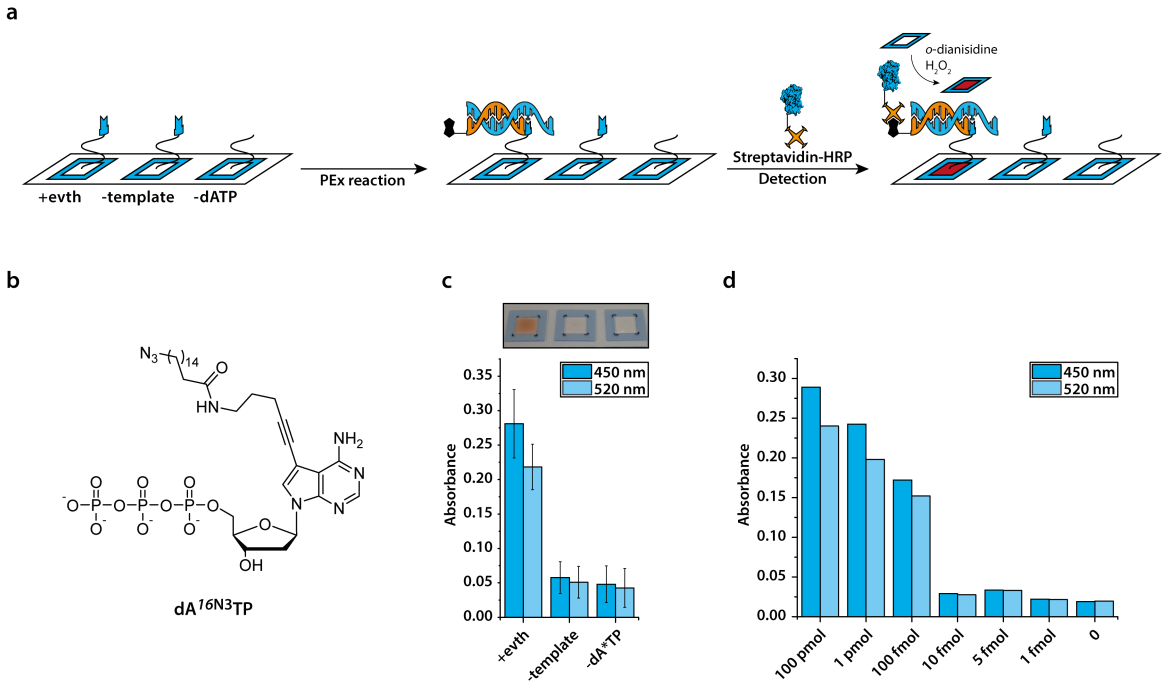

Figure 21: PEx experiments with a solid-phase immobilized nucleotide. a) Schematic representation of the setup. An amine-functionalized dATP is spotted on an NHS-activated glass slide within reaction chambers contained by a self-adhesive frame. A PEx reaction with 5'-biotin labeled primer is conducted within the reaction chamber. Streptavidin-HRP conjugate is added to each well and after a short incubation period, all unbound reagents are removed by washing. Finally, a colorigenic HRP substrate solution is added. b) Chemical structure of the amino-functionalized dATP derivative **8.** c) Quantification and image of the aforementioned assay, n=3. d) Evaluation of the LOD of the slide assay via a dilution series of template concentration. n=1-2.

With the knowledge gained during the experiments with HRP nucleotides with primers immobilized on solid phase, an alternative setup was envisioned. This time, the nucleotide itself should be bound to the solid phase and then employed in a PEx reaction with the 5'-biotin-labeled primer. Doing so, the primer would only be bound to the solid phase if a successful incorporation of the immobilized nucleotide is achieved. The 5'-biotin modification could then be used to detect the incorporation by the application of streptavidin-coupled HRP, similar to the assay described before (*a*). Several advantages were expected from this assay: First, the glass surface should minimize unspecific binding of any of the reagents to the surface. Second, the HRP itself is removed from the PEx reaction which should further decrease unspecific binding and background reactions. Third, handling and washing of the glass slides is easier as no transfer of the beads to a spin column is required. Fourth, the 5'-biotin modification can be utilized by many streptavidin conjugated reporter system and hence is more versatile than the direct HRP conjugation.

In addition to all these benefits, the glass slide is many orders of magnitude larger than any nucleotide modification that has been reported to be incorporated by DNA polymerases before. Thus, a successful

incorporation in this setup would prove that the modification can be almost infinitely large if the linker connecting it to the nucleobase is long enough.

For these experiments, a deoxyadenine derivative, equipped with a C16-aminolinker on its C7-deaza position (dA^{16N3}TP, Figure *21b*), kindly provided by Jana Balintova, was used. The nucleotide was spotted on an NHS-activated glass slide within reaction chambers formed by self-adhesive frames (*Figure 21a*). A negative control with no nucleotide spotted onto the surface was prepared as a control alongside the other samples. All reaction chambers were subsequently treated with 6-amino-hexanoic acid to block remaining NHS-groups and to generate a negative charge on the surface in order to minimize adhesion of the DNA strand to the glass surface. Following this, the reaction chambers were washed several times. The PEx reaction was carried out with RT-*KTq* DNA polymerase and the BRAF mismatched template sequence (matching the dATP used here) at 55°C with the slide lying on the metal surface of a thermoblock. Evaporation of the reaction mixture was prevented by placing plastic cover slips on top of the reaction chambers. Subsequent to the PEx reaction, the chambers were washed thoroughly, incubated with Streptavidin-HRP conjugate and again washed. Finally, the HRP dye solution containing *o*-dianisidine and hydrogen peroxide was added and the colorigenic reaction was followed by the naked eye and absorbance measurement (Figure *21c*).

Barely any absorbance was observed for the control reactions with no dATP spotted on the surface (right) or no template present in the reaction (middle). Only if the reaction contained all necessary reagents, a distinct staining of the reaction chamber was observed (left). Hence, the immobilized dATP derivative **7** was successfully incorporated into the primer strand by RT-*KTq* DNA polymerase despite the macroscopic cargo attached to it. This is most likely facilitated by the large linker consisting not only of the C16-alkylchain between the nucleotide and the amino group on the linker, but also the NHS-activated hydrogel on the surface of the glass slides with a thickness of 100 nm in the hydrated state.[188] Combined, the linker is long enough to circumvent any spatial conflicts between the DNA polymerase and the cargo.

Next, the LOD of the new setup was determined by employing a dilution series of the template (*Figure 21d*). Due to the limitation of the assay to three reaction chambers per slide, the data points were split up between four slides with the employed amount of template partially overlapping for comparison. By naked eye and absorbance measurement, the assay was allowed a positive readout down to 100 fmol of template. No significant staining was observed below 10 fmol, 5 fmol or 1 fmol compared to the no template control. With a LOD between 100 fmol and 10 fmol this setup performed more than tenfold worse

than the assay on the streptavidin coated sepharose beads. The use of the glass slides did not substantially decrease background staining and detection times again had to be limited to 1 min.

Hence, the successful incorporation of an immobilized dATP with its macroscopic cargo demonstrates the scope of nucleotide modifications in PEx experiments. By utilizing a secondary detection, a benefit in sensitivity compared to the approaches used before was expected. However, no advantages regarding the naked eye detection application were gained with this setup.

3.6 – PEx based LAMP Detection on Solid Phase

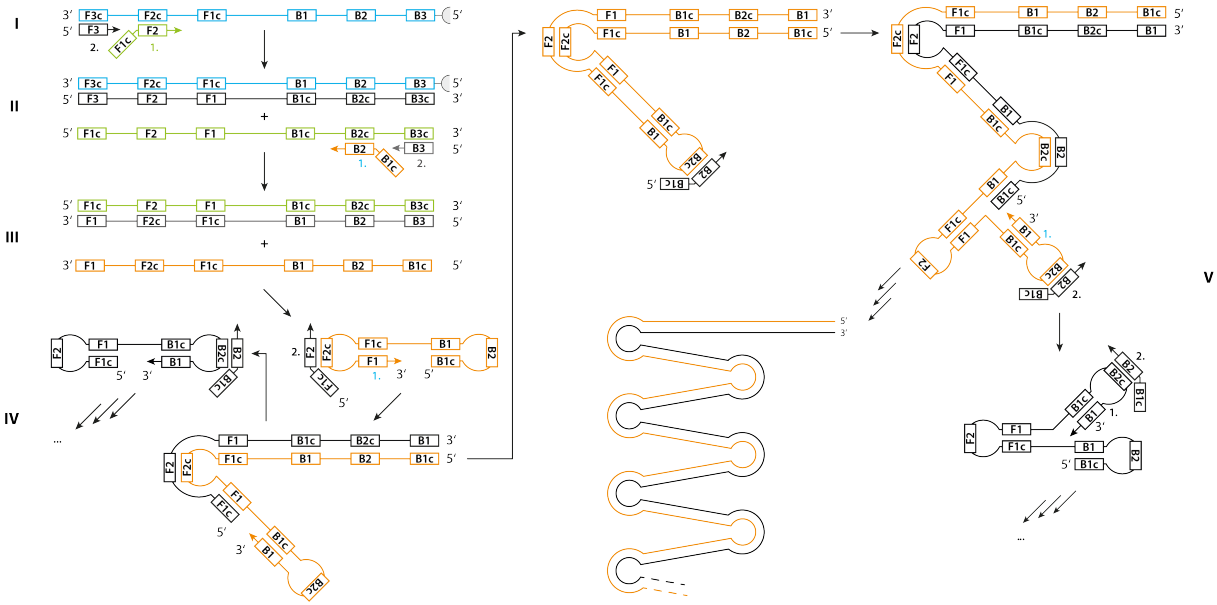

Figure 22: Scheme of the classic loop-mediated isothermal amplification reaction. Six distinct areas of the template (F1c, F2c, F3c, B1, B2 and B3) are targeted by a set of four primers (outer primers: black/grey, inner primers: green/orange) comprising two inner primers and two outer primers. Subsequent elongation of the inner primers and strand displacement by the extension of the outer primers leads to a dump bell-like structure in which self-primed DNA synthesis and displacement by new inner primers leads to the generation of concatemers and cauliflower-like structures of different sizes as amplification products. Inner primers & elongation products: green/orange, outer primers & elongation products: black/grey; c = complementary.

To increase the applicability of the approach compared to the HRP-based setups, a more sensitive detection system should be utilized. In this regard, LAMP stood out because of its low detection limit, isothermal procedure and rapid amplification that suit the envisioned POC-character of the assay.[53-54, 138]

In classic LAMP, a set of four different primers and a DNA polymerase with strand displacement properties are used to target six distinct areas of the template sequence (Figure *22* blue, F1-F3, B1-B3). The two inner primers (green in step I and orange in step II) comprise a site complementary to a sequence in the target oligonucleotide and a 5' overhang that is complementary to a site within the elongated primer (F1c, B1c). After the inner primer is elongated, the outer primer (black) binds upstream of the inner primer at the target sequence and its elongation by the strand displacement DNA polymerase releases the prolonged inner primer (Figure *22*, step I). The procedure is then repeated at the other side of the released, elongated inner primer (step II), generating a new sequence that is similar to the target sequence, but instead of the outer primer binding site, it is now on both sides equipped with a sequence

complementary to an area inside the oligonucleotide (orange, step III). Annealing of these complementary sequences will lead to a dumb bell-like structure in which first the self-primed 3' end is elongated by the DNA polymerase to open the dumb bell-end on the other side and second, the annealing and elongation of new inner primer releases the stem-loop generated in the first step (step IV). Thus, a new self-primed 3'-end is formed with which the cycle of self-primed elongation and release by an inner primer is continued. In the end, a mixture of stem-loop like DNA concatemers and cauliflower-like structures with various repeat count is obtained (step V). The reaction can be monitored by e.g. the addition of dyes used for nucleic acid staining or turbidity analysis of precipitating magnesium phosphate. Furthermore, the use of low-buffered reaction mixtures allows amplification monitoring with pH sensitive indicator dyes by the naked eye, as during the DNA polymerase reaction, a proton is released for each nucleotide incorporation.[189]

Due to the use of four different primers in the initiation step of the amplification, LAMP assays are considered to offer great specificity in amplification. Optionally, a third set of primers ("loop primers") that anneal to the single-stranded loop regions of the DNA concatemers can be included to accelerate the amplification.[190]

LAMP assays have also been adapted to cover SNP genotyping and RNA detection.[191-194] However, in order to work as intended, the primers needed for the amplification have to meet certain requirements in regards to their melting temperature, spacing and concentrations.[53] Thus, the design of suitable LAMP primers can be tedious, even when done with specific design software. While setting up the LAMP reaction, further problems can occur such as the amplification of non-template controls, which drastically impedes the reliability of LAMP assays.[195-197] While optimization of the assay parameters can help to reduce non-template amplification, this process again requires a lot of time and effort.

Therefore, combining an established LAMP assay with the simple setup and robustness of a PEx reaction would allow sensitive detection of diverse targets without the necessity to individually optimize a LAMP assay for each target. Following the approaches before, the LAMP template sequence should thereby be covalently attached to a nucleotide. The nucleotide could be incorporated into an immobilized primer during the PEx reaction in dependence of the presence and sequence of a target nucleic acid. After the removal of all unbound modified nucleotides, a LAMP assay could be carried out in order to detect the incorporation event.

Oligonucleotide modified dNTPs have been described before in studies utilizing them as barcodes or as a reporter system with DNAzyme properties.[86] A LAMP template sequence, however, has to harbor six distinct binding sites in fixed spacing. Typical sequences hence consist of around 200 or more nucleotides, which vastly exceeds the oligonucleotides that have been successfully incorporated before with up to 40 nucleobases.

The chosen LAMP template is a 245 base sequence taken from the genome of the Lambda phage.[189-190] In order to be accessible in reasonable yields by solid phase synthesis and ligation, the sequence was shortened 61 nucleotides in the middle area and split up into two halves with lengths of 91 and 93. For conjugation to the nucleotide, the oligonucleotide representing the 5'-end of the target sequence was equipped with a 5'-dibenzocyclooctyne (DBCO) modification (Figure *23*). The 3'-half of the sequence was phosphorylated on its 5'-end to allow splint ligation with T4 DNA ligase, which was carried out at 16°C overnight in presence of two equivalents of a 30-mer splint.

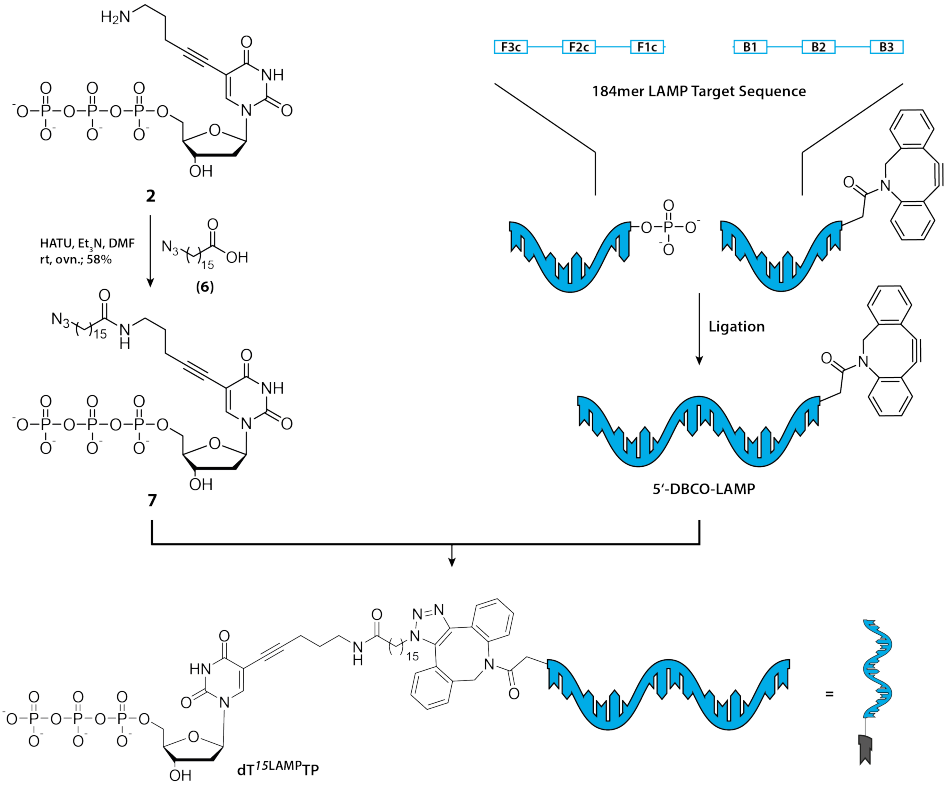

Figure 23: Synthesis of LAMP template-conjugated dTTP analogs. left: **2**, DMF, HATU, triethylamine, rt, ovn.; right: The two modified halves of the LAMP template are ligated by splint ligation with T4 DNA ligase yielding a 5'-DBCO-modified 184mer. The click reaction between the azide-functionalized nucleotide and the LAMP template is carried out in PBS buffer at room temperature overnight and the product is purified by ion-exchange HPLC at 85°C.

To accompany the 5'-DBCO modified LAMP sequence, an azide-functionalized nucleotide was prepared. Starting from 16-bromohexadecanoic acid, 16-azidohexadecanoic acid (**6**) was synthesized fol-

lowing reported procedures with sodium azide in DMF.[198] Compound **6** was then coupled to compound **2** using similar conditions as for the thiol-modified deoxythymidines **3**-**5** with HATU and a sterically hindered base in DMF yielding compound **7**. Conjugation of **7** and the LAMP template by strain-promoted 1,3-dipol cycloaddition was achieved in PBS buffer overnight and the product was purified by ion exchange HPLC and centrifugal filtration. The generated conjugate only has a slightly higher volume than the HRP-conjugate (approx. 57,000Å^3 compared to 43,000 Å^3), but assuming a linear secondary structure, the LAMP target exceeds the HRP-conjugate by far in its extensiveness (Figure *24a*).

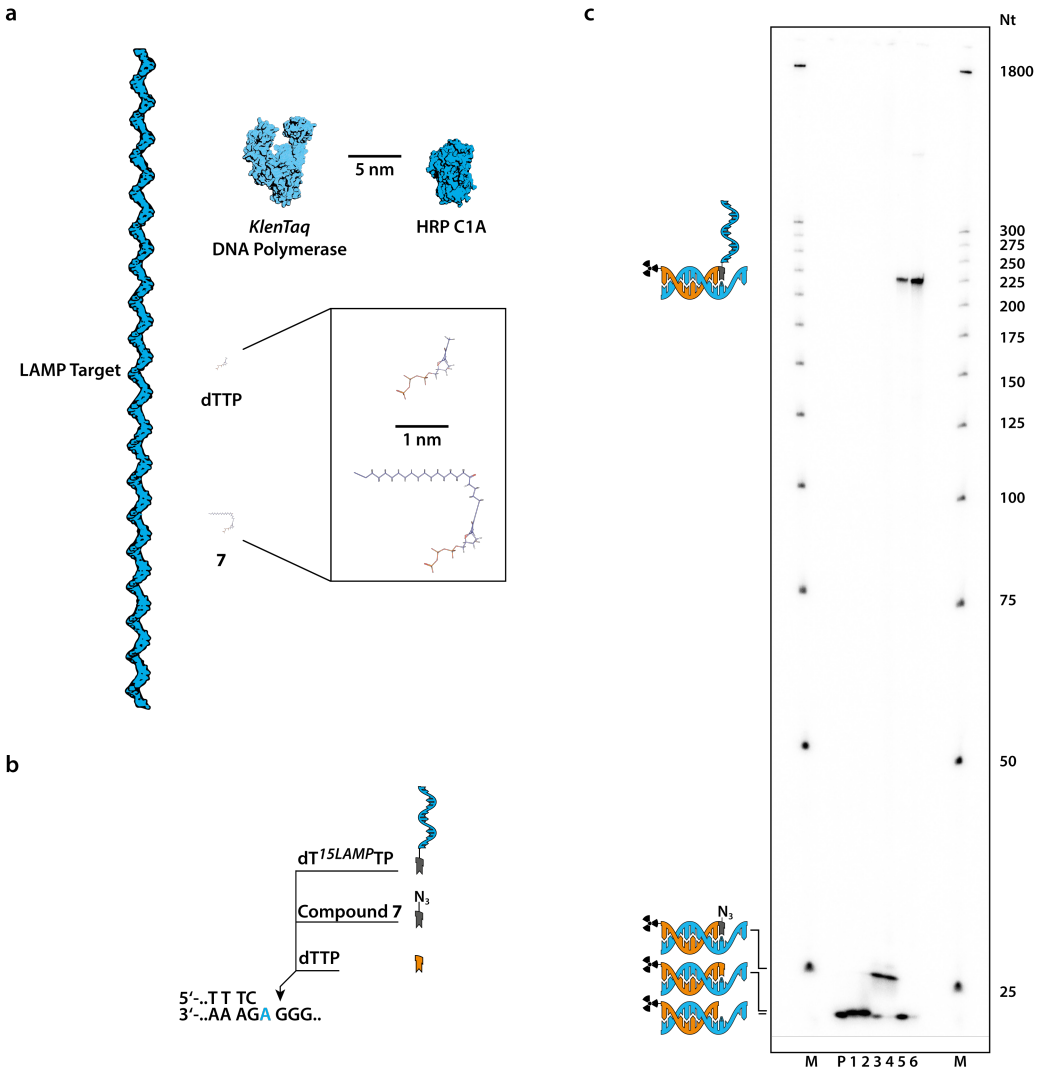

Figure 24: PEx experiment employing the LAMP-conjugated dTTP. a) The LAMP target sequence, *KlenTaq* DNA polymerase, natural dTTP and compound 7 drawn to size. b) Partial sequence of the incorporation site in the BRAF sequence context and the three different nucleotides used in this experiment. c) PEx experiment with *KlenTaq* DNA polymerase at 55°C with 1 µM dT^{15LAMP}TP. **P:** Primer, **1:** dTTP, 1 min, **2:** dTTP, 30 min; **3:** Compound **7**, 1 min, **4:** Compound **7**, 30 min; **5:** dT^{15LAMP}TP, 1 min, **6:** dT^{15LAMP}TP, 30 min; **M:** Marker.

PEx experiments in solution were conducted with dT^{15LAMP}TP in comparison with natural dTTP and the azide-modified derivative **7** with KTq DNA polymerase on the BRAF sequence context used for the same experiments with dT^{nHRP}TPs (Figure *24b*). Samples of the PEx reaction were again quenched and

analyzed by dPAGE. For dTTP, the expected small shift for a mono-incorporation (Figure *24c*) was observed. Employment of compound **7** led to a slightly larger shift in gel migration as anticipated for the long alkyl chain impeding migration through the gel matrix. Finally, dT^{15LAMP}TP led to a clear shift, similar as seen for the enzyme-conjugated nucleotides. The band corresponding to the LAMP sequence-conjugated nucleotide runs at approx. 225 nt, which is consistent with the combined volume of the 21-mer primer, the 184-mer LAMP sequence and the connecting alkyl linker. Therefore, not only the conjugation between the LAMP sequence and the nucleotide was confirmed, but it was also shown that DNA polymerases are able to incorporate nucleotides equipped with ssDNA that is considerably longer than the sequence context used for incorporation.

Having the nucleotide-attached LAMP target in hand, the LAMP reaction itself should be optimized. The assay was conducted as reported in the original publication with Bst 2.0 DNA polymerase, 350 µM for each dNTP and 0.2/0.4/1.6 µM primers (outer/loop/inner) at 65°C and monitored by real-time SYBR green I fluorescence detection.[189] Using these conditions, the positive control containing 10 nM of the ligated LAMP target amplified at a Cq value of 15.4, but all non-template controls showed a similar amplification ranging from Cq 26.4 to 46.6 (Figure *25a*).

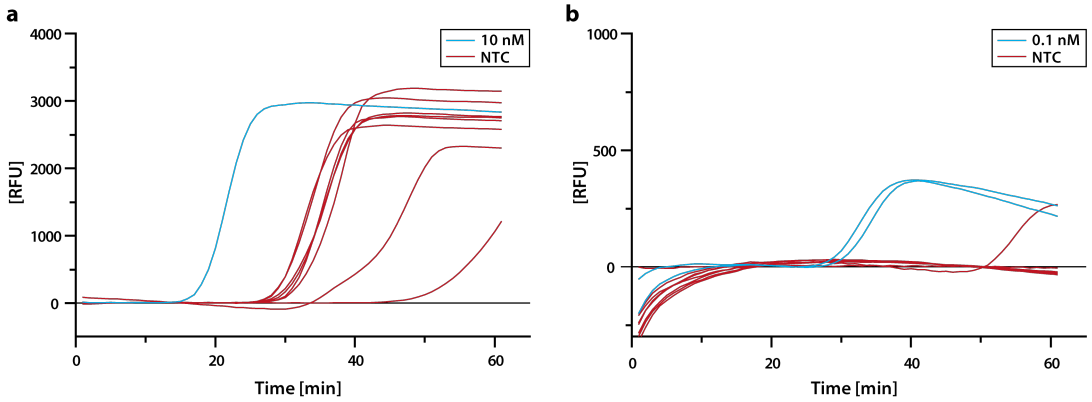

Figure 25: Representative results for real-time monitoring of the LAMP with SYBR green I in realtime cycler. a) LAMP Assay using the conditions reported by Tanner *et al.* with Bst 2.0 DNA polymerase at 65°C, 0.2/0.4/1.6 µM outer/loop/inner primers, 8 mM $MgSO_4$ and 350 µM dNTP each. b) Optimized conditions with Isotherm2G DNA Polymerase at 55°C, 0.2/0.4/1.6 µM outer/loop/inner primers, 2 mM $MgSO_4$ and 200 µM dNTP each.

To ensure that this behavior was not caused by a contamination with LAMP target, the experiment was repeated several times with freshly prepared reagents. However, amplification of non-template controls was persistent in all runs. Melting point analysis of the samples did not yield any conclusions in regard to the source of this behavior with some false positives ranging around the positive control and others at completely different temperatures. Similar issues were reported in other studies with persistent non-template amplification in LAMP assays[195-197].

To overcome these issues, a screening of LAMP conditions was carried out including different DNA polymerases, incubation temperatures, primer ratios and concentrations of dNTPs, Mg^{2+}, SYBR green I and betaine. In the end, the assay conditions were changed to Isotherm2G DNA polymerase, 55°C reaction temperature, 200 µM dNTP each with SYBR green I and remaining primer concentrations at their original levels (0.2/0.4/1.6 µM outer/loop/inner primer). Primers were denatured prior to the addition to the master mix in order to minimize the effect of primer dimers or the presence of any self-primed secondary structures. With the optimized conditions, 0.1 nM of the ligated LAMP target were detected at Cq 28 with no to minimal false positive reactions, which amplified at sufficiently delayed time points (Cq 51, Figure *25b*).

In order to reduce possible unspecific binding of dT$^{15\text{LAMP}}$TP and to improve the washing steps of the assay as well as the practicability, streptavidin coated 8-well plates were used as the solid phase. These plates have been tested with HRP-conjugates, yielding similar results as the streptavidin coated beads. However, the plates do not allow real-time monitoring of the reaction. Therefore, an endpoint readout by agarose gel electrophoresis had to be used.

Starting, the wells were incubated with 5' biotinylated primer in PBS and subsequently blocked with (+)-biotin. After several washing steps, 50 µl of PEx reaction mixture was added containing 100 nM *KlenTaq* DNA polymerase, 1 µM dT$^{16\text{LAMP}}$TP and 200 nM BRAF template (Figure *26a*, lane 1). Controls were set up without BRAF template (lane 2) or with dTTP instead of the LAMP target modified nucleotide (lane 3). Following 30 mins of incubation at 55°C in a monitored water bath, the reaction mixture was removed. After the plates were washed intensively with 1x *KlenTaq* reaction buffer, PBS buffer, deionized water and 1x Isotherm2G reaction buffer, the LAMP reaction mixture was applied. Furthermore, an additional sample (lane 4) was treated equally as the other samples but was incubated in plain 1x *KlenTaq* reaction buffer instead of a PEx reaction mixture. Here, the LAMP reaction was spiked with 2 nM of LAMP target to serve as a positive control. The LAMP reaction was incubated at 55°C in the water bath for 20 mins and stopped by rapid cooling of the wells in ice water. Samples were taken and directly subjected to 2.5% agarose gel electrophoresis.

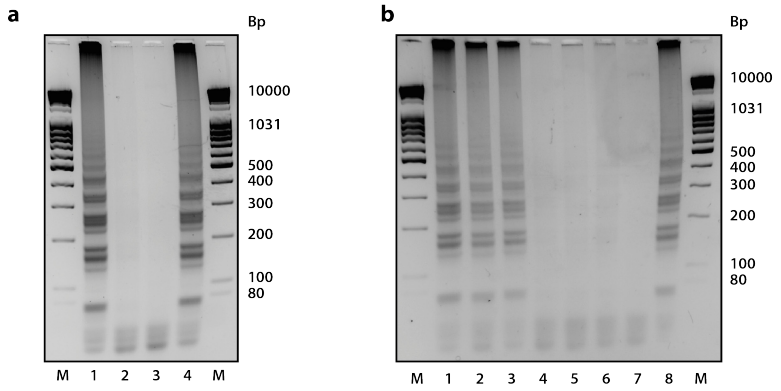

Figure 26: Agarose gels of PEx-based LAMP detection of DNA targets. A PEx reaction as depicted in *Figure 24b* employing a LAMP target conjugated dTTP derivative and *KlenTaq* DNA polymerase was performed on a immobilized primer in presence or in absence of the matched PEx template. Subsequently, the wells were washed and a LAMP reaction mixture was added. Samples of each well were taken and analyzed on a 2.5% agarose gel. Picture colors were inverted to improve contrast. a) Result for the assay with **1:** 200 nM (10 pmol) matched BRAF template, **2:** no BRAF template, **3:** 200 nM BRAF template but natural dTTP instead of dT^{15LAMP}TP, **4**: no PEx reactions but LAMP reaction spiked with LAMP target sequence as a positive control, **M:** marker. b) Determination of the current LOD. Assay was performed as in a with **1:** 200 nM/10 pmol template, **2:** 20 nM/1 pmol, **3:** 2 nM/100 fmol, **4:** 0.2 nM/10 fmol, **5:** 20 pM/1 fmol, **6:** no template, **7:** natural dTTP, **8:** target spiked LAMP control, **M:** marker.

On the agarose gel, a ladder-like pattern of bands was observed for well 1 (Figure *26a*). The pattern is consistent with the positive control in well 4, which proves the specific amplification of the LAMP target. No amplification was observed for both negative controls 2 and 3. Hence, a LAMP reaction can be utilized to detect the presence of a PEx template using LAMP target-conjugated dTTP derivatives.

However, the detection limit of the assay as it stands was found to be way higher than expected for a LAMP assay (Figure *26b*). Using the same conditions as in Figure *26a*, the assay was only viable to detect 100 fmol of the BRAF template used in the primer extension (Figure *26b*, lane 3) and thus is around 20-fold less sensitive than the HRP-based assay. As LAMP has been reported to enable the detection in the low two digit range of target sequence copy numbers, the shortfall in sensitivity observed here is most likely caused by a lack of optimization. First, due to the issue with non-template amplification, the LAMP reaction times are kept low with only 20 min of amplification. The real-time experiments displayed in Figure *25b* show that with optimized conditions, the exponential phase of the amplification of 0.1 nM LAMP target is observed at around 29 min. Therefore, the threshold of a maximum of 10 nM of dTTP-conjugated LAMP target (when a 1:1 conversion of BRAF template to conjugate incorporation is assumed) seen in the LOD assay is consistent with the real-time data. Further optimization of the LAMP

assay is therefore strongly needed to avoid the amplification in any non-template controls and thus enable longer incubation times.

Second, the general approach of the assay includes the employment of a vast amount of LAMP target in the sample. Due to the sensitivity of LAMP, an amplification will be observed as soon as small trace amounts of the conjugate are not removed by the washing steps or are covalently immobilized by misincorporation by the DNA polymerase. Thus, reaction and washing conditions would have to be thoroughly screened in order to minimize this risk.

Finally, the use of an endpoint readout is not desirable for the assay because it does not allow to differentiate between early and late amplification as e.g. in template vs. non-template reactions. Real-time monitoring could be accomplished by running the assay in a plate reader with a suitable fluorescence detector for SYBR green I detection. Additionally, several techniques have been reported for the real-time monitoring of LAMP reactions that do not rely on complex machinery. Among those, the detection by pH sensitive dyes in low-buffered reaction solutions is among the most interesting, as it provides a clear and easy readout via the naked eye. The employment of such a real-time readout would moreover immensely ease the optimization of the assay.

In summary, a LAMP target sequence derived from the genome of the Lambda phage was generated and conjugated to an azide-functionalized dTTP derivative via click chemistry. PEx experiments with the LAMP conjugate revealed that *KlenTaq* DNA polymerase is able to incorporate the modified nucleotide into a primer strand in spite of the length of the attached oligonucleotide. As in the experiments with HRP-conjugated nucleotides, dT$^{15\text{LAMP}}$TP was employed in solid phase primer extension reactions in which the modification should serve as reporter for the presence of the PEx template. Amplification in the adjacent LAMP reaction was thereby only observed if the PEx template was added to the PEx reaction and hence the assay setup successfully combined the robustness and simple setup of PEx based assays with the rapid and sensitive amplification of LAMP. However, the full potential of LAMP could not be exploited as the permanent occurrence of non-template amplification restricted the assay to short incubation times and thus led to a LOD that is around 20-fold higher than for the HRP-based assay. Further optimization will therefore have to address the specificity issues with the LAMP assay as well as the washing procedure and the readout used on the solid support.

4 – Summary and Outlook

Synthetically modified nucleotides are crucial for many biotechnological applications.[84, 93, 100, 109-110] When employed in DNA polymerase catalyzed reactions, the attributes of the modification can be used to draw conclusions about e.g. the sequence of the template strand or for the enrichment of specific nucleic acids. Key to this approach is the premise that the modified nucleotide is still accepted as a substrate by DNA polymerases albeit their evolutionary 'training' to process the natural substrates with high fidelity. Crystallographic studies were able to show, that modifications placed on the C5-position of pyrimidine and the C7 position of deaza-purines can be encompassed by a channel within the DNA polymerase which minimizes the perturbation in processing caused by the spatially more demanding nucleotide. This channel directly connects the active site of the DNA polymerase with its surface.[114-115] Hence, a linker between the nucleotide and the modification, which spans the length of the channel, allows the usage of bigger modifications.[84, 120] In this regard, nucleotides modified with small single-stranded DNA fragments have been reported.[86, 168] Additionally, the untemplated addition of protein-modified nucleotides to the 3' of a DNA strand by a terminal transferase has been demonstrated by Sørensen and coworkers.[121] However, this incorporation randomly extends single stranded DNA and therefore does not allow any conclusions about the employed DNA strand.

To elucidate the size limitations of synthetic modifications in reactions catalyzed by replicative DNA polymerases, macromolecule-conjugated nucleotides should be synthesized and employed in PEx experiments. The attributes of the macromolecule should then be harnessed as a readout for the incorporation that is visible without any training or machinery.

In a first effort, thymidine derivatives with thiol-functionalized alkyl linkers were synthesized. The linkers differed in length to study the influence of the span on the incorporation behavior. Utilizing the Michael reaction, the nucleotides were coupled to maleimide-functionalized Horseradish peroxidase, a glycosylated 44 kDa plant enzyme.[150-152] After purification by IEX-FPLC, the chimeric protein-nucleotide hybrids retained their enzymatic activity. The two conjugates with the shortest and the longest linker (dT^{7HRP}TP and dT^{15HRP}TP) were subsequently employed in PEx reaction with the A-family DNA polymerases *KlenTaq* and *KF exo*$^-$. Both incorporated the two nucleotides despite them being several orders of magnitude larger than the natural substrate. A clear bias towards the longer linker was observed when compared to natural dTTP in competition experiments where dT^{15HRP}TP was processed 5.5-fold better than dT^{7HRP}TP by KTq DNA polymerase and 3.2-fold better by *KF exo*$^-$ DNA polymerase. This indicated

that a longer linker facilitates the incorporation as more spacing between the two enzymes provides a higher degree of flexibility. Incorporation was in total higher for *KlenTaq* DNA polymerase than for *KF exo*⁻ DNA polymerase possibly caused by less structural interference and more conformational dynamics at the elevated reaction temperature (55°C vs 37°C). For dT^{15HRP}TP the incorporation on basis of a RNA template was shown utilizing a *KlenTaq* variant with reverse transcriptase activity (RT-*KTq*).[58]

Knowing that the conjugates can be processed by replicative DNA polymerases, the better accepted conjugate dT^{15HRP}TP was employed in PEx experiments with a streptavidin-bead immobilized primer strand.[169] Here, the incorporation of the modified nucleotide leads to a covalent attachment of the enzyme to the solid support. Following the PEx reaction, all unbound conjugate can hence be removed by filtration and the bound enzyme can be detected by the addition of a colorigenic substrate solution. Due to the sequence specificity and the template dependency of the employed DNA polymerase, a signal should only be observed in case a matched template is present in the reaction mixture.

With dT^{15HRP}TP, the addition of an HRP dye solution allowed the detection of amounts as low as 5 fmol of the template sequence by the naked eye for KTq and *KF exo-* DNA polymerase with strong discrimination against a T:T mismatched template. When using RT-KTq, the assay was moreover also able to detect RNA targets. The specificity of the approach was thereby demonstrated by the detection of femtomole amounts of *E. coli* 16S rRNA in the presence of an excess of human RNA.

Harnessing the difference in incorporation opposite RNA bases equipped with epigenetic markers, the assay allowed to sense the presence of a single methyl group in the sequence of human 18S rRNA, which could in future be used as a method for the fast and direct sensing of methylation sites.[81, 185]

Considering the transition to a more practical solid phase that does not require a filtration by centrifugation, the proposed assay could theoretically be conducted with very little to no machinery in less than an hour and would therefore meet the criteria raised by POC testing.[135-138] However, several drawbacks would have to be faced in advance:

First, unspecific binding of the conjugates restrains the lower limit of detection and thus hampers the detection of target sequences in lower concentrations. Second, to achieve the detection of clinically relevant amounts of nucleic acid targets, the signal provided by a single HRP incorporation per target sequence is insufficient. Therefore, either a signal amplification (e.g. a HRP multimer attached to the nucleotide[199]) or a multiple incorporation of the conjugates would be necessary. The feasibility of multiple incorporation of the conjugates was shown for *KlenTaq* DNA polymerase where at least four of the

conjugates equipped with the longest linker could be incorporated even in a consecutive fashion. No multiple incorporation was observed for the shorter linker, suggesting that the extra spacing is important to decrease spatial interference of the two enzymes. However, an attempted multiple incorporation on the *E. coli* 16S rRNA did not yield any increase in signal intensity, which is most likely caused by the presence of a stem loop close to the primer binding site. Due to the lacking strand displacement ability of RT-*KTq* DNA polymerase, the primer extension most likely stalls when encountered with the stem loop. This directly points to the third drawback: The streptavidin-coated sepharose beads do not support heating to high temperatures. Therefore, no annealing step can be performed on the beads and the assay as it stands now and thus it is limited to single-stranded DNA and RNA targets.

To overcome these drawbacks, the assay would have to optimized in several regards. Most importantly, a solid support and washing procedure that reduces the unspecific binding of the conjugates is desired to enable longer incubation and detection times and thus allow for the whole potential of HRP to unfold. If this solid support would also tolerate denaturation conditions and thus enable the detection of double stranded targets with a reliable multiple incorporation, HRP-conjugates could become relevant for diagnostic purposes. So far multiple solid supports have been evaluated but have shown their own individual draw backs which rendered them unsuitable for the improvement of the assay. Annealing of the biotinylated primer with the target prior to the immobilization could provide access to double stranded targets but would necessitate the purification of the nucleic acid samples as the biotin found e.g. in blood serum could block the beads.[200] Furthermore, the employment of DNA polymerases with strand displacement activity could help to overcome double stranded structures such as stem loops in multiple incorporation.

To circumvent some of these issues an alternative approach was tested using a dATP derivative directly coupled to a glass slide as the modified nucleotide. Here the C16-linker on nucleotide combined with the hydrogel spacers of the glass slide allowed the incorporation of nucleotide despite it being attached to a macroscopic object by its nucleobase. The biotinylated primer, which is immobilized by the incorporation of the nucleotide, was then detected via a colorigenic reaction after the addition of a streptavidin-HRP. However, this approach suffered from its own drawbacks and the laborious handling of the slides and ultimately failed to improve the LOD.

Finally, in order to show the versatility of the approach as well as to increase the sensitivity, dTTP analogs coupled to a 184-mer single stranded DNA sequence were synthesized. The sequence derived from the Lambda phage genome served as the target of a loop-mediated isothermal amplification assay.[189-190]

Unlike in the direct amplification of a target sequence by LAMP, the nucleotide-target conjugate was used in a PEx based approach to sense the presence and sequence of the PEx template. This way, the laborious set up of LAMP assays for each individual target with the sophisticated primer design and need for extensive optimization would be substituted by an easy to set up and adapt PEx assay in which a single, robust LAMP assay would serve as the readout.

The target-nucleotide conjugate was successfully incorporated by *KlenTaq* DNA polymerase in PEx experiments in solution as well as on a solid support, where, similar to the HRP in the first effort, the cargo was used as a reporter for the PEx reaction. However, the LAMP assay used to detect the covalently bound target sequence suffered from poor specificity in solution. Even after thorough optimization, false-positive amplification was observed regularly. Therefore, the amplification times in experiments with immobilized primers had to be limited and thus, with a detection limit 20-fold higher than with the HRP-conjugates, the approach so far did not result in the increased sensitivity that was envisioned. The use of a more reliable LAMP assay as well as the employment of more practicable readout mechanisms could greatly improve the approach. However, the general assay design comes with a risk since a comparably large amount of LAMP target is added to each well in the PEx reaction. Insufficient washing and unspecific binding would therefore also lead to the observation of 'false'-positives. Hence, the washing protocols will have to be carefully worked out to ensure complete removal of unbound conjugates.

In general, a size limit of nucleotide modifications seems non-existent, provided that a linker of sufficient length is used to diminish any interference of the cargo with the DNA polymerase. With further optimizations, PEx based approaches employing modified nucleotides with large, functional cargos could be of relevance for diagnostic approaches as they are a robust, simple and fast platform that allows a readout by the naked eye.

Aside from the diagnostic PEx application demonstrated in this work, the direct introduction of large modifications into DNA is also of importance to other areas of research. For example, proteins are frequently used for the functionalization of DNA nanostructures.[201-203] Here, the controllable and predictable folding of DNA scaffolds can be used e.g. to study the influence of the spacing on protein interaction and activity, a scenario in which accurate placing of the functionalities is indispensable.[204]

DNA-DNA conjugates, as generated in the LAMP project, can be used as barcodes in screening approaches[86], as amplifier probes in branched DNA assays[205] or as branching points in DNA hydrogels[206].

Additionally, DNA-functionalized nanoparticles have emerged in several fields of research including "(bio)sensing, labeling, targeted imaging, cellular delivery, diagnostics, therapeutics, theranostics, bioelectronics, and biocomputing to name just a few amongst many others".[207]

Most methods applied so far for the generation of DNA with large modifications include non-covalent binding via antibodies and aptamers or two-step procedures in which functionalized nucleotides are incorporated and subsequently reacted with activated macromolecules.[203, 208-210] The ability to directly incorporate conjugates enzymatically enables the site-specific introduction of proteins and other large conjugates in one step and thus can help to simplify the generation of the aforementioned hybrids.

5 - Zusammenfassung und Ausblick

Synthetisch modifizierte Nukleotide sind für viele biotechnologische Anwendungen unabdingbar.[84, 93, 100, 109-110] Wenn sie in von DNA-Polymerasen katalysierten Reaktionen eingesetzt werden, können über die Eigenschaften bestimmter Modifikationen z.B. Rückschlüsse über die Sequenz des Templatstrangs gezogen oder eine bestimmte Zielsequenz angereichert werden. Voraussetzung ist, dass die modifizierten Nukleotide von DNA-Polymerasen weiterhin als Substrat erkannt werden, obwohl diese Enzyme faktisch im Laufe ihrer Evolution dahingehend optimiert wurden, natürlich vorkommende Substrate mit hoher Selektivität einzubauen. Mit Hilfe von Kristallographiestudien konnte gezeigt werden, dass sich Modifikationen an der C5-Position von Pyrimidinen oder der C7-Position von Deazapurinen in Kanäle im Inneren der DNA Polymerase fügen können, was störende Einflüsse bei der Prozessierung der deutlich vergrößerten Nukleotide minimiert. Diese Kanäle verbinden das aktive Zentrum der DNA-Polymerase direkt mit seiner Oberfläche.[114-115] Wenn sich also zwischen Nukleotid und Modifikation ein Linker von einer solchen Länge befindet, dass die gesamte Länge des Kanals überbrückt werden kann, ist theoretisch auch die Nutzung von großen Modifikationen möglich.[84, 120] In diesem Zusammenhang wurde bereits der Einbau von Nukleotiden beschrieben, welche mit kurzen, einzelsträngigen DNA-Fragmenten gekoppelt waren.[86, 168] Darüber hinaus wurde von Sørensen und Mitarbeitern auch die templatunabhängige Addition von Protein-modifizierten Nukleotiden an das 3‘-Ende von DNA-Strängen durch eine terminale Nukleotidyltransferase beschrieben.[121] Da dieser Einbau jedoch das Ende des DNA Einzelstrangs willkürlich verlängert, lässt sich dieser Ansatz nicht dazu nutzen, Rückschlüsse über die Sequenz des DNA-Strangs zu ziehen.

Um die Größenbeschränkung von synthetischen Modifikationen in durch replikative DNA-Polymerasen katalysierten Reaktionen zu ermitteln, sollten Makromolekül-konjugierte Nukleotide synthetisiert und in Primerverlängerungsreaktionen (PEx-Reaktion) eingesetzt werden. Im Anschluss sollte über intrinsische Eigenschaften des Makromoleküls ein Readout für die Reaktionen etabliert werden, der ohne jegliche Schulung oder Geräte deutbar ist.

Im ersten Ansatz wurden dazu Desoxythymidinanaloga (dTTP-Analoga) mit Thiol-funktionalisierten Alkyllinkern synthetisiert. Die Analoga unterschieden sich dabei in der Länge des Alkyllinkers, um eine Untersuchung des Einflusses der Linkerlänge auf das Einbauverhalten des Nukleotids zu ermöglichen. Mit Hilfe der Michaelreaktion wurden die Nukleotide an Maleimid-funktionalisierte Meerrettichper-

oxidase (Horseradish Peroxidase, HRP) gekoppelt.[150-152] Auch nach der Aufreinigung durch Ionenaustauschchromatographie konnten die so entstandenen Chimäre aus 44 kDa Glycoprotein und Nukleotid dabei ihre Aktivität beibehalten. Die zwei Nukleotide mit dem kürzesten und dem längsten Linker (dT^{7HRP}TP and dT^{15HRP}TP) wurden anschließend zusammen mit den DNA-Polymerasen der A-Familie, *KlenTaq* und *KF exo*$^-$, in PEx-Reaktionen eingesetzt. Obwohl die modifizierten Nukleotide mehrere Größenordnungen größer sind als die natürlichen Substrate, konnten sie von beiden DNA-Polymerasen eingebaut werden. In Kompetitionsexperimenten mit natürlichem dTTP wurde weiterhin beobachtet, dass das Nukleotid mit dem längeren Linker von den DNA-Polymerasen bevorzugt wird. Hier wurde dT^{15HRP}TP im Falle der *KlenTaq* DNA-Polymerase 5,5-mal besser akzeptiert als dT^{7HRP}TP. Im Falle der *KF exo*$^-$ DNA-Polymerase wurde dT^{15HRP}TP 3,2-mal besser akzeptiert als dT^{7HRP}TP. Dies legt nahe, dass ein längerer Linker den Einbau des Nukleotids vereinfacht, da der größere Abstand beiden Enzymen das System flexibler macht. Generell wurde für *KlenTaq* DNA-Polymerase höhere Einbauraten beobachtet als für *KF exo*$^-$ DNA-Polymerase, was vermutlich sowohl an geringeren strukturellen Interferenzen als auch an der größeren Komformationsdynamik bei erhöhten Temperaturen liegt (55°C vs. 37°C). Für dT^{15HRP}TP wurde außerdem der Einbau auf Basis eines RNA-Templates mit Hilfe einer *KlenTaq* DNA-Polymerase, welche über Reverse Transkriptase-Aktivität verfügt (RT-*KTq*), gezeigt.[58]

Mit dem Wissen, dass die Konjugate von replikativen DNA-Polymerasen prozessiert werden können, sollte das besser akzeptierte Konjugat dT^{15HRP}TP in PEx-Reaktionen eingesetzt werden bei denen der Primerstrang auf Streptavidin-funktionalisierten Sepharosekügelchen immobilisiert ist.[169] Dabei führt der Einbau des modifizierten Nukleotids zu einer kovalenten Bindung des Enzymes an die Festphase. Nach der PEx-Reaktioen kann daher alles ungebundene Konjugat durch Filtration entfernt und das gebundene Enzym durch eine farbgebende Substratlösung detektiert werden. Durch die Sequenzspezifität und die Templatabhängigkeit der verwendeten DNA-Polymerase sollte somit nur dann eine Farbentwicklung beobachtet werden können, wenn das Templat mit der korrekten Sequenz in der Reaktionslösung enthalten ist.

Mit Hilfe von dT^{15HRP}TP wurden nach Zugabe des Farbreagenz für *KlenTaq* DNA-Polymerase und *KF exo*$^-$ DNA-Polymerase Mengen von nur 5 fmol der Templatsequenz verlässlich detektiert, wobei eine klare Unterscheidung zwischen der korrekten Basenpaarung an der Einbaustelle und einer möglichen T:T-Fehlpaarung möglich war. Die Verwendung der RT-*KTq* DNA-Polymerase erlaubte zusätzlich die Detektion von RNA-Sequenzen. Die Spezifität des Tests wurde hier durch die Detektion von Femtomol-Mengen an *E. coli* 16S rRNA in der Gegenwart eines Überschusses an menschlicher RNA gezeigt.

Das unterschiedliche Einbauverhalten gegenüber RNA-Basen, welche epigenetische Marker tragen, konnte dafür verwendet werden, die Anwesenheit einzelner Methylgruppen in menschlicher 18S rRNA aufzuzeigen. Dies könnte in Zukunft als Methode zur schnellen und direkten Identifizierung von Metyhlierungsstellen genutzt werden.[81, 185]

Wenn man den Wechsel auf eine praktikablere Festphase voraussetzt, die keine Filtration durch Zentrifugation bedingt, könnte der Test theoretisch mit einem Minimum an bzw. ohne Geräte in unter einer Stunde durchgeführt werden und würde somit die Kriterien für POC-Testverfahren erfüllen.[135-138] Hierfür müsste das System allerdings in mehreren Punkten optimiert werden:

Zum einen beeinträchtigt die unspezifische Bindung der Konjugate an die Festphase das Detektionslimit und verhindert somit die Detektion der Zielsequenzen in geringeren Konzentrationen. Zum andern ist das Signal, welches durch einen einzelnen Einbau einer HRP pro Zielsequenz erzeugt wird, zu gering um die Detektion von klinisch relevanten Proben zu erlauben. Daher wäre entweder eine Signalamplifikation (z.B. durch ein an das Nukleotid gekoppeltes HRP-Multimer[199]) oder der mehrfache Einbau der Konjugate notwendig. Die Durchführbarkeit eines Mehrfacheinbaus wurde für *KlenTaq* DNA-Polymerase gezeigt. Hier wurden mindestens vier der Konjugate mit dem längsten Linker eingebaut und das überdies sogar direkt aufeinanderfolgend. Für den kürzeren Linker konnte kein Mehrfacheinbau beobachtet werden. Dies bedeutet, dass der zusätzliche Abstand zwischen beiden Enzymen wichtig ist, da er die räumliche Beeinträchtigung minimiert. Ein versuchter Mehrfacheinbau in einem Experiment mit *E. coli* 16S rRNA lieferte jedoch keinen Anstieg der Signalintensität, was sehr wahrscheinlich durch das Vorkommen einer Haarnadelstruktur kurz nach der Bindestelle des Primers zu erklären ist. Durch die fehlende Strangverdrängungsaktivität der verwendeten RT-*KTq* DNA-Polymerase stockt die Primerverlängerung sobald sie die Haarnadelstruktur erreicht. Hier wird auch der letzte Nachteil des Tests deutlich: Die verwendeten, Streptavidin-beschichteten Sepharosekügelchen können nicht auf hohe Temperaturen erhitzt werden. Daher kann auf den Kügelchen vor dem Test kein Annealingschritt vollzogen werden, weshalb der Test momentan auf einzelsträngige DNA- und RNA-Zielsequenzen beschränkt ist.

Um diese Nachteile zu überwinden, müsste das Nachweisverfahren in vielerlei Hinsicht optimiert werden. Hier wären vor allem eine Festphase und ein Waschverfahren wünschenswert, die die unspezifische Bindung der Konjugate minimieren. Dies würde längere Inkubations- und Detektionszeiten ermöglichen und so das volle Potential der HRP erschließen. Wenn diese Festphase dann zusätzlich die Denaturierung der Proben bei hohen Temperaturen tolerieren und somit die Detektion von doppelsträngigen

Sequenzen mitsamt verlässlichem Mehrfacheinbau ermöglichen würde, könnten HRP-Konjugate in Zukunft an Revelanz für diagnostische Verfahren gewinnen. Die Evaluation mehrerer Festphasen erbrachte jedoch, dass diese wiederum ihre eigenen, individuellen Nachteile besitzen, welche sie für die Verbesserung des Nachweisverfahrens unbrauchbar machten.

Das Annealen der biotinylierten Primer an die Zielsequenz vor der Immobilisierung könnte doppelsträngige Zielsequenzen zugänglich machen, würde aber die vorherige Aufreinigung der Nukleinsäureproben erfordern da das natürliche Biotin, welches z.B. in Blutserum zu finden ist, die Streptavidinmoleküle auf der Oberfläche der Kügelchen blockieren könnten.[200] Darüber hinaus könnte der Einsatz von DNA-Polymerasen mit Strangverdrängungsaktivität dabei helfen doppelsträngige Abschnitte wie zum Beispiel Haarnadelstrukturen beim Mehrfacheinbau zu überwinden.

Um einige der Probleme zu umgehen, wurde ein alternativer Ansatz getestet, in dem ein an eine Glasoberfläche gekoppeltes dATP-Analog als modifiziertes Nukleotid verwendet wurde. Der enthaltene C16-Linker in Kombination mit den Hydrogelspacern der Glasplatte ermöglichte dabei den Einbau des Nukleotids, ungeachtet der Tatsachsache, dass ein makroskopisches Objekt an die Nukleobase gebunden ist. Der biotinylierte Primer, welcher durch den Einbau des Nukleotids immobilisiert wird, konnte anschließend nach der Zugabe von Streptavidin-funktionalisierter HRP durch eine Farbreaktion detektiert werden. Die aufwendige Handhabung der Glasplatten und die Tatsache, dass das Detektionslimit mit diesem Ansatz nicht gesenkt werden konnte führte jedoch zur Aufgabe dieser Strategie.

Um die Vielfältigkeit des PEx-Ansatzes zu verdeutlichen und gleichzeitig die Sensitivität zu erhöhen, wurden letztendlich dTTP-Analoga synthetisiert, an die ein 184mer einer einzelsträngigen DNA Sequenz gekoppelt war. Diese Sequenz, welche aus dem Genom der Lambdaphage stammt, sollte anschließend als Templat einer ‚loop-mediated isothermal amplification'-Reaktion (LAMP-Reaktion) dienen.[189-190] Im Gegensatz zur direkten Amplifikation der Zielsequenz durch LAMP wurde das DNA-Nukleotid-Konjugat zunächst in einem PEx-basierten Ansatz eingesetzt, um die Präsenz und die Sequenz des PEx-Templats zu ermitteln. Auf diese Art und Weise würde die aufwendige Etablierung der LAMP-Reaktion für jede Zielsequenz mit seinem komplexen Primerdesign und der notwendigen, ausführlichen Optimierung durch die sehr leicht zu etablierende und flexible PEx-Reaktion ersetzt werden. Somit könnte eine einzige, robuste LAMP-Reaktion als Readout dienen.

Das DNA-Nukleotide-Konjugat wurde in PEx-Reaktionen sowohl in Lösung als auch auf der Festphase erfolgreich durch *KlenTaq* DNA-Polymerase eingebaut. Hierbei diente, ähnlich zur HRP, die Modifikation wieder als Reporter für die PEx-Reaktion. Die LAMP-Reaktion wies dabei zunächst in Lösung eine sehr geringe Spezifität auf, sodass sogar nach eingehender Optimierung häufig falsch-positive Reaktionen erhalten wurden. Aus diesem Grund musste die Reaktionszeit in den Experimenten auf Festphase begrenzt werden und der Ansatz erreichte mit einem Detektionslimit, welches 20-fach höher als das der HRP-Konjugate lag, nicht die erhoffte bessere Sensitivität.

Die Verwendung eines verlässlicheren LAMP-Systems in Kombination mit einem praktikablerem Readout könnte diesen Ansatz hier deutlich verbessern. Dieser birgt jedoch generell ein hohes Risiko, da im PEx-Schritt hohe Mengen der LAMP-Sequenz in jedes Reaktionsgefäß gegeben werden müssen. Unzureichende Waschschritte sowie unspezifische Bindung können daher das Auftreten von ‚falsch-positiven' Reaktionen stark begünstigen. Die Waschschritte müssen daher sehr sorgfältig ausgearbeitet werden, um das vollständige Entfernen der ungebundenen Konjugate zu gewährleisten.

Unter der Voraussetzung, dass ein Linker von ausreichender Länge verwendet wird, scheint eine Größenbeschränkung für modifizierte Nukleotide in DNA-Polymerasen basierten Reaktionen nicht zu existieren. Nach weiteren Optimierungen könnten PEx-basierte Ansätze, in denen Nukleotide mit großen, funktionellen Makromolekülen eingesetzt werden, an Relevanz für diagnostische Verfahren gewinnen, da sie ein robustes, einfaches und schnelles Nachweisverfahren verkörpern, das einen Readout mit bloßem Auge ermöglicht.

Neben den diagnostischen Ansätzen, die in dieser Arbeit vorgestellt wurden, ist die Möglichkeit, große Modifikationen enzymatisch direkt in DNA einzuführen, auch für andere Forschungszweige entscheidend. Beispielsweise werden Proteine häufig für die Funktionalisierung von DNA-Nanostrukturen genutzt.[201-203] Dabei kann die kontrollierte und vorhersehbare Faltung des DNA-Gerüsts unter anderem dazu dienen den Einfluss des Abstands auf die Interaktion und Aktivität von Proteinen zu erforschen; ein Szenario für das die punktgenaue Einbringung der Funktionalitäten unabdingbar ist.[204]

DNA-DNA-Konjugate, wie sie im LAMP-Projekt hergestellt wurden, können als Strichcode in Screeningansätzen verwendet werden[86], als Verstärkersonde in ‚branched DNA'-Verfahren[205] oder als Verzweigungspunkte in DNA-Hydrogelen.[206]

Darüber hinaus haben DNA-funktionalisierte Nanopartikel in viele Forschungsfelder Einzug gefunden, darunter „unter anderem Biosensing, die Kennzeichnung von Nanopartikeln, zielgerichtete Bildgebungsverfahren, die zellgenaue Verabreichung von Medikamenten, die Diagnostik, die Therapie und Theranostik, Bioelektronik sowie Biocomputing“.[207]

Viele Methoden, die bisher für die Herstellung von DNA-Konjugaten mit großen Modifikationen verwendet wurden, nutzen die nichtkovalente Bindung über Antikörper und Aptamere oder zweistufige Verfahren, in welchen chemisch funktionalisierte Nukleotide eingebaut werden, die nachträglich mit den aktivierten Makromolekülen zur Reaktion gebracht werden.[203, 208-209] Die Möglichkeit solche Konjugate direkt enzymatisch einzubauen, gestattet daher Proteine und andere große Modifikationen sequenz-spezifisch in nur einem Schritt einzuführen und kann somit dabei helfen die vorher genannten DNA-Hybride einfacher herzustellen.

6 – Experimental Part

6.1 Chemical Synthesis

6.1.1 – Chemicals and buffers

Commercially available chemicals used for chemical synthesis were purchased in high purity (98%+) from Carbosynth, Sigma-Aldrich Chemie/Merck, TCI Chemicals, Arcos, Roth, VWR or ABCR GmbH and used without any prior purification. If not stated otherwise, the reactions were performed under the exclusion of air and moisture in anhydrous, HPLC grade solvents from Sigma-Aldrich and VWR.

TEAB buffer for IEX-FPLC purification

5 kg of dry ice are evaporated in a sealed 5 L plastic laboratory bottle. The gas is passed into a second 5 L laboratory bottle filled with approx. 3 L water and 5 mol NEt_3 (697 mmol) until the two phases have mixed and the pH falls below 8. The pH is then adjusted to 7.5 with acetic acid and the bottle is filled up to 5 L with MQ to give a 1 M TEAB buffer.

TEAA buffer for RP-HPLC purification

1 mol of acetic acid was diluted in approx. 600 ml of MQ water. 1 mol of triethylamine were slowly added to the solution and it was stirred for several minutes until it reached room temperature again. The pH was adjusted to 7 using acetic acid and the solution was filled up to 1 L to yield a 1 M triethylammonium acetate buffer (TEAA).

6.1.2 – Instruments and standard techniques

NMR spectroscopy

NMR spectra were recorded in deuterated solvents on either Bruker Avance III 600 or Bruker Avance III 400 spectrometers at room temperature. The data was analyzed with MestReNova NMR software Versions 12.0.3. The spectra were referenced using the undeuterated impurities of the deuterated solvents as an internal standard.[211]

Yield determination for nucleotides / UV/Vis-spectroscopy

Due to the presence of unknown amounts of water in the lyophilized nucleoside triphosphates, the yields were determined by UV/Vis-Spectrometry. The compounds were solubilized in an exact volume of MQ and absorbance was measured on a Nanodrop ND-1000 Spectrophotometer (PeqLab) in the nucleic acid mode. The concentration of the nucleotide solution was then calculated using the Lambert-Beer law with ε(290 nm) = 13300 for dTTP derivatives.

Bis(tributylammonium)pyrophosphate

In order to generate the Bis(tributylammonium)pyrophosphate used in triphosphate synthesis, a column packed with Amberlite IR-120 (proton form, Merck) was first washed until the flow-through reached a pH of 5. 10 mmol disodium pyrophosphate were then dissolved in 50 mL MQ and passed through the column. The flow-through was dropped into an ice-cold solution of 20 mmol tributylamine (2 eq., 4.8 mL) in 40 mL ethanol. After the flow-through reached a pH of 5 again, the ethanol solution was evaporated under reduced pressure, co-evaporated twice with 10 mL of ethanol, three times with 10 mL anhydrous DMF and finally the residue was diluted in 20 mL of anhydrous DMF to yield a 0.5 M solution of Bis(tributylammonium)pyrophosphate.

IEX-FPLC purification of compound 2

After the phosphorylation, the triphosphate species is purified on a Äkta Purifier FPLC System equipped with a DEAE sephadex A-25 column at 4°C. A gradient from 0.1 M TEAB buffer to 1 M TEAB buffer is applied and peaks are detected at 215, 254 and 280 nm by the internal UV-detector.

RP-HPLC purification of functionalized nucleoside triphosphates

HPLC purification of compounds **3-5** and **7** was accomplished on a Prominence HPLC System with preparative LC-20AP pumps (Shimadzu) and a Nucleodur RP-18 HTec column (16 mm diameter, Macherey-Nagel). The residue of the evaporation was applied as an aqueous solution and the reaction components were separated on a gradient running from 5% acetonitrile in 50 mM TEAA buffer to 100% acetonitrile in 50 mins at a flow of 8 ml/min.

IEX-HPLC purification of dT^{11}^{HRP}TP

IEX-HPLC of compound **4** was accomplished on a Prominence HPLC System with preparative LC-20AP pumps (Shimadzu) with a 250/4 DNAPac PA-100 from Dionex. A gradient was run from buffer A (25 mM Tris, pH 8) to buffer B (25 mM Tris, pH 8, 0.5 NaClO4, 1 ml/min flow rate).

Mass Spectrometry

ESI-HRMS data of compounds **3-5** and **7** were recorded on a Bruker microTOF II mass spectrometer in negative mode *via* direct inject. The obtained data was referenced to sodium formate clusters as an internal standard.

6.1.3 – Synthesis of 5-(trifluoroacetamidopentynyl)-2'-deoxyuridine 1[86, 146-147]

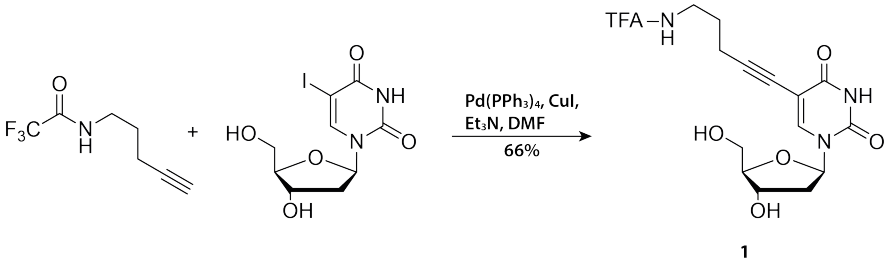

Figure 27: Synthesis of 5-(trifluoroacetamidopentynyl)-2'-deoxyuridine from 5-Iodo-2'-deoxyuridine.

500 mg of 5-iodo-2'-deoxyuridine (1.4 mmol) were placed in a 100 ml round bottom flask. 54 mg CuI (0.2 eq., 0.28 mmol) and 163 mg $Pd(PPh_3)_4$ (0.1 eq., 0.1 mmol) were added and the flask was flushed with inert gas on a Schlenck line. After the solids were dissolved in 20 ml dry DMF, 501 mg N-(4-pentynyl)-trifluoroacetamide (2 eq., 2.8 mmol) was added followed by 1.95 ml NEt_3 (10 eq., 14 mmol). The reaction was stirred at room temperature for 12 h before the solvent was removed under reduced pressure. The residue was purified by column chromatrography (0% to 10% MeOH in DCM) to yield 66% of compound **1** was a white solid**.**

^{1}H NMR (400 MHz, Methanol-d4): δ 8.28 (s, 1H, H-5), 6.28 (t, ^{3}J = 6.6 Hz, 1H, H-1'), 4.43 (dt, ^{3}J = 6.8, 3.6 Hz, 1H, H-3'), 3.97 (q, ^{3}J = 3.3 Hz, 1H, H-4'), 3.81 (dd, ^{2}J = 12.0 Hz, ^{3}J = 3.1 Hz, 1H, H-5'a), 3.74 (dd,

^{2}J = 12.0 Hz, ^{3}J = 3.5 Hz, 1H, H-5'b), 3.46 (t, ^{3}J = 7.0 Hz, 2H, -NHCH2-), 2.48 (t, ^{3}J = 7.0 Hz, 2H, -CH2CH2CCH-), 2.38 – 2.19 (m, 2H, H-2'), 1.86 (p, ^{3}J = 7.0 Hz, 2H, -CH2CH2CH2-). ^{13}C NMR (101 MHz, Methanol-d4): δ 151.3, 144.52, 118.96, 93.68, 89.09, 86.93, 72.03, 62.62, 41.65, 39.83, 28.58, 17.57.

R_f (MQ:MeCN 3:1) = 0.2

6.1.4 – Synthesis of 5-(aminopentynyl)-2'-deoxyuridine triphosphate 2

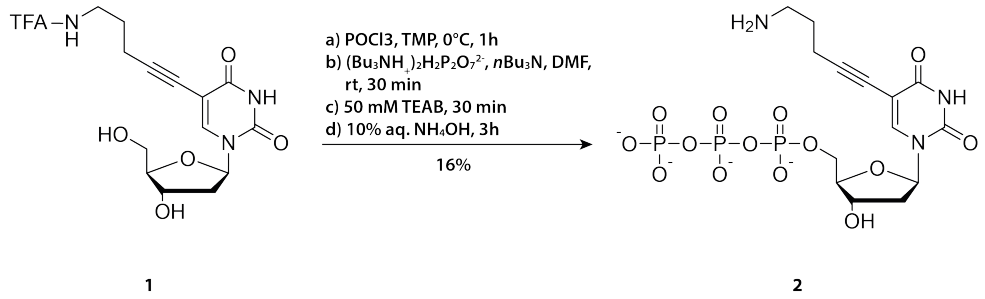

Figure 28: Triphosphate synthesis converting compound **1** to the deprotected nucleoside triphosphate **2**.

To a solution of 100 mg of compound **1** (247 µmol) and 77 mg proton sponge (1.5 eq., 370 µmol) in distilled 5 ml $POMe_3$, 26 µl (1.2 eq., 288 µmol) $POCl_3$ were added at 0°C. Following 1 h of stirring, 589 µl (10 eq., 2.47 mmol) tributylamine and 2.5 ml of a 0.5 M bis(tributylammonium)-pyrophosphate solution (5 eq., 1.24 mmol) were added simultaneously with syringes and the solution was allowed to reach room temperature during 30 min of stirring. The reaction was quenched by the addition of 10 ml 0.1 M TEAB buffer and 30 min of stirring. The reaction mixture was washed three times with 10 ml EE before the water phase was concentrated under reduced pressure. The residue was subjected to IEX-FPLC purification. Peaks containing the product (identified by MS) were pooled, lyophilized and stirred in 10% ammonium hydroxide for 3 h to remove the TFA protecting group. Subsequently, the deprotected nucleoside triphosphate was purified on RP-HPLC to yield 16% of compound **2** as determined with ε(290 nm) = 13300 $M^{-1}{\cdot}cm^{-1}$ in an aqueous solution on a Nanodrop ND1000 Spectrophotometer.

^{1}H NMR (400 MHz, D2O): δ 8.18 (s, 1H, H-6), 6.32 (t, ^{3}J = 6.6 Hz, 1H, H-1'), 4.69-4.63 (m, 1H, H-3'), 4.31-4.16 (m, 3H, H-4', H-5' a/b), 3.21 (q, ^{3}J = 7.3 Hz, 18 H, Et3N), 2.60 (t, 1H, ^{3}J = 6.4 Hz, 2H, -CH2CH2CH2NH-), 2.47-2.31 (m, 2H, H-2' a/b), 2.03-1.93 (p, ^{3}J = 6.8 Hz, 2H, -CH2CH2CH2NH-), 1.29 (t, 27 H, ^{3}J = 6.4 Hz, Et3N). ^{31}P NMR (162 MHz, D2O): δ -9.1 (d, ^{2}J = 20.1 Hz, Pγ), -11.36 (d, ^{2}J = 19.6 Hz, Pα), -22.4 (t, ^{2}J = 20.1 Hz, Pβ). HR-ESI-MS (m/z): $[M-H]^-$ = calcd: 548.0242; found: 548.0249.

6.1.5 – Synthesis of C5-thiol modified dTTP derivatives 3-5

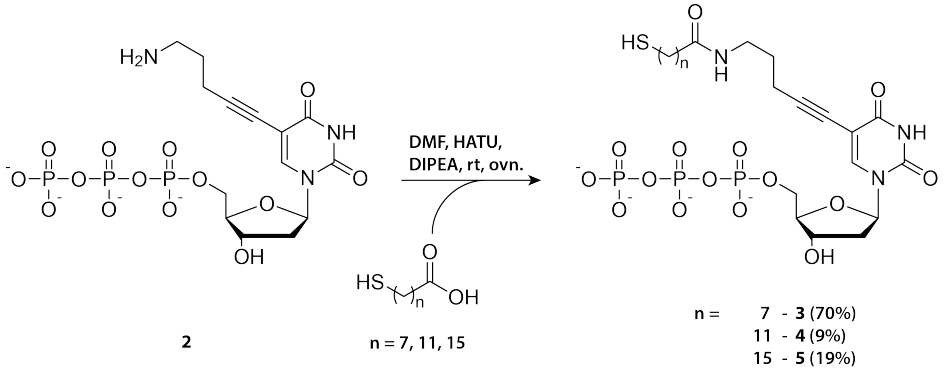

Figure 29: Conjugation of nucleoside triphosphate **2** with ω-thiol-alkyllinkers to yield compounds **3**-**5**.

To a solution of 25.0 µmol 5-(aminopentynyl)-2'-deoxyuridinetriphosphate tetrabutylammonium salt (**2**) in 1 ml DMF, 37.5 µmol (1.5 eq., 9.7 mg) of DIPEA were added. In parallel, 27.5 µmol (1.1 eq.) of the mercaptocarboxylic acid, 37.5 µmol (1.5 eq., 9.7 mg) DIPEA and 25 µmol HATU (1 eq., 9.5 mg) were dissolved in 1 ml DMF and stirred for 30 min. Both mixtures were then combined and stirred at room temperature for additional 12 h. The solvent was removed under reduced pressure and the residual oil was subjected to C_{18}-RP-HPLC (95% 50 mM triethylammonium acetate (TEAA) buffer to 100% MeCN). The yield was determined by Nanodrop ND1000 Spectrophotometer with ε(290 nm) = 13300 $M^{-1}{\cdot}cm^{-1}$. The compounds were diluted in MQ and kept as a stock solution at -20 °C.

5-(5-(8-mercaptooctanamido)pent-1-yn-1-yl)deoxyuridine 3:

Yield: 70% of **3** as triethylammonium salt.

^{1}H NMR (400 MHz, Methanol-d_4): δ 7.99 (s, 1H, H-C(6)), 6.24 (t, ^3J = 6.8 Hz, 1H, H-C(1')), 4.62–4.57 (m, 1H, H-C(3')), 4.32–4.26 (m, 1H, H-C(5'a)), 4.22-4.15 (m, 1H, H-C(5'b)), 4.09-4.05 (m, 1H, H-C(4')), 3.20 (q, ^3J = 7.3 Hz, 17H, -$CH_2CH_2CH_2$NH-, Et_3N), 2.48 (t, ^3J = 7.3 Hz, 2H, H-C(L8)), 2.44 (t, ^3J = 6.8 Hz, 2H, -$CH_2CH_2CH_2$NH-), 2.29-2.25 (m, 2H, H-2'), 2.20 (t, ^3J = 7.4 Hz, 2H, H-C(L2)), 1.77 (p, ^3J = 6.8 Hz, 2H, -$CH_2CH_2CH_2$NH-), 1.63-1.55 (m, 4H, H-C(L3+7)), 1.43-1.36 (m, 2H, H-C(L6)), 1.31 (t, ^3J = 7.1 Hz, 25H, H-C(L4-5), Et_3N). ^{31}P NMR (162 MHz, Methanol-d_4) δ -10.20 (d, ^2J = 20.9 Hz), -11.15 (d, ^2J = 20.8 Hz), -23.41 (t, ^2J = 21.1 Hz). HR-ESI-MS (*m/z*): $[M-H]^-$ = calcd: 706.0996; found: 706.0991

5-(5-(12-mercaptohexadecanamido)pent-1-yn-1-yl)deoxyuridine 4:

Yield: 9% of **4** as triethylammonium salt.

^{1}H NMR (400 MHz, Methanol-d_4): δ 8.03 (s, 1H, H-C(6)), 6.27 (t, ^{3}J = 6.9 Hz, 1H, H-C(1')), 4.67 – 4.60 (m, 1H, H-C(3')), 4.36 – 4.27 (m, 1H, H-C(5'a)), 4.24-4.16 (m, 1H, H-C(5'b)), 4.12-4.07 (m, 1H, H-C(4')), 3.22 (qt, ^{3}J = 7.0 Hz, 10H, -$CH_2CH_2CH_2$NH-, Et_3N,), 3.09 (t, ^{3}J = 7.3 Hz, 2H, **L12**), 2.47 (t, ^{3}J = 6.8 Hz, 2H, -$CH_2CH_2CH_2$NH-), 2.33-2.26 (m, 2H, H-2'), 2.23 (t, ^{3}J = 7.4 Hz, 2H, H-C(L2)), 1.81 (p, ^{3}J = 6.7 Hz, 2H, -$CH_2CH_2CH_2$NH-), 1.71 (p, ^{3}J = 7.4 Hz, 2H, H-C(L11)), 1.61 (p, ^{3}J = 7.1 Hz, 2H, H-C(L3)), 1.51-1.42 (m, 2H, H-C(L10)), 1.39-1.30 (m, 30H, H-C(L4-9), Et_3N). ^{31}P NMR (162 MHz, Methanol-d_4) δ -9.95 (d, ^{2}J = 20.8 Hz), -11.05 (d, ^{2}J = 20.8 Hz), -22.94 (m). HR-ESI-MS (*m/z*): $[M-H]^-$ = calcd: 762.1633; found: 762.1586

5-(5-(16-mercaptohexadecanamido)pent-1-yn-1-yl)deoxyuridine 5:

Yield: 19% of **5** as triethylammonium salt.

^{1}H NMR (600 MHz, Methanol-d_4) δ 8.02 (s, 1H, H-C(6)), 6.26 (t, ^{3}J = 6.8 Hz, 1H, H-C(1')), 4.64-4.60 (m, 1H, H-C(3')), 4.34 – 4.29 (m, 1H, H-C(5'a)), 4.23 – 4.18 (m, 1H, H-C(5'b)), 4.11-4.08 (m, 1H, H-C(4')), 3.22 (q, ^{3}J = 7.2, 20H, Et_3N, -$CH_2CH_2CH_2$NH-), 2.51 (t, ^{3}J = 7.3 Hz, 2H, H-C(L16)), 2.47 (t, ^{3}J = 6.8 Hz, 2H, -$CH_2CH_2CH_2$NH-), 2.32-2.27 (m, 2H, H-C(2')), 2.22 (t, ^{3}J = 7.6 Hz, 2H, H-C(L2)), 1.80 (p, ^{3}J = 6.8 Hz, 2H, -$CH_2CH_2CH_2$NH-), 1.61 (p, ^{3}J = 7.3 Hz, 4H, H-C(L3+15)), 1.47-1.38 (m, 4H, H-C(L4/14)), 1.37-1.28 (m, 54H, H-C(5-13), Et_3N). ^{31}P NMR (243 MHz, Methanol-d_4): δ = -10.48 (d, ^{2}J = 21.2 Hz), -11.39 (d, ^{2}J = 21.6 Hz), -23.84 (t, ^{2}J = 21.8 Hz). HR-ESI-MS (*m/z*): $[M-H]^-$ = calcd: 818.2259; found: 818.2279.

6.1.6 – Synthesis of C5-azide modified pyrimidines

Synthesis of 16-azidohexadecanoic acid[198]

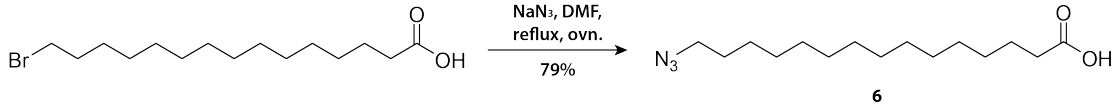

Figure 30: Synthesis of 16-azidohexadecanoic acid starting from 16-bromohexadecanoic acid.

To a stirred solution of 16-bromohexadecanoic acid (1 g, 2.98 mmol) in DMF, NaN_3 was added (0.39 g, 5.96 mmol, 2 eq.). The reaction was refluxed for 16 h and then extracted three times with 50 ml ethyl acetate. The combined organic phase was washed with water three times and brine, dried over $MgSO_4$ and the solvent was evaporated under reduced pressure to yield 16-azidohexadecanoic acid (0.7 g, 79%).

^{1}H NMR (400 MHz, CDCl3) δ 3.25 (t, ^3J=7.0 Hz, 2H, H-C(L16)-, 2.35 (t, ^3J=7.5 Hz, 2H, H-C(L2)-, 1.69-1.54 (m, 4H, H-C(L3+15)-), 1.42-1.21 (m, 22H, H-C(L4+14)-). ^{13}C NMR (101 MHz, CDCl3): δ 179.75, 51.66, 34.12, 29.76, 29.72, 29.68, 29.63, 29.57, 29.38, 29.30, 29.21, 28.99, 26.87, 24.84

5-(5-(16-azidohexadecanamido)pent-1-yn-1-yl)deoxyuridine (7)

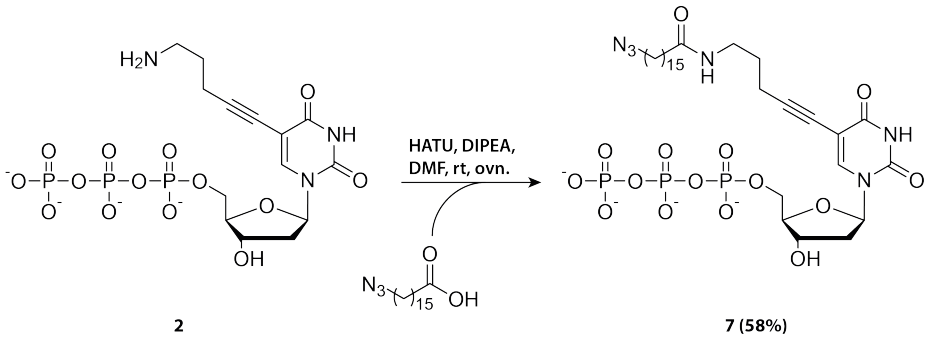

Figure 31: Synthesis of azide functionalized dTTP derivate **7**

To a solution of 18.9 µmol (10.3 mg) 5-(aminopentynyl)-2'-deoxyuridinetriphosphate tetrabutylammonium salt (**2**) in 1 ml DMF, 94.5 µmol (5 eq., 9.5 mg) of NEt_3 were added. In parallel, 37.8 µmol (2 eq, 11.2 mg) of 16-azidohexadecanoic acid, 94.5 µmol (5 eq, 9.5 mg) NEt_3 and 37.8 µmol HATU (2 eq., 14.4 mg) were dissolved in 1 ml DMF and stirred for 30 min. Both mixtures were then combined and stirred at room temperature for additional 12 h. The solvent was removed under reduced pressure and the residual oil was subjected to C_{18}-RP-HPLC (95% 50 mM triethylammonium acetate (TEAA) buffer to 100% MeCN). **7** was obtained in 58% yield as determined by Nanodrop ND1000 spectrometer with

ε(290 nm) = 13300 $M^{-1}\cdot cm^{-1}$. The compound was diluted in MQ and kept as a 10 mM stock solution at -20 °C.

^{1}H NMR (400 MHz, Methanol-d_4) δ 8.01 (s, 1H, H-C(6)), 6.26 (t, ^{3}J = 6.8 Hz, 1H, H-C(1')), 4.63-4.57 (m, 1H, H-C(3')), 4.34 – 4.26 (m, 1H, H-C(5'a)), 4.23 – 4.17 (m, 1H, H-C(5'b)), 4.11-4.06 (m, 1H, H-C(4')), 3.29 (t, ^{3}J = 6.9, 2H, H-C(L16)-), 3.22 (q, ^{3}J = 7.1, 17H, -$CH_2CH_2CH_2$NH-, Et_3N,), 2.46 (t, ^{3}J = 6.9 Hz, 2H, H-C(L2)), 2.32-2.25 (m, 2H, H-C(2')), 2.1 (t, ^{3}J = 7.5, 2H, -$CH_2CH_2CH_2$NH-), 2.20 (t, ^{3}J = 7.6 Hz, 2H, H-C(L2)), 1.79 (p, ^{3}J = 6.8 Hz, 2H, -$CH_2CH_2CH_2$NH-), 1.60 (p, ^{3}J = 6.8 Hz, 4H, H-C(L3+15)), 1.45-1.27 (m, 51H, H-C(4-14), Et_3N). ^{31}P NMR (243 MHz, Methanol-d_4): δ = -10.44 (d, ^{2}J = 20.5 Hz), -11.33 (d, ^{2}J = 21.3 Hz), -23.72 (t, ^{2}J = 21.3 Hz). HR-ESI-MS (*m/z*): $[M-H]^-$ = calcd: 827.2552; found: 827.2562.

6.2 – Biochemical Experiments

6.2.1 – Chemicals and materials

Chemicals used for the preparations of buffers and solutions in biochemical experiments were purchased from Sigma-Aldrich/Merck, Roth, Fluka, Acros Organics, Riedel-de-Haën, and VWR in "per analysis" or molecular biology grade and used without any further purification.

Table 1: List of chemicals and materials used in biochemical experiments and their manufacturers

Chemical/Material	Manufacturer
[gamma-32P]Adenosine 5'-triphosphate	Hartmann Analytics
1.5 ml reacton tubes	Brand
10 mM solution of amino-functionalized dATP derivative 8	Provided by Jana Balintova
15 and 50 ml Falcon tubes	Peske
200 µl PCR tubes	TreffLab
25 Bp DNA Step ladder	Promega
2-Mercaptoethanol	Merck
384 Well Lightcycler Plate	Sarstedt
6-Aminohexanoic acid	Sigma-Aldrich
Amicon 4 ml, MWCO 3,000	Merck
Deoxynucleotides	Jena Bioscience
Direct-zol RNA Kit	Zymo Research
Gel Loading Dye, Purple 6x	NEB
Gel Red	Biotium
HiTrap® Q HP 1 ml anion exchange column	GE Healthcare
Human total brain rRNA	Invitrogen
Hydrogen peroxide 30%	Merck
Low Molecular Weight Ladder (LMW)	NEB
MinElute Reaction clean up Kit	Qiagen
Nexterion H NHS-activated glass slides	SCHOTT Technical Glass Solutions
o-dianisidine dihydrochloride	Sigma-Aldrich
PCR foil seal	4titude
Pierce Spin Columns	Thermo Fisher Scientific
Pierce Streptavidin Coated Plates, Clear, 8-Well Strip	Thermo Fisher Scientific

Pipette tips w/ filter Biosphere	Sarstedt
Pipette tips: TipOne	StarLab
RNA, 16S- and 23S-ribosomal, *E. coli* MRE600	Roche
Rotiphorese sequencing gel concentrate (19:1)	Roth
Rotiphorese® Gel 30	Roth
Sephadex G-25	GE Healthcare
Streptavidin Sepharose® High Performance	GE Healthcare
SYBR Green I	Sigma-Aldrich
Vivaspin columns 6 MWCO 10,000	Sartorius AG
Whatman 0.2 µm membrane filters, RC58	GE Healthcare
Whatman Chromatography paper	GE Healthcare

6.2.2 – Instruments

Table 2: List of instruments employed and their manufacturers

Instrument	Manufacturer
Agarose gel system	Fisher Scientific
Åkta Pure chromatography system	GE Healthcare
Centrifuge 5810R	Eppendorf
Centrifuge Mini Sprout	Biozym
Centrifuge Minispin	Eppendorf
Gel dryer (Model 583)	Bio-Rad
Molecular Imager ChemiDoc XRS System	Bio-Rad
Multichannel pipettes (Transferpette S-12)	Brand
Nanodrop Spectrophotometer ND-1000	PeqLab
PAGE System I: Sequi-Gen GT	Bio-Rad
PAGE System II	Workshop at the University of Konstanz
pH electrode SevenEasy	Mettler Toledo
Phosphoimager I: Molecular Imager FX	Bio-Rad
Phosphoimager II: Typhoon FLA 7000	GE Healthcare
Pipettes: Research Plus	Eppendorf

PowerPac 3000 Power supply	Bio-Rad
PowerPac High Voltage	Bio-Rad
PowerShot A60 Digital Camera	Canon
Prominence Analytical HPLC System	Shimadzu
Radiography screens and cassettes	Fuji
Real-time PCR cycler CFX 384	Bio-Rad
Thermoblock QBTP	Grant
Thermocycler PEx in solution: T-Gradient	Biometra
Thermocycler PEx on beads: LifeTouch	Bioer
ThermoMixer F2.0	Eppendorf
Vortex	Heidolph

6.2.3 – Software

Table 3: Softwares used for analysis, plotting and editing of data, graphs and illustrations

Software	Manufacturer
Adobe Illustrator 2017	Adobe
CFX Manager	Bio-Rad
ChemOffice 17	Perkin Elmer
GraphPad Prism 6.0.1	GraphPad Softwar
Image Lab 6.0.1	Bio-Rad
MestReNova 12.0.3	MestReLab
Origin 2015	Origin Lab Corp.
PyMol, Version 1.3	Schrödinger, LLC, New York, USA
Quantity One	Bio-Rad
Unicorn 6.3	GE Healthcare
WinCoot 0.8.9.1	Paul Emsley, Kevin Cowtan

6.2.4 – Buffers and solutions

All buffers were prepared with MQ water and filtered sterile before use.

Table 4: Composition and names of all buffers that were not commercially available.

Buffer name	Composition
10x Isotherm2G reaction buffer	800 mM Tris-HCl, 200 mM ammonium sulfate, 100 mM potassium chloride, 10 mM DTT, 0.2% Tween 20, 20 mM magnesium sulfate, pH 8.5
10x KTq reaction buffer	500 mM Tris-HCl, 160 mM ammonium sulfate, 25 mM magnesium chloride, 1% Tween 20, pH 9.2
10x TBE buffer	900 mM Tris, 900 mM boric acid, 20 mM EDTA, pH 8.0
1x TAE buffer	40 mM Tris-HCl, 40 mM acetic acid, 1 mM EDTA, pH 8.3
Binding buffer (beads)	200 mM sodium phosphate, 1.5 M sodium chloride
Conjugation buffer	150 mM sodium chloride, 100 mM sodium phosphate, pH 7
Detection buffer (HRP)	100 mM sodium citrate, pH 5
HRP dye solution	1 mM o-dianisidine dihydrochloride, 1 mM hydrogen peroxide in detection buffer
IEX-FPLC buffer A	20 mM Tris-HCl, pH 9
IEX-FPLC buffer B	20 mM Tris-HCl, 1 M sodium chloride, pH 9
IEX-HPLC buffer A	25 mM Tris-HCl, pH 8
IEX-HPLC buffer B	25 mM Tris-HCl, 0.5 M sodium perchlorate, pH 8
PBS buffer	137 mM sodium chloride, 2.7 mM potassium chloride, 10 mM sodium hyrogenphosphate, 1.8 mM potassium dihydrogenphosphate, pH 7.4
SDS separation gel buffer	1.5 M Tris-HCl, pH 8.9
SDS stacking gel buffer	Tris-HCl, pH 6.8
Slide spotting buffer	100 mM sodium borate, 0.01% Tween, pH 9
Slide washing buffer	500 mM sodium chloride, 100 mM sodium phosphate, pH 7, 0.1% Tween
Stopping solution	80% v/v formamide, 20 mM EDTA, 0.025% w/v bromphenol blue, 0.025% w/v xylene cyanol
Streptavidin-plate washing buffer	25 mM Tris-HCl, 150 mM sodium chloride, 0.1% BSA, 0.05% Tween 20, pH 7.2

6.2.5 – Oligonucleotides

All oligonucleotides were purchased from Metabion or biomers.net with HPLC or PAGE purification.

Table 5: Sequences of all oligonucleotides used. Bold letters indicate the nucleotide opposite the incorporation site.

Name	Sequence
5'-biotin 16S rRNA primer[173]	5'-biotin-TEG-d(GCA GTT TCC CAG ACA TTA C)-3'
5'-biotin BRAF primer	5´-biotin-d(TTT TTT TTT TTT TTT TTT TGA CCC ACT CCA TCG AGA TTT C)-3'
5'-biotin primer epigenetic on synth. RNA	5'-Biotin-TEG-d(ACTACAAGCCCCAAAAGCAG)-3'
BRAF primer	5´-d(GAC CCA CTC CAT CGA GAT TTC)-3'
BRAF template (DNA)	5´-d(TGC CTG GTG TTT GGG **A**GA AAT CTC GAT GGA GTG GGT C)-3'
BRAF template (RNA)	5´-(UGC CUG GUG UUU GGG **A**GA AAU CUC GAU GGA GUG GGU C)-3'
Human 18S rRNA 2OMe468 primer	5'-Biotin-TEG-d(ATT TGC GCG CCT GCT GCC T)-3'
Human 18S rRNA 6mA1832 primer	5'-Biotin-TEG-d(GTT CAC CTA CGG AAA CCT TG)-3'
LAMP backward inner primer[190]	5'-d(GAG AGA ATT TGT ACC ACC TCC CAC CGG GCA CAT AGC AGT CCT AGG GAC AGT)
LAMP backward loop primer[190]	5'-d(ACC ATC TAT GAC TGT ACG CC)
LAMP backward outer primer[190]	5'-d(GGA CGT TTG TAA TGT CCG CTC C)
LAMP forward inner primer[190]	5'-d(CAG CCA GCC GCA GCA CGT TCG CTC ATA GGA GAT ATG GTA GAG CCG C)
LAMP forward loop primer[190]	5'-d(CTG CAT ACG ACG TGT CT)
LAMP forward outer primer[190]	5'-d(GGC TTG GCT CTG CTA ACA CGT T)
LAMP_Splint	5'-d(GGC TGG CTG TCC AGT GAG AGA ATT TGT ACC)

LAMP_Target_A	5'-DBCO-d(GGA CGT TTG TAA TGT CCG CTC CGG CAC ATA GCA GTC CTA GGG ACA GTG GCG TAC AGT CAT AGAT GGT CGG TGG GAG GTG GTA CAA ATT CTC TC)-3'
LAMP_Target_B	5'-P-d(ACT GGA CAG CCA GCC GCA GCA CGT TCC TGC ATA CGA CGT GTC TGC GGC TCT ACC ATA TCT CCT ATG AGC AAC GTG TTA GCA GAG CCA AGC C)
Match template	5´-d(GGT CTA GCT ACA G**A**G AAA TCT CGA TGG AGT GGG TC)-3'
Mismatch template	5´-d(GGT CTA GCT ACA G**T**G AAA TCT CGA TGG AGT GGG TC)-3'
Multiple incorporation template (consec.)	5´-d(T GCC TGG TGT TTG GG**A AAA AAA AAA A**GA AAT CTC GAT GGA GTG GGT C)-3'
Multiple incorporation template (iterative)	5'-d(T **A**G GG**A** TCT **A**TT T**A**C TT**A** CCG **A**TT C**A**T TT**A** CGC **A**GT C**A**G GC**A** TTC **A**GA AAT CTC GAT GGA GTG GGT C)-3'
Synthetic RNA template for epigenetics	5'-(AUA GGG GAA UGG GCC GUU CAU CUG CUA AAA GG**A** CUG CUU UUG GGG CUU GUA GU)-3'
Synthetic RNA template for epigenetics	5'-(AUA GGG GAA UGG GCC GUU CAU CUG CUA AAA GG**A(2'OMe)** CUG CUU UUG GGGCUUGUAGU)-3'
Synthetic RNA template for epigenetics	5'-(AUA GGG GAA UGG GCC GUU CAU CUG CUA AAA GG**A(6m)** CUG CUU UUG GGG CUU GUA GU)-3'

6.2.6 – Proteins and Enzymes

If not stated otherwise, the enzymes were used in the buffers and according to the protocols provided by the vendors.

Table 6: Proteins and enzymes used for the experiments in this work and their manufacturers

Protein/Enzyme	Manufacturer
Bst 2.0WS DNA polymerase	NEB
Calf intestinal alkaline phosphatase (CIP)	NEB
Isotherm2G DNA polymerase	myPOLS Biotech GmbH
***KF exo*⁻ DNA polymerase**	NEB
***KlenTaq* DNA polymerase**	Provided by Kim Leitner
Maleimide-activated HRP	Sigma-Aldrich
Pronase	Sigma-Aldrich
Proteinase K	Sigma-Aldrich
RT-*KTq* DNA polymerase	Provided by Kim Leitner
Streptavidin-HRP conjugate	Sigma-Aldrich
T4 DNA Ligase	NEB
T4 Polynucleotide kinase	NEB

6.2.7 – Determination of RNA/DNA concentrations

For synthetic oligonucleotides, molar attenuation coefficients were used as given by the manufacturers. Coefficients for newly generated sequences were calculated with the IDT OligoAnalyzer 3.1 using the nearest neighbor model.

Concentration of RNA extracts were, if not given by the manufacturer, measured using the Nanodrop ND-1000 spectrometer at 260 nm in the nucleic acid mode.

6.2.8 – General procedure for agarose gels

35 µl GelRed nucleic acid stain were mixed with 35 ml 0.8% or 2.5% agarose solution in 1x TAE buffer. The mixture was poured into a gel chamber and cooled until the gel solidified. Samples were diluted in purple loading dye and run at 120 V in 1x TAE buffer. The gel was then analysed by UV staining in a Chemidoc™ XRS system (Bio-Rad).

6.2.9 – Conjugation of Nucleotides and malHRP

2 mg of maleimide-activated HRP (malHRP, Sigma) were reconstituted in 250 µl conjugation buffer. The concentration was determined by Nanodrop Spectrometer with ε(403 nm) = 102000 M^{-1} cm^{-1}.[158] 75 µl of the solution were then mixed with 5 eq. of the thiol-modified nucleotides 3-5 and incubated overnight in a thermoshaker at 30 °C. The solution was subjected to anion exchange FPLC (HiTrap Q HP, *GE Life Science*) with a gradient from 20 mM Tris-HCl buffer (IEX-FPLC buffer A, pH 9) to 1 M NaCl in 20 mM Tris-HCl (IEX-FPLC buffer B, pH 9). The fractions containing the conjugate were identified by ESI-MS or PEx/dPAGE. To remove the FPLC buffer, the pooled fractions were purified *via* *Vivaspin* 6 (10,000 MWCO, Sartorius) and subsequently washed with conjugation buffer. The thusly concentrated conjugate was then incubated with 1.5 mM 2-mercaptoethanol in conjugation buffer overnight to block remaining maleimide groups. Excess 2-mercaptoethanol was removed by *Vivaspin* concentration and repeated washing with MQ. The final concentration of the obtained conjugate was determined *via* Nanodrop spectrometry with ε(403 nm) = 102000 M^{-1} cm^{-1}. The conjugates were stored at -20°C.

6.2.10 – Mass spectrometry of dT^{nHRP}TP

Samples were analyzed using an Agilent 1200 Series HPLC and a Nucleodur 300-5 150/2 C4ec column (Machery-Nagel) with a flow of 0.3 ml/min. 1.5 mM ammonium acetate was co-injected post-column with a flow of 10 µl/min. The data was acquired on a Bruker microTOFII spectrometer. The resulting spectra were deconvoluted using the maximum entropy algorithm provided by Bruker.

6.2.11 – Calculation of nucleotide and conjugate volumes

To calculate the volumina, the structures of the nucleoside triphosphates were generated in PyMol molecular graphics system V1.7.4 based on the 1HCH pdb file and entered into 3V webserver. The LAMP target sequence was rendered in WinCoot as an ideal ssDNA in B-Form and entered into 3V webserver.[212]

6.2.12 – 5'-Radioactive labeling of ODNs

DNA oligonucleotide primers were radioactively labeled at the 5' terminus with a ^{32}P containing phosphate group using T4 PNK (NEB) and [γ-^{32}P]ATP. The reaction contained primer (0.4 µM), PNK reaction buffer (1 x), [γ-^{32}P]ATP (0.8 µCi/µl) and T4 PNK (0.4 U/µl) in a total volume of 50 µl and was incubated for 1 h at 37 °C. The reaction was stopped by denaturing the T4 PNK for 2 min at 95° C and buffers and excess [γ-^{32}P]ATP were removed by gel filtration (MicroSpin Sephadex G-25). Addition of unlabeled primer (20 µl, 10 µM) led to a final concentration of 3 µM of diluted radioactive labeled primer.

For comparison, a marker was labeled as well. For the HRP-conjugates nucleotides, low molecular weight ladder (2 µl) was labeled as the primers. The labeled ladder was diluted 10x in stopping solution.

LAMP-target coupled nucleotides were compared to 25 bp DNA step ladder. The ladder was first dephosphorylated with CIP according to the protocol provided by the manufacturer of the enzyme. After denaturation, the reaction was purified with a MinElute Clean up Kit (10 µl elution volume) and 500 ng of the purified, dephosphorylated ladder were subjected to the labeling procedure. In the end, the labeled ladder was diluted 10x with stopping solution.

6.2.13 – General Procedure for primer Extension (PEx) in solution and dPAGE of dT$^{n\text{HRP}}$TP conjugates

To 1x polymerase buffer, 150 nM primer (100 nM for competition experiments) and 200 nM template were added. The mixture was annealed at 95 C for 5 min. Subsequently, DNA polymerase was added (*KF exo*$^-$ 0.5 U, *KTq* 100 nM and *RT-KTq* 500 nM) and the reaction was started by addition of the dNTP(s) (1 µM final concentration, 10 µM for competition experiments). Time points were collected by quenching 2 µl of the reaction mixture with 10 µl stopping solution (80% v/v formamide, 20 mM EDTA, 0.025% w/v bromphenol blue, 0.025% w/v xylene cyanol).

Denaturing polyacrylamide gels (9 %) were prepared by polymerization of a solution of urea (8.3 M) and bisacrylamide/acrylamide (9 %) in TBE buffer using ammonium peroxodisulfate (APS, 0.08 %) and *N*,*N*,*N*',*N*'-tetramethylethylene-diamine (TEMED, 0.04 %). Immediately after addition of APS and TEMED, the solution was filled in a sequencing gel chamber (Bio-Rad) and left for polymerization for at least 45 min. After addition of TBE buffer (1 x) to the electrophoresis unit, gels were pre-warmed by electrophoresis at 100 W for 30 min and samples were added and separated during electrophoresis (100 W) for approx. 1.5 h. The gel was transferred to *Whatman* filter paper, dried at 80 °C *in vacuo* using a gel dryer (model 583, *Bio-Rad*) and exposed to an imager screen. Readout was performed with a molecular imager (FX, *Bio-Rad*).

6.2.14 – General procedure for SDS-PAGE of PEx experiments with dT$^{n\text{HRP}}$TP

12.5% SDS polyacrylamide gels were prepared by adding 4.2 ml Rotiphorese Gel 30 to 3.3 ml MQ mixed with 2.5 ml separation gel buffer, 100 µl 10% SDS solution, and 10 µl TEMED. Polymerization was started with 75 µl 10% APS solution. The solution was filled into the gel chamber and covered with isopropanol. After the gel has solidified, the isopropanol was removed and a mixture of 0.65 ml Rotiphorese Gel 30, 3.1 ml MQ, 1.25 ml stacking gel buffer, 20 µl 10% SDS solution, 5 µl TEMED and 35 µl APS was placed on top of the separation gel. Gels were stored in a humid environment for up to a week at 4°C. 1.5 µl of the quenched PEx samples were directly applied in the stopping solution and run at 5 W.

6.2.15 – Primer Extension on streptavidin-coated sepharose beads[168-169]

10 µl of a streptavidin-coated sepharose bead slurry (*GE Healthcare*) were spun down (2400 x g) and the supernatant was discharged carefully. The beads were then washed two times with 40 µl 1 x binding

buffer before 9.5 µl binding buffer and 0.5 µl 5'-biotinylated primer (100 µM were added. Following 10 min of incubation with gentle mixing, 5.5 µl of 1 mM (D)-+-biotin in binding buffer were added to block the remaining streptavidin moieties. After further 5 min, the beads were spun down again and washed one time with 40 µl binding buffer and two times with the polymerase buffer. For the primer extension reaction, 22.4 µl MQ, 3 µl 10x polymerase buffer and 1 µl template (amount indicated in each experiment) were added to the beads and the mixture was mixed every minute for 10 min to prevent the beads from settling down in the tube. Subsequently, 0.6 µl DNA polymerase solution (final concentrations: *KF exo*$^-$ 0.3 U, *KlenTaq* 100 nM, *RT-KTq* 200 nM) and 3 µl of 10 µM dNTP were added (1 µM final). The reaction mixture was incubated at room temperature (*KF exo*$^-$, 15 min) or at 55°C (*RT-KTq*/*KTq* DNA polymerase, 3-10 mins), then the beads were spun down and transferred to an empty spin column cartridge. After removing the reaction mixture by short spin centrifugation in a table top centrifuge, the beads were washed four times with 100 µl detection buffer in the same way. Subsequently, they were transferred back to reaction tubes, the supernatant was discharged and 20 µl of the developing solution were applied (1 mM *o*-dianisidine/hydrogen peroxide in detection buffer). The reaction was quenched by the addition of 5 µl of 10 N sulfuric acid after 1 min. Pictures were taken with a *Canon PowerShot* A620 digital camera.

Variations in particular experiments:

Initial solid phase experiment: 10 min PEx time

E. Coli 16S rRNA detection: 5 min PEx time

Multiple incorporation on DNA templates: 10 min PEx time

Epigenetics on synth. RNA templates: 2.5 min PEx time, 100 fmol template

Epigenetics on RNA extracts: 3 min PEx time, 250 ng extracted RNA, 100 ng unmethylated RNA

6.2.16 – Extraction of HeLa total RNA

HeLa cells were kindly provided by Sandra Lange within the group. The RNA was extracted according to the protocol of the Direct-zol MiniPrep RNA kit (Zymo Research) and the obtained RNA extracts were analysed on a 0.8% agarose gel with 1% GelRed staining. Band intensities under UV light were assessed in Quantity One to evaluate the 18s rRNA content and the total RNA concentration was adjusted to 100 ng/µl.

6.2.17 – Preparation of LAMP target sequence and conjugation to compound 7

The split LAMP target sequence was splint ligated using T4 DNA ligase. 1 nmol of sequences LAMP_TARGET_A and LAMP_TARGET_B (10 µM) were mixed with 2 nmol (20 µM) of the split sequence in a total volume of 98 µl of 1x T4 ligase buffer provided by the manufacturer. The mixture was heated to 95°C for 2 min and slowly cooled down to 25°C. Subsequently, 2 µl of T4 Ligase (800 U) were added and the reaction was incubated at 16°C overnight.

The mixture was then diluted to 200 µl with MQ and subjected to 95°C for 5 min. Ion-exchange HPLC was performed at 85°C column temperature using 100 µl of the solution on an analytical HPLC system with a semi-preparative Thermo Scientific™ Dionex™ DNAPac™ PA100 column and a gradient from IEX-HPLC buffer A (25 mM Tris-HCl, pH 8) to IEX-HPLC buffer B (25 mM Tris-HCl, 0.5 M sodium perchlorate, pH 8).

Peaks demonstrating an absorbance at λ = 260 nm were collected and pooled in Amicon 4 centrifugal filters. After repeated washing with MQ, the ligated LAMP target was transferred to a 1.5 ml reaction tube and absorbance was measured by NanoDrop ND-1000 spectrometry at 260 nm with ε(403 nm) = 1752400 M^{-1} cm^{-1}.

To conjugate the 5'-DBCO labeled LAMP target sequence with compound **7**, the above generated oligonucleotide was incubated with 10 eq of the nucleotide in 1x PBS (pH 7.4) overnight. IEX-HPLC and Amicon purification were repeated to yield the 5'-triphosphate-labeled LAMP target sequence.

6.2.18 – PEx in solution with LAMP target conjugated compound 7

To 1x polymerase buffer, 150 nM primer and 200 nM template were added. The mixture was annealed at 95 C for 5 min. Subsequently, DNA polymerase was added (*KTq* 100 nM) and the reaction was started by addition of the dNTP (1 µM final concentration). Time points were collected by quenching 2 µl of

the reaction mixture with 10 µl stopping solution (80% v/v formamide, 20 mM EDTA, 0.025% w/v bromphenol blue, 0.025% w/v xylene cyanol).

Denaturing polyacrylamide gels (9 %) were prepared by polymerization of a solution of urea (8.3 M) and bisacrylamide/acrylamide (9 %) in TBE buffer using ammonium peroxodisulfate (APS, 0.08 %) and *N*,*N*,*N*',*N*'-tetramethylethylene-diamine (TEMED, 0.04 %). Immediately after addition of APS and TEMED, the solution was filled in a sequencing gel chamber (Bio-Rad) and left for polymerization for at least 45 min. After addition of TBE buffer (1 x) to the electrophoresis unit, gels were pre-warmed by electrophoresis at 100 W for 30 min and samples were added and separated during electrophoresis (100 W) for approx. 1.5 h. The gel was transferred to *Whatman* filter paper, dried at 80 °C *in vacuo* using a gel dryer and exposed to an imager screen. Readout was performed with a molecular imager FX.

6.2.19 – LAMP assay in solution

To avoid contaminations, all LAMP reactions were pipetted with Biosphere filter tips. LAMP target used for the positive controls was pipetted with a second pipette set.

Initial LAMP reactions were performed according to the conditions reported by Tanner and co-workers with 8 U Bst 2.0WS DNA polymerase, 1x SYBR I, 0.2/0.4/1.6 µM LAMP primers (outer/loop/inner), 10 nM 5'-DBCO LAMP target (positive control), 350 µM/dNTP, 65°C in 1x isothermal amplification buffer (NEB) with 8 mM $MgSO_4$.[189]

LAMP reactions in optimized conditions were carried out using 200 µM dNTPs, 0.2/0.4/1.6 µM primers (outer/loop/inner), 1x SYBR I, 4 U of Isotherm2G DNA polymerase (myPOLS Biotech GmbH) and 0.1 nM 5'-DBCO LAMP target (positive control) in a total of 10 µl of 1x Isotherm2G buffer at 55°C for the indicated amount of time. Fluoresence of SYBR I was measured in 1 min intervals minute in a Bio-Rad CFX384 Touch™ Real-Time PCR Detection System. Following the amplification, melting point measurement was carried out with a gradient from 55°C to 95°C in 0.5°C steps.

6.2.20 – Primer Extension and LAMP assay on plates

Pierce Streptavidin coated 8-well strips (Thermo Fisher) were washed twice with 200 µl of 1x plate washing buffer. Subsequently, 1 µl of 500 µM 5'-biotin BRAF primer in 100 µl 1x PBS buffer were added to each well. After 15 min of incubation at room temperature, the primer solution was removed and 200 µl of 1 mM (D)-+-biotin in 1x PBS were added. After 5 min of incubation the liquid was removed and the

wells were washed once with 200 µl of PBS buffer and twice with 200 µl of 1x KTq reaction buffer. Following this, 50 µl of PEx reaction mixture (100 nM KTq DNA polymerase, 200 nM BRAF template, 200 nM dT^{15LAMP}TP in a total of 50 µl 1x KTq buffer) were applied, the wells were sealed with PCR foil seal and incubated at 55°C (measured with a digital thermometer) in a shallow water bath on a thermal block for 30 min.

The supernatant was removed and the wells were washed first twice with 100 µl 1x KTq buffer, then three times with 1x PBS buffer and finally rinsed for 2 min under a water tap with distilled water. All liquid was removed and the wells were finally washed with 200 µl of 1x Isotherm2G buffer. 50 µl of LAMP reaction mixture (200 µM dNTPs, 0.2/0.4/1.6 µM primers (outer/loop/inner), 1x SYBR I, 4 U Isotherm2G) were employed in each well. For the positive control, 2 nM 5'DBCO LAMP target were added. The wells were incubated at 55°C as for the primer extension. Amplification was stopped by rapidly cooling the wells to 0°C in an ice bath. Samples were instantly collected and run on a 2.5% agarose gel. The gel was read out using GelRed staining under UV light on a Chemidoc™ XRS system (Bio-Rad).

6.2.21 – PEx reaction with immobilized dATP on glass plates

Distinct reaction chambers were created with Thermo Fisher Gene Frames (1 cm x 1 cm) on Schott Nexterion H NHS activated glass slides. The reaction chambers were either treated with 20 µl spotting buffer and 20 µl 10 µM compound **7** (dA^{15NH2}TP) or 40 µl 0.5x spotting buffer (negative control) for 3 h. The supernatant was removed and 40 µl 25 mM 6-aminohexanoic acid in spotting buffer was added to block remaining NHS groups for 60 mins. Subsequently, the chambers were washed twice each with 100 µl MQ water and 1x KlenTaq reaction buffer. 25 µl PEx reaction solution containing 4 µM BRAF primer, 40 nM RT-KTq DNA Polymerase and 4 µM BRAF mismatch template were applied and the slides were incubated on a thermoblock for 45 min. For the washing procedure, the position of the frames was marked on the slides and the frames were removed. The slides were washed under MQ and slide washing buffer several times before new frames were put on the slides. 0.5 mg/ml of Streptavidin-HRP conjugate (Thermo Fisher) in 25 µl washing buffer was employed in each reaction chamber and incubated at rt for 30 mins. The chambers were then washed 5x with warm slide washing buffer and 3x with warm HRP detection buffer. Finally, 40 µl of o-dianisidine dye solution were added and the colorigenic was quenched after 1 min by the addition of 10 µl 10 N sulfuric acid. Absorbance was measured at

450 nm and 520 nm with NanoDrop ND-1000 using the UV/Vis mode. Pictures were taken with a *PowerShot* A620 digital camera (Canon).

7 - Literature

[1] G. Mendel, Versuche über Pflanzenhybriden, *Verhandlungen des naturforschenden Vereines in Brünn* **1866**, *IV*, 3–47.

[2] F. Miescher, Über die chemische Zusammensetzung der Eiterzellen, *Hoppe-Seyler's Medicinisch-chemische Untersuchungen* **1871**, *4*, 441-460.

[3] A. Kossel, A. Neumann, Über das Thymin, ein Spaltungsprodukt der Nukleinsäure, *Berichte der deutschen chemischen Gesellschaft* **1893**, *26*.

[4] P. Levene, W. Jacobs, Über die Hefe-Nucleinsäure, *Berichte der deutschen chemischen Gesellschaft* **1909**, 2474-2478.

[5] P. Levene, W. Jacobs, Über Inosinsäure, *Berichte der deutschen chemischen Gesellschaft* **1909**, 1198-1203.

[6] P. Levene, The structure of yeast nucleic acid, *Journal of Biological Chemistry* **1919**, 415-424.

[7] R. Altmann, *Über Nukleinsäuren*, Physiologische Abteilung Leipzig, **1889**.

[8] P. Portin, The birth and development of the DNA theory of inheritance: sixty years since the discovery of the structure of DNA, *Journal of Genetics* **2014**, *93*, 293-302.

[9] F. Griffith, The Significance of Pneumococcal Types, *The Journal of Hygiene* **1928**, *27*, 113-159.

[10] O. T. Avery, C. M. Macleod, M. McCarty, Studies on the Chemical Nature of the Substance Inducing Transformation of Pneumococcal Types : Induction of Transformation by a Desoxyribonucleic Acid Fraction Isolated from Pneumococcus Type Iii, *The Journal of Experimental Medicine* **1944**, *79*, 137-158.

[11] E. Chargaff, E. Vischer, et al., The composition of the desoxypentose nucleic acids of thymus and spleen, *Journal of Biological Chemistry* **1949**, *177*, 405-416.

[12] A. D. Hershey, M. Chase, Independent functions of viral protein and nucleic acid in growth of bacteriophage, *The Journal of General Physiology* **1952**, *36*, 39-56.

[13] J. D. Watson, F. H. Crick, The structure of DNA, *Cold Spring Harbor Symposia on Quantitative Biology* **1953**, *18*, 123-131.

[14] R. E. Franklin, R. G. Gosling, Evidence for 2-chain helix in crystalline structure of sodium deoxyribonucleate, *Nature* **1953**, *172*, 156-157.

[15] M. H. Wilkins, A. R. Stokes, H. R. Wilson, Molecular structure of deoxypentose nucleic acids, *Nature* **1953**, *171*, 738-740.

[16] J. D. Watson, F. H. Crick, Genetical implications of the structure of deoxyribonucleic acid, *Nature* **1953**, *171*, 964-967.

[17] J. D. Watson, F. H. Crick, Molecular structure of nucleic acids; a structure for deoxyribose nucleic acid, *Nature* **1953**, *171*, 737-738.

[18] A. Travers, G. Muskhelishvili, DNA structure and function, *The FEBS Journal* **2015**, *282*, 2279-2295.

[19] E. Chargaff, Chemical specificity of nucleic acids and mechanism of their enzymatic degradation, *Experientia* **1950**, *6*, 201-209.

[20] M. Mandelkern, J. G. Elias, D. Eden, et al., The dimensions of DNA in solution, *Journal of Molecular Biology* **1981**, *152*, 153-161.

[21] D. B. Haniford, D. E. Pulleyblank, The in-vivo occurrence of Z DNA, *Journal of Biomolecular Structure and Dynamics* **1983**, *1*, 593-609.

[22] A. Nordheim, M. L. Pardue, E. M. Lafer, et al., Antibodies to left-handed Z-DNA bind to interband regions of Drosophila polytene chromosomes, *Nature* **1981**, *294*, 417-422.

[23] R. E. Franklin, R. G. Gosling, Molecular Configuration in Sodium Thymonucleate, *Nature* **1953**, *171*, 740-741.

[24] A. Ghosh, M. Bansal, A glossary of DNA structures from A to Z, *Acta Crystallographica Section D* **2003**, *59*, 620-626.

[25] P. A. Levene, E. S. London, The structure of thymonucleic acid., *Journal of Biological Chemistry* **1929**, *83*, 793-802.

[26] J. Brachet, Ribonucleic acids and the synthesis of cellular proteins, *Nature* **1960**, *186*, 194-199.

[27] J. Brachet, Recherches sur la synthese de l'acide thymonucleique pendant le developpement de l'oeuf d'Oursin, *Archives de Biologie* **1933**, *44*, 519-576.

[28] F. H. Crick, On protein synthesis, *Symposia of the Society for Experimental Biology* **1958**, *12*, 138-163.

[29] S. Hormeno, B. Ibarra, J. L. Carrascosa, et al., Mechanical properties of high-G.C content DNA with a-type base-stacking, *Biophysical Journal* **2011**, *100*, 1996-2005.

[30] T. Lindahl, Instability and decay of the primary structure of DNA, *Nature* **1993**, *362*, 709-715.

[31] D. Elliott, M. Ladomery, *Molecular biology of RNA*, Second edition. ed., Oxford University Press, Oxford, **2016**.

[32] A. Kornberg, I. R. Lehman, M. J. Bessman, et al., Enzymic synthesis of deoxyribonucleic acid, *Biochimica et Biophysica Acta* **1956**, *21*, 197-198.

[33] M. J. Bessman, I. R. Lehman, E. S. Simms, et al., Enzymatic Synthesis of Deoxyribonucleic Acid: II. General properties of the reaction, *Journal of Biological Chemistry* **1958**, *233*, 171-177.

[34] M. Garcia-Diaz, K. Bebenek, Multiple functions of DNA polymerases, *Critical Reviews in Plant Sciences* **2007**, *26*, 105-122.

[35] E. Johansson, N. Dixon, Replicative DNA polymerases, *Cold Spring Harbor Perspectives in Biology* **2013**, *5*.

[36] S. Korolev, M. Nayal, W. M. Barnes, et al., Crystal structure of the large fragment of Thermus aquaticus DNA polymerase I at 2.5-A resolution: structural basis for thermostability, *Proceedings of the National Academy of Sciences of the United States of America* **1995**, *92*, 9264-9268.

[37] A. J. Berdis, Mechanisms of DNA polymerases, *Chemical Reviews* **2009**, *109*, 2862-2879.

[38] C. Castro, E. D. Smidansky, J. J. Arnold, et al., Nucleic acid polymerases use a general acid for nucleotidyl transfer, *Nature Structural & Molecular Biology* **2009**, *16*, 212-218.

[39] M. Meselson, F. W. Stahl, The Replication of DNA in Escherichia Coli, *Proceedings of the National Academy of Sciences of the United States of America* **1958**, *44*, 671-682.

[40] F. J. Bollum, Thermal Conversion of Nonpriming Deoxyribonucleic Acid to Primer, *Journal of Biological Chemistry* **1959**, *234*, 2733-2734.

[41] E. A. Motea, A. J. Berdis, Terminal deoxynucleotidyl transferase: the story of a misguided DNA polymerase, *Biochimica et Biophysica Acta* **2010**, *1804*, 1151-1166.

[42] W. Yang, P. J. Weng, Y. Gao, A new paradigm of DNA synthesis: three-metal-ion catalysis, *Cell & Bioscience* **2016**, *6*, 51.

[43] P. McInerney, P. Adams, M. Z. Hadi, Error Rate Comparison during Polymerase Chain Reaction by DNA Polymerase, *Molecular Biology International* **2014**, *2014*, 287430.

[44] K. A. Eckert, T. A. Kunkel, DNA polymerase fidelity and the polymerase chain reaction, *Genome Research* **1991**, *1*, 17-24.

[45] R. Saiki, S. Scharf, F. Faloona, et al., Enzymatic amplification of beta-globin genomic sequences and restriction site analysis for diagnosis of sickle cell anemia, *Science* **1985**, *230*, 1350-1354.

[46] K. Mullis, F. Faloona, S. Scharf, et al., Specific Enzymatic Amplification of DNA In Vitro: The Polymerase Chain Reaction, *Cold Spring Harbor Symposia on Quantitative Biology* **1986**, *51*, 263-273.

[47] A. Chien, D. B. Edgar, J. M. Trela, Deoxyribonucleic acid polymerase from the extreme thermophile Thermus aquaticus, *Journal of bacteriology* **1976**, *127*, 1550-1557.

[48] M. Takagi, M. Nishioka, H. Kakihara, et al., Characterization of DNA polymerase from Pyrococcus sp. strain KOD1 and its application to PCR, *Applied and Environmental Microbiology* **1997**, *63*, 4504-4510.

[49] R. K. Saiki, D. H. Gelfand, S. Stoffel, et al., Primer-directed enzymatic amplification of DNA with a thermostable DNA polymerase, *Science* **1988**, *239*, 487-491.

[50] G. T. Walker, M. C. Little, J. G. Nadeau, et al., Isothermal in vitro amplification of DNA by a restriction enzyme/DNA polymerase system, *Proceedings of the National Academy of Sciences of the United States of America* **1992**, *89*, 392-396.

[51] J. Aschenbrenner, A. Marx, DNA polymerases and biotechnological applications, *Current Opinion in Biotechnology* **2017**, *48*, 187-195.

[52] S. Ishino, Y. Ishino, DNA polymerases as useful reagents for biotechnology – the history of developmental research in the field, *Frontiers in microbiology* **2014**, *5*.

[53] T. Notomi, H. Okayama, H. Masubuchi, et al., Loop-mediated isothermal amplification of DNA, *Nucleic Acids Research* **2000**, *28*, E63.

[54] X. Kong, W. Qin, X. Huang, et al., Development and application of loop-mediated isothermal amplification (LAMP) for detection of Plasmopara viticola, *Scientific Reports* **2016**, *6*, 28935.

[55] Y. Wang, Y. Wang, H. Xu, et al., Rapid and Sensitive Detection of Listeria ivanovii by Loop-Mediated Isothermal Amplification of the smcL Gene, *PLoS One* **2015**, *9*, e115868.

[56] R. Laos, J. M. Thomson, S. A. Benner, DNA polymerases engineered by directed evolution to incorporate non-standard nucleotides, *Frontiers in microbiology* **2014**, *5*, 565-565.

[57] V. Pinheiro, J. Ong, P. Holliger, in *Protein Engineering Handbook, Vol. 3*, Wiley-VCH, **2012**, pp. 279-302.

[58] N. Blatter, K. Bergen, O. Nolte, et al., Structure and Function of an RNA-Reading Thermostable DNA Polymerase, *Angewandte Chemie International Edition* **2013**, *52*, 11935-11939.

[59] I. A. Roundtree, M. E. Evans, T. Pan, et al., Dynamic RNA Modifications in Gene Expression Regulation, *Cell* **2017**, *169*, 1187-1200.

[60] G. R. Wyatt, S. S. Cohen, The bases of the nucleic acids of some bacterial and animal viruses: the occurrence of 5-hydroxymethylcytosine, *The Biochemical journal* **1953**, *55*, 774-782.

[61] T. Pfaffeneder, B. Hackner, M. Truß, et al., The Discovery of 5-Formylcytosine in Embryonic Stem Cell DNA, *Angewandte Chemie International Edition* **2011**, *50*, 7008-7012.

[62] Y.-F. He, B.-Z. Li, Z. Li, et al., Tet-Mediated Formation of 5-Carboxylcytosine and Its Excision by TDG in Mammalian DNA, *Science* **2011**, *333*, 1303-1307.

[63] W. E. Cohn, E. Volkin, Nucleoside-5′-Phosphates from Ribonucleic Acid, *Nature* **1951**, *167*, 483-484.

[64] I. Alseth, B. Dalhus, M. Bjørås, Inosine in DNA and RNA, *Current Opinion in Genetics & Development* **2014**, *26*, 116-123.

[65] B. F. Vanyushin, S. G. Tkacheva, A. N. Belozersky, Rare Bases in Animal DNA, *Nature* **1970**, *225*, 948-949.

[66] G. R. Wyatt, Recognition and estimation of 5-methylcytosine in nucleic acids, *The Biochemical journal* **1951**, *48*, 581-584.

[67] B. E. H. Maden, in *Progress in Nucleic Acid Research and Molecular Biology, Vol. 39* (Eds.: W. E. Cohn, K. Moldave), Academic Press, **1990**, pp. 241-303.

[68] T. Kiss, Small nucleolar RNA-guided post-transcriptional modification of cellular RNAs, *The EMBO Journal* **2001**, *20*, 3617-3622.

[69] L. D. Moore, T. Le, G. Fan, DNA Methylation and Its Basic Function, *Neuropsychopharmacology* **2012**, *38*, 23.

[70] R. Jaenisch, A. Bird, Epigenetic regulation of gene expression: how the genome integrates intrinsic and environmental signals, *Nature Genetics* **2003**, *33*, 245.

[71] D. B. Dunn, J. D. Smith, The occurrence of 6-methylaminopurine in deoxyribonucleic acids, *Biochemical Journal* **1958**, *68*, 627-636.

[72] R. Desrosiers, K. Friderici, F. Rottman, Identification of Methylated Nucleosides in Messenger RNA from Novikoff Hepatoma Cells, *Proceedings of the National Academy of Sciences of the United States of America* **1974**, *71*, 3971-3975.

[73] G. Zheng, John A. Dahl, Y. Niu, et al., ALKBH5 Is a Mammalian RNA Demethylase that Impacts RNA Metabolism and Mouse Fertility, *Molecular Cell* **2013**, *49*, 18-29.

[74] W. Xiao, S. Adhikari, U. Dahal, et al., Nuclear m6A Reader YTHDC1 Regulates mRNA Splicing, *Molecular Cell* **2016**, *61*, 507-519.

[75] X. Wang, Boxuan S. Zhao, Ian A. Roundtree, et al., N6-methyladenosine Modulates Messenger RNA Translation Efficiency, *Cell* **2015**, *161*, 1388-1399.

[76] X. Wang, Z. Lu, A. Gomez, et al., N6-methyladenosine-dependent regulation of messenger RNA stability, *Nature* **2013**, *505*, 117.

[77] W. A. Decatur, M. J. Fournier, rRNA modifications and ribosome function, *Trends in Biochemical Sciences* **2002**, *27*, 344-351.

[78] S. Xue, M. Barna, Specialized ribosomes: a new frontier in gene regulation and organismal biology, *Nature Reviews Molecular Cell Biology* **2012**, *13*, 355.

[79] K. E. Sloan, A. S. Warda, S. Sharma, et al., Tuning the ribosome: The influence of rRNA modification on eukaryotic ribosome biogenesis and function, *RNA biology* **2016**, *14*, 1138-1152.

[80] M. Frommer, L. E. McDonald, D. S. Millar, et al., A genomic sequencing protocol that yields a positive display of 5-methylcytosine residues in individual DNA strands, *Proceedings of the National Academy of Sciences of the United States of America* **1992**, *89*, 1827-1831.

[81] J. Aschenbrenner, A. Marx, Direct and site-specific quantification of RNA 2′-O-methylation by PCR with an engineered DNA polymerase, *Nucleic Acids Research* **2016**, *44*, 3495-3502.

[82] W. H. Prusoff, Synthesis and biological activities of iododeoxyuridine, an analog of thymidine, *Biochimica et Biophysica Acta* **1959**, *32*, 295-296.

[83] S. C. Srivastava, S. K. Raza, R. Misra, 1,N6-etheno deoxy and ribo adenosine and 3,N4-etheno deoxy and ribo cytidine phosphoramidites. Strongly fluorescent structures for selective introduction in defined sequence DNA and RNA molecules, *Nucleic Acids Research* **1994**, *22*, 1296-1304.

[84] D. R. Bentley, S. Balasubramanian, H. P. Swerdlow, et al., Accurate whole human genome sequencing using reversible terminator chemistry, *Nature* **2008**, *456*, 53-59.

[85] T. M. Tarasow, S. L. Tarasow, B. E. Eaton, RNA-catalysed carbon-carbon bond formation, *Nature* **1997**, *389*, 54-57.

[86] A. Baccaro, A. L. Steck, A. Marx, Barcoded nucleotides, *Angewandte Chemie International Edition* **2012**, *51*, 254-257.

[87] H. J. Schaeffer, S. Gurwara, R. Vince, et al., Novel substrate of adenosine deaminase, *Journal of Medicinal Chemistry* **1971**, *14*, 367-369.

[88] L. Eyer, R. Nencka, E. de Clercq, et al., Nucleoside analogs as a rich source of antiviral agents active against arthropod-borne flaviviruses, *Antiviral Chemistry and Chemotherapy* **2018**, *26*, 2040206618761299.

[89] F. Cramer, Modified nucleotides as tools in nucleic acid research, *Accounts of Chemical Research* **1969**, *2*, 338-344.

[90] S. Obika, D. Nanbu, Y. Hari, et al., Synthesis of 2′-O,4′-C-methyleneuridine and -cytidine. Novel bicyclic nucleosides having a fixed C3, -endo sugar puckering, *Tetrahedron Letters* **1997**, *38*, 8735-8738.

[91] M. Petersen, J. Wengel, LNA: a versatile tool for therapeutics and genomics, *Trends in Biotechnology* **2003**, *21*, 74-81.

[92] F. Eckstein, Nucleoside Phosphorothioates, *Annual Review of Biochemistry* **1985**, *54*, 367-402.

[93] M. Hocek, Synthesis of Base-Modified 2′-Deoxyribonucleoside Triphosphates and Their Use in Enzymatic Synthesis of Modified DNA for Applications in Bioanalysis and Chemical Biology, *The Journal of Organic Chemistry* **2014**, *79*, 9914-9921.

[94] V. T. Dien, M. Holcomb, A. W. Feldman, et al., Progress Toward a Semi-Synthetic Organism with an Unrestricted Expanded Genetic Alphabet, *Journal of the American Chemical Society* **2018**, *140*, 16115-16123.

[95] M. D. Matteucci, M. H. Caruthers, Synthesis of deoxyoligonucleotides on a polymer support, *Journal of the American Chemical Society* **1981**, *103*, 3185-3191.

[96] S. L. Beaucage, M. H. Caruthers, Deoxynucleoside phosphoramidites—A new class of key intermediates for deoxypolynucleotide synthesis, *Tetrahedron Letters* **1981**, *22*, 1859-1862.

[97] L. Gjonaj, G. Roelfes, Selective chemical modification of DNA with alkoxy- and benzyloxyamines, *Organic & Biomolecular Chemistry* **2015**, *13*, 6059-6065.

[98] C.-X. Song, C. He, Bioorthogonal Labeling of 5-Hydroxymethylcytosine in Genomic DNA and Diazirine-Based DNA Photo-Cross-Linking Probes, *Accounts of Chemical Research* **2011**, *44*, 709-717.

[99] S. Klimašauskas, E. Weinhold, A new tool for biotechnology: AdoMet-dependent methyltransferases, *Trends in Biotechnology* **2007**, *25*, 99-104.

[100] M. Hollenstein, Nucleoside Triphosphates — Building Blocks for the Modification of Nucleic Acids, *Molecules* **2012**, *17*, 13569.

[101] M. M. Masud, A. Ozaki-Nakamura, F. Satou, et al., Enzymatic synthesis of modified DNA by PCR, *Nucleic Acids Research Supplement* **2001**, 21-22.

[102] B. D. Preston, L. A. Loeb, Enzymatic synthesis of site-specifically modified DNA, *Mutation Research* **1988**, *200*, 21-35.

[103] T. W. Kim, J. C. Delaney, J. M. Essigmann, et al., Probing the active site tightness of DNA polymerase in subangstrom increments, *Proceedings of the National Academy of Sciences of the United States of America* **2005**, *102*, 15803-15808.

[104] E. T. Kool, H. O. Sintim, The difluorotoluene debate—a decade later, *Chemical Communications* **2006**, 3665-3675.

[105] Rais A. Ganai, E. Johansson, DNA Replication—A Matter of Fidelity, *Molecular Cell* **2016**, *62*, 745-755.

[106] M. Hollenstein, Nucleoside triphosphates -building blocks for the modification of nucleic acids, *Molecules* **2012**, *17*, 13569-13591.

[107] G. Gao, M. Orlova, M. M. Georgiadis, et al., Conferring RNA polymerase Activity to a DNA polymerase: A single residue in reverse transcriptase controls substrate selection, *Proceedings of the National Academy of Sciences of the United States of America* **1997**, *94*, 407-411.

[108] S. L. Beaucage, in *Comprehensive Natural Products Chemistry* (Eds.: S. D. Barton, K. Nakanishi, O. Meth-Cohn), Pergamon, Oxford, **1999**, pp. 153-249.

[109] S. Jäger, G. Rasched, H. Kornreich-Leshem, et al., A Versatile Toolbox for Variable DNA Functionalization at High Density, *Journal of the American Chemical Society* **2005**, *127*, 15071-15082.

[110] A. Hottin, A. Marx, Structural Insights into the Processing of Nucleobase-Modified Nucleotides by DNA Polymerases, *Accounts of Chemical Research* **2016**, *49*, 418-427.

[111] M. Hocek, M. Fojta, Cross-coupling reactions of nucleoside triphosphates followed by polymerase incorporation. Construction and applications of base-functionalized nucleic acids, *Organic & Biomolecular Chemistry* **2008**, *6*, 2233-2241.

[112] N. Boge, M. I. Jacobsen, Z. Szombati, et al., Synthesis of DNA strands site-specifically damaged by c8-arylamine purine adducts and effects on various DNA polymerases, *Chemistry - A European Journal* **2008**, *14*, 11194-11208.

[113] S. E. Lee, A. Sidorov, T. Gourlain, et al., Enhancing the catalytic repertoire of nucleic acids: a systematic study of linker length and rigidity, *Nucleic Acids Research* **2001**, *29*, 1565-1573.

[114] K. Bergen, A. L. Steck, S. Strutt, et al., Structures of KlenTaq DNA Polymerase Caught While Incorporating C5-Modified Pyrimidine and C7-Modified 7-Deazapurine Nucleoside Triphosphates, *Journal of the American Chemical Society* **2012**, *134*, 11840-11843.

[115] S. Obeid, A. Baccaro, W. Welte, et al., Structural basis for the synthesis of nucleobase modified DNA by Thermus aquaticus DNA polymerase, *Proceedings of the National Academy of Sciences of the United States of America* **2010**, *107*, 21327-21331.

[116] M. Kuwahara, J. Nagashima, M. Hasegawa, et al., Systematic characterization of 2'-deoxynucleoside- 5'-triphosphate analogs as substrates for DNA polymerases by polymerase chain reaction and kinetic studies on enzymatic production of modified DNA, *Nucleic Acids Research* **2006**, *34*, 5383-5394.

[117] H. Sawai, A. Ozaki-Nakamura, M. Mine, et al., Synthesis of new modified DNAs by hyperthermophilic DNA polymerase: substrate and template specificity of functionalized thymidine analogues bearing an sp3-hybridized carbon at the C5 alpha-position for several DNA polymerases, *Bioconjugate Chem* **2002**, *13*, 309-316.

[118] M. M. Masud, A. Ozaki-Nakamura, M. Kuwahara, et al., Modified DNA bearing 5-(methoxycarbonyl-methyl)-2 '-deoxyuridine: Preparation by PCR with thermophilic DNA polymerase and post-synthetic derivation, *Chembiochem* **2003**, *4*, 584-588.

[119] H. M. Kropp, K. Betz, J. Wirth, et al., Crystal structures of ternary complexes of archaeal B-family DNA polymerases, *PLoS One* **2017**, *12*, e0188005.

[120] A. Baccaro, A. Marx, Enzymatic Synthesis of Organic-Polymer-Grafted DNA, *Chemistry – A European Journal* **2010**, *16*, 218-226.

[121] R. S. Sorensen, A. H. Okholm, D. Schaffert, et al., Enzymatic ligation of large biomolecules to DNA, *ACS Nano* **2013**, *7*, 8098-8104.

[122] I. Sarac, M. Hollenstein, Terminal Deoxynucleotidyl Transferase in the Synthesis and Modification of Nucleic Acids, *Chembiochem* **2018**.

[123] M. Delarue, J. B. Boule, J. Lescar, et al., Crystal structures of a template-independent DNA polymerase: murine terminal deoxynucleotidyltransferase, *The EMBO Journal* **2002**, *21*, 427-439.

[124] N. Sukumar, J. B. Boule, N. Expert-Bezancon, et al., Crystallization of the catalytic domain of murine terminal deoxynucleotidyl transferase, *Acta Crystallographica Section D* **2000**, *56*, 1662-1664.

[125] Z. Hatahet, A. A. Purmal, S. S. Wallace, A Novel Method for Site-Specific Introduction of Single Model Oxidative DNA Lesions into Oligodeoxyribonucleotides, *Nucleic Acids Research* **1993**, *21*, 1563-1568.

[126] A. J. Jeffreys, V. Wilson, S. L. Thein, Individual-Specific Fingerprints of Human DNA, *Nature* **1985**, *316*, 76-79.

[127] I. S. Shergill, M. Williamson, L. Gommersall, et al., Basic principles of real-time quantitative PCR AU - Arya, Manit, *Expert Review of Molecular Diagnostics* **2005**, *5*, 209-219.

[128] A. L. Shaffer, W. Wojnar, W. Nelson, Amplification, detection, and automated sequencing of gibbon interleukin-2 mRNA by Thermus aquaticus DNA polymerase reverse transcription and polymerase chain reaction, *Analytical Biochemistry* **1990**, *190*, 292-296.

[129] L. Ugozzoli, R. B. Wallace, Allele-specific polymerase chain reaction, *Methods* **1991**, *2*, 42-48.

[130] J. Aschenbrenner, M. Drum, H. Topal, et al., Direct sensing of 5-methylcytosine by polymerase chain reaction, *Angewandte Chemie International Edition* **2014**, *53*, 8154-8158.

[131] F. Sanger, S. Nicklen, A. R. Coulson, DNA sequencing with chain-terminating inhibitors, *Proceedings of the National Academy of Sciences of the United States of America* **1977**, *74*, 5463-5467.

[132] F.-M. Ana, G. Sofia, L. C. Maria, NGS Technologies as a Turning Point in Rare Disease Research , Diagnosis and Treatment, *Current Medicinal Chemistry* **2018**, *25*, 404-432.

[133] S. A. E. Marras, S. Tyagi, F. R. Kramer, Real-time assays with molecular beacons and other fluorescent nucleic acid hybridization probes, *Clinica Chimica Acta* **2006**, *363*, 48-60.

[134] M. Schena, Genome analysis with gene expression microarrays, *BioEssays* **1996**, *18*, 427-431.

[135] T. R. Kozel, A. R. Burnham-Marusich, Point-of-Care Testing for Infectious Diseases: Past, Present, and Future, *Journal of Clinical Microbiology* **2017**, *55*, 2313-2320.

[136] P. Maffert, S. Reverchon, W. Nasser, et al., New nucleic acid testing devices to diagnose infectious diseases in resource-limited settings, *European Journal of Clinical Microbiology & Infectios Disease* **2017**, *36*, 1717-1731.

[137] A. Niemz, T. M. Ferguson, D. S. Boyle, Point-of-care nucleic acid testing for infectious diseases, *Trends in Biotechnology* **2011**, *29*, 240-250.

[138] P. Wang, L. J. Kricka, Current and Emerging Trends in Point-of-Care Technology and Strategies for Clinical Validation and Implementation, *Clinical Chemistry* **2018**, *64*, 1439-1452.

[139] M. Vincent, Y. Xu, H. Kong, Helicase-dependent isothermal DNA amplification, *EMBO reports* **2004**, *5*, 795-800.

[140] G. T. Walker, M. S. Fraiser, J. L. Schram, et al., Strand displacement amplification--an isothermal, in vitro DNA amplification technique, *Nucleic Acids Research* **1992**, *20*, 1691-1696.

[141] W. A. Al-Soud, P. Rådström, Purification and Characterization of PCR-Inhibitory Components in Blood Cells, *Journal of Clinical Microbiology* **2001**, *39*, 485-493.

[142] W. A. Al-Soud, L. J. Jönsson, P. Rådström, Identification and Characterization of Immunoglobulin G in Blood as a Major Inhibitor of Diagnostic PCR, *Journal of Clinical Microbiology* **2000**, *38*, 345-350.

[143] J. M. Bienvenue, L. A. Legendre, J. P. Ferrance, et al., An integrated microfluidic device for DNA purification and PCR amplification of STR fragments, *Forensic Science International: Genetics* **2010**, *4*, 178-186.

[144] M. Bates, A. Zumla, Rapid infectious diseases diagnostics using Smartphones, *Annals of translational medicine* **2015**, *3*, 215-215.

[145] L. Xie, T. Wang, T. Huang, et al., Dew inspired breathing-based detection of genetic point mutation visualized by naked eye, *Scientific Reports* **2014**, *4*, 6300.

[146] G. L'Abbé, S. Leurs, I. Sannen, et al., Synthesis of thiazolo[4,3-a]isoindoles by intramolecular cycloaddition-elimination reactions of 4-methyl-5-(substituted)imino-Δ2-1,2,3,4-thiatriazolines, *Tetrahedron* **1993**, *49*, 4439-4446.

[147] K. Sonogashira, Y. Tohda, N. Hagihara, A convenient synthesis of acetylenes: catalytic substitutions of acetylenic hydrogen with bromoalkenes, iodoarenes and bromopyridines, *Tetrahedron Letters* **1975**, *16*, 4467-4470.

[148] T. Kovács, L. Ötvös, Simple synthesis of 5-vinyl- and5-ethynyl-2′-deoxyuridine-5′-triphosphates, *Tetrahedron Letters* **1988**, *29*, 4525-4528.

[149] L. P. Miranda, P. F. Alewood, Accelerated chemical synthesis of peptides and small proteins, *Proceedings of the National Academy of Sciences of the United States of America* **1999**, *96*, 1181-1186.

[150] L. M. Shannon, E. Kay, J. Y. Lew, Peroxidase Isozymes from Horseradish Roots: I. Isolation and physical properties, *Journal of Biological Chemistry* **1966**, *241*, 2166-2172.

[151] J. Everse, K. E. Everse, M. B. Grisham, *Peroxidases in chemistry and biology*, CRC Press, Boca Raton, Fla., **1991**.

[152] N. C. Veitch, Horseradish peroxidase: a modern view of a classic enzyme, *Phytochemistry* **2004**, *65*, 249-259.

[153] J. W. Tams, K. G. Welinder, Glycosylation and thermodynamic versus kinetic stability of horseradish peroxidase, *FEBS Letters* **1998**, *421*, 234-236.

[154] J. B. Adams, Regeneration and the kinetics of peroxidase inactivation, *Food Chemistry* **1997**, *60*, 201-206.

[155] B. S. Chang, K. H. Park, D. B. Lund, Thermal Inactivation Kinetics of Horseradish Peroxidase, *Journal of Food Science* **1988**, *53*, 920-923.

[156] H. Zollner, *Handbook of enzyme inhibitors*, 2nd, rev. and enlarged ed., VCH, Weinheim, Federal Republic of Germany ; New York, NY, USA, **1993**.

[157] S. Aldrich, Product Specification P1709, 08.02.2019, https://www.sigmaaldrich.com/Graphics/COfAInfo/SigmaSAPQM/SPEC/P1/P1709/P1709-2MG_____SIGMA____.pdf

[158] P. I. Ohlsson, K. G. Paul, Molar Absorptivity of Horseradish-Peroxidase, *Acta Chemica Scandinavica Series B - Organic Chemistry and Biochemistry* **1976**, *30*, 373-375.

[159] D. Strzelecka, S. Chmielinski, S. Bednarek, et al., Analysis of mononucleotides by tandem mass spectrometry: investigation of fragmentation pathways for phosphate- and ribose-modified nucleotide analogues, *Scientific Reports* **2017**, *7*, 8931.

[160] S. Obeid, M. Yulikov, G. Jeschke, et al., Enzymatic Synthesis of Multiple Spin-Labeled DNA, *Angewandte Chemie International Edition* **2008**, *47*, 6782-6785.

[161] T. Ohbayashi, M. Kuwahara, M. Hasegawa, et al., Expansion of repertoire of modified DNAs prepared by PCR using KOD Dash DNA polymerase, *Organic & Biomolecular Chemistry* **2005**, *3*, 2463-2468.

[162] A. R. Kore, Solid-phase synthesis of new ribo and deoxyribo BrdU probes for labeling and detection of nucleic acids, *Tetrahedron Letters* **2009**, *50*, 793-795.

[163] H. Davies, G. R. Bignell, C. Cox, et al., Mutations of the BRAF gene in human cancer, *Nature* **2002**, *417*, 949.

[164] W. M. Barnes, The fidelity of Taq polymerase catalyzing PCR is improved by an N-terminal deletion, *Gene* **1992**, *112*, 29-35.

[165] M. Drum, R. Kranaster, C. Ewald, et al., Variants of a Thermus aquaticus DNA Polymerase with Increased Selectivity for Applications in Allele- and Methylation-Specific Amplification, *PLoS One* **2014**, *9*, e96640.

[166] G. I. Berglund, G. H. Carlsson, A. T. Smith, et al., The catalytic pathway of horseradish peroxidase at high resolution, *Nature* **2002**, *417*, 463.

[167] H. M. Kropp, S. L. Durr, C. Peter, et al., Snapshots of a modified nucleotide moving through the confines of a DNA polymerase, *Proceedings of the National Academy of Sciences of the United States of America* **2018**, *115*, 9992-9997.

[168] D. Verga, M. Welter, A. L. Steck, et al., DNA polymerase-catalyzed incorporation of nucleotides modified with a G-quadruplex-derived DNAzyme, *Chemical Communications* **2015**, *51*, 7379-7381.

[169] A.-L. Steck, Oligonucleotide-modified Nuclotides, Ph.D. Thesis, University of Konstanz, **2013**.

[170] A. Claiborne, I. Fridovich, Chemical and enzymatic intermediates in the peroxidation of o-dianisidine by horseradish peroxidase. 1. Spectral properties of the products of dianisidine oxidation, *Biochemistry* **1979**, *18*, 2324-2329.

[171] B. Porstmann, T. Porstmann, E. Nugel, Comparison of chromogens for the determination of horseradish peroxidase as a marker in enzyme immunoassay, *Journal of Clinical Chemistry and Clinical Biochemistry* **1981**, *19*, 435-439.

[172] Z. A. Crannell, B. Rohrman, R. Richards-Kortum, Equipment-Free Incubation of Recombinase Polymerase Amplification Reactions Using Body Heat, *PLoS One* **2014**, *9*, e112146.

[173] K. B. M. Sauter, A. Marx, Evolving Thermostable Reverse Transcriptase Activity in a DNA Polymerase Scaffold, *Angewandte Chemie International Edition* **2006**, *45*, 7633-7635.

[174] J. S. Towner, P. E. Rollin, D. G. Bausch, et al., Rapid diagnosis of Ebola hemorrhagic fever by reverse transcription-PCR in an outbreak setting and assessment of patient viral load as a predictor of outcome, *Journal of Virology* **2004**, *78*, 4330-4341.

[175] F. Mwingira, B. Genton, A. N. Kabanywanyi, et al., Comparison of detection methods to estimate asexual Plasmodium falciparum parasite prevalence and gametocyte carriage in a community survey in Tanzania, *Malaria Journal* **2014**, *13*, 433.

[176] A. Bacconi, G. S. Richmond, M. A. Baroldi, et al., Improved sensitivity for molecular detection of bacterial and Candida infections in blood, *Journal of Clinical Microbiology* **2014**, *52*, 3164-3174.

[177] T. D. Simon, B. Van Yserloo, K. Nelson, et al., Use of quantitative 16S rRNA PCR to determine bacterial load does not augment conventional cerebrospinal fluid (CSF) cultures among children undergoing treatment for CSF shunt infection, *Diagnostic Microbiology and Infectious Disease* **2014**, *78*, 188-195.

[178] K. Zwirglmaier, W. Ludwig, K.-H. Schleifer, Recognition of individual genes in a single bacterial cell by fluorescence in situ hybridization – RING-FISH, *Molecular Microbiology* **2004**, *51*, 89-96.

[179] G. Quereux, G. Herbreteau, A. C. Knol, et al., Efficient treatment of a metastatic melanoma patient with a combination of BRAF and MEK inhibitors based on circulating tumor DNA analysis: a case report, *BMC Research Notes* **2017**, *10*, 320.

[180] P. Yarza, P. Yilmaz, E. Pruesse, et al., Uniting the classification of cultured and uncultured bacteria and archaea using 16S rRNA gene sequences, *Nature Reviews Microbiology* **2014**, *12*, 635-645.

[181] K. B. Ignatov, E. V. Barsova, A. F. Fradkov, et al., A strong strand displacement activity of thermostable DNA polymerase markedly improves the results of DNA amplification, *Biotechniques* **2014**, *57*, 81-87.

[182] The enzyme-linked immunosorbent assay (ELISA), *Bulletin of the World Health Organization* **1976**, *54*, 129-139.

[183] S. Zhang, A. Garcia-D'Angeli, J. P. Brennan, et al., Predicting detection limits of enzyme-linked immunosorbent assay (ELISA) and bioanalytical techniques in general, *Analyst* **2014**, *139*, 439-445.

[184] J. Balintova, M. Welter, A. Marx, Antibody-nucleotide conjugate as a substrate for DNA polymerases, *Chemical Science* **2018**, *9*, 7122-7125.

[185] J. Aschenbrenner, Engineering of DNA polymerases for direct detection of modified nucleotides in DNA and RNA, Ph.D. Thesis, University of Konstanz, **2017**.

[186] S. Sharma, V. Marchand, Y. Motorin, et al., Identification of sites of 2 '-O-methylation vulnerability in human ribosomal RNAs by systematic mapping, *Scientific Reports* **2017**, *7*.

[187] N. Liu, M. Parisien, Q. Dai, et al., Probing N6-methyladenosine RNA modification status at single nucleotide resolution in mRNA and long noncoding RNA, *RNA (New York, N.Y.)* **2013**, *19*, 1848-1856.

[188] Schott, Nexterion H Product FAQ, 08.02.2019, https://www.schott.com/nexterion/english/application/faq/hydrogel.html

[189] N. A. Tanner, Y. H. Zhang, T. C. Evans, Visual detection of isothermal nucleic acid amplification using pH-sensitive dyes, *Biotechniques* **2015**, *58*, 59-68.

[190] K. Nagamine, T. Hase, T. Notomi, Accelerated reaction by loop-mediated isothermal amplification using loop primers, *Molecular and Cellular Probes* **2002**, *16*, 223-229.

[191] S. Ikeda, K. Takabe, M. Inagaki, et al., Detection of gene point mutation in paraffin sections using in situ loop-mediated isothermal amplification, *Pathology International* **2007**, *57*, 594-599.

[192] M. Iwasaki, T. Yonekawa, K. Otsuka, et al., Validation of the Loop-Mediated Isothermal Amplification Method for Single Nucleotide Polymorphism Genotyping with Whole Blood, *Genome Letters* **2003**, *2*, 119-126.

[193] H.-t. Chen, J. Zhang, L.-n. Ma, et al., Rapid pre-clinical detection of classical swine fever by reverse transcription loop-mediated isothermal amplification, *Molecular and Cellular Probes* **2009**, *23*, 71-74.

[194] H. M. Pham, C. Nakajima, K. Ohashi, et al., Loop-Mediated Isothermal Amplification for Rapid Detection of Newcastle Disease Virus, *Journal of Clinical Microbiology* **2005**, *43*, 1646-1650.

[195] E. Suleman, M. S. Mtshali, E. Lane, Investigation of false positives associated with loop-mediated isothermal amplification assays for detection of Toxoplasma gondii in archived tissue samples of captive felids, *Journal of Veterinary Diagnostic Investigation* **2016**, *28*, 536-542.

[196] K. Nagai, N. Horita, M. Yamamoto, et al., Diagnostic test accuracy of loop-mediated isothermal amplification assay for Mycobacterium tuberculosis: systematic review and meta-analysis, *Scientific Reports* **2016**, *6*, 39090.

[197] K. Senarath, R. B. Usgodaarachchi, V. Navaratne, et al., *Non Specific Amplification with the LAMP Technique in the Diagnosis of Tuberculosis in Sri Lankan Settings, Vol. 02*, **2014**.

[198] J. A. Morales-Serna, O. Boutureira, A. Serra, et al., Synthesis of Hyperbranched β-Galceramide-Containing Dendritic Polymers that Bind HIV-1 rgp120, *European Journal of Organic Chemistry* **2010**, *2010*, 2657-2660.

[199] A. J. Gross, I. W. Sizer, The Oxidation of Tyramine, Tyrosine, and Related Compounds by Peroxidase, *Journal of Biological Chemistry* **1959**, *234*, 1611-1614.

[200] B. A. Clevidence, M. W. Marshall, J. J. Canary, Biotin Levels in Plasma and Urine of Healthy-Adults Consuming Physiological Doses of Biotin, *Nutrition Research* **1988**, *8*, 1109-1118.

[201] H. Yan, S. H. Park, G. Finkelstein, et al., DNA-templated self-assembly of protein arrays and highly conductive nanowires, *Science* **2003**, *301*, 1882-1884.

[202] G. Bernardinelli, B. Hogberg, Entirely enzymatic nanofabrication of DNA-protein conjugates, *Nucleic Acids Research* **2017**, *45*, e160.

[203] C. M. Niemeyer, Semi-synthetic DNA-protein conjugates: novel tools in analytics and nanobiotechnology, *Biochemical Society Transactions* **2004**, *32*, 51-53.

[204] A. Shaw, V. Lundin, E. Petrova, et al., Spatial control of membrane receptor function using ligand nanocalipers, *Nature Methods* **2014**, *11*, 841-846.

[205] G. J. Tsongalis, Branched DNA technology in molecular diagnostics, *American Journal of Clinical Pathology* **2006**, *126*, 448-453.

[206] A. Finke, H. Bußkamp, M. Manea, et al., Designer Extracellular Matrix Based on DNA–Peptide Networks Generated by Polymerase Chain Reaction, *Angewandte Chemie International Edition* **2016**, *55*, 10136-10140.

[207] A. Samanta, I. L. Medintz, Nanoparticles and DNA - a powerful and growing functional combination in bionanotechnology, *Nanoscale* **2016**, *8*, 9037-9095.

[208] C. B. Rosen, A. L. B. Kodal, J. S. Nielsen, et al., Template-directed covalent conjugation of DNA to native antibodies, transferrin and other metal-binding proteins, *Nature Chemistry* **2014**, *6*, 804.

[209] S. H. Weisbrod, A. Marx, Novel strategies for the site-specific covalent labelling of nucleic acids, *Chemical Communications* **2008**, 5675-5685.

[210] J. B. Trads, T. Torring, K. V. Gothelf, Site-Selective Conjugation of Native Proteins with DNA, *Accounts of Chemical Research* **2017**, *50*, 1367-1374.

[211] G. R. Fulmer, A. J. M. Miller, N. H. Sherden, et al., NMR Chemical Shifts of Trace Impurities: Common Laboratory Solvents, Organics, and Gases in Deuterated Solvents Relevant to the Organometallic Chemist, *Organometallics* **2010**, *29*, 2176-2179.

[212] N. R. Voss, M. Gerstein, 3V: cavity, channel and cleft volume calculator and extractor, *Nucleic Acids Research* **2010**, *38*, W555-562.

8 - Appendix

8 - Appendix

Compound 3

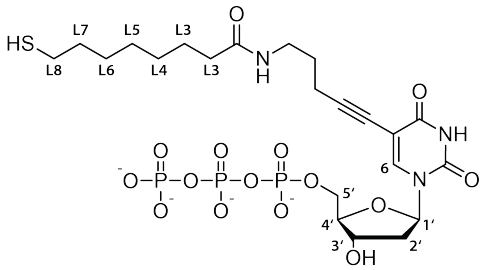

^{1}H NMR: (400 MHz, MeOD)

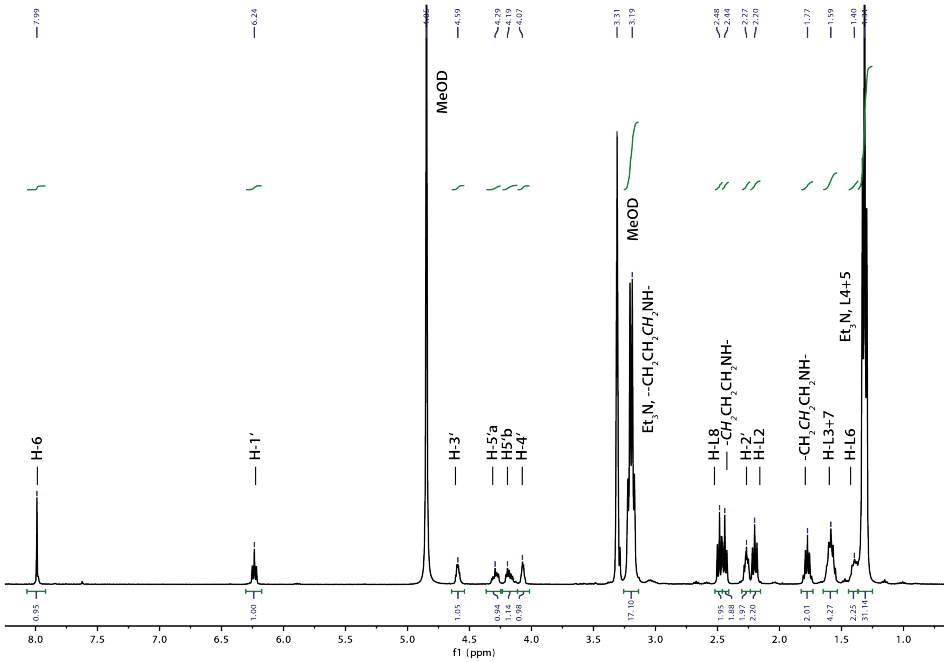

^{31}P NMR: (162 MHz, MeOD)

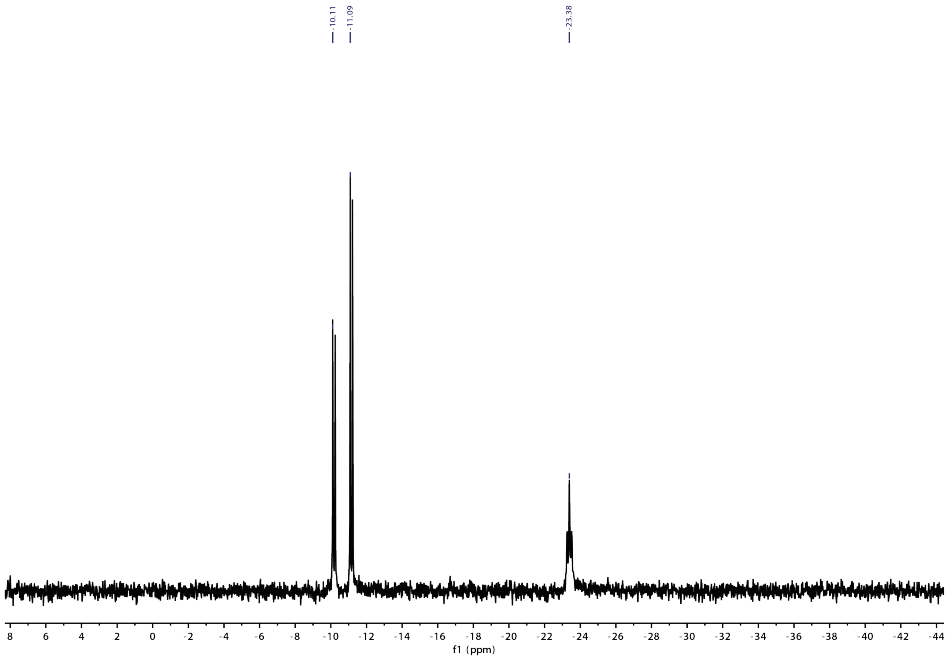

Compound 4

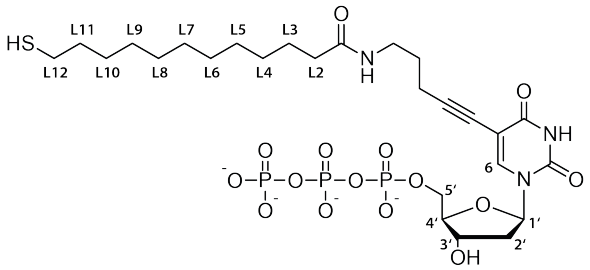

^{1}H NMR: (400 MHz, MeOD)

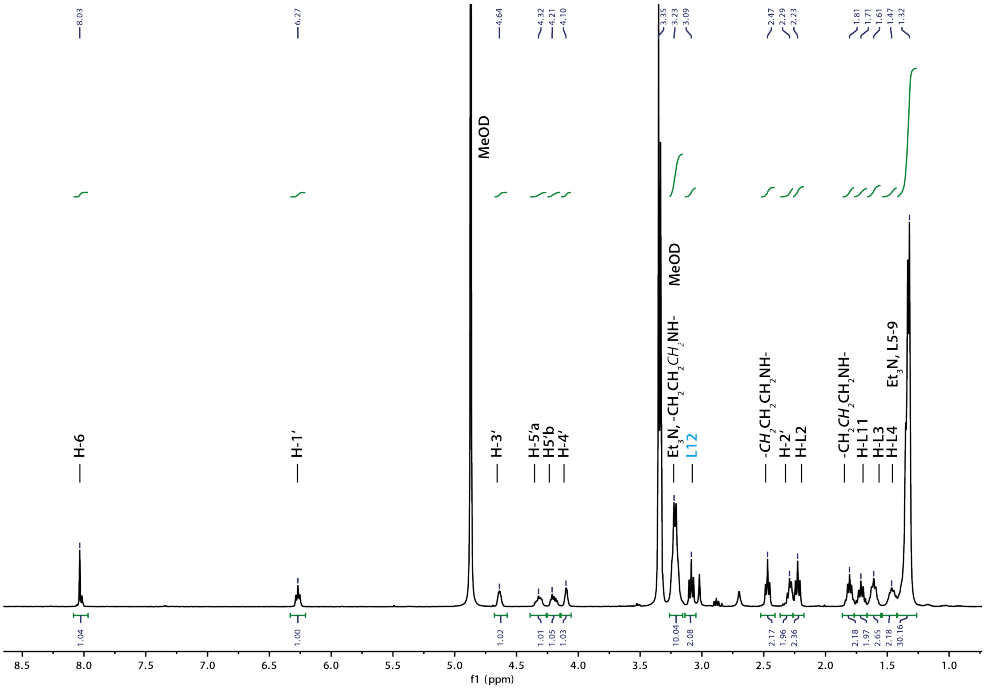

^{31}P NMR: (162 MHz, MeOD)

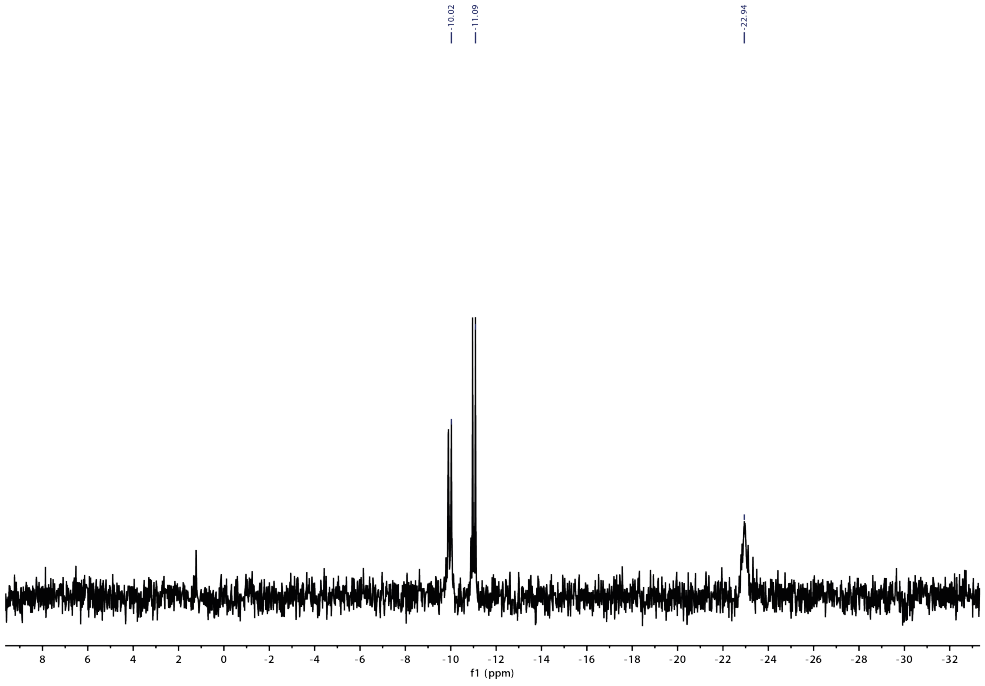

8 - Appendix

Compound 5

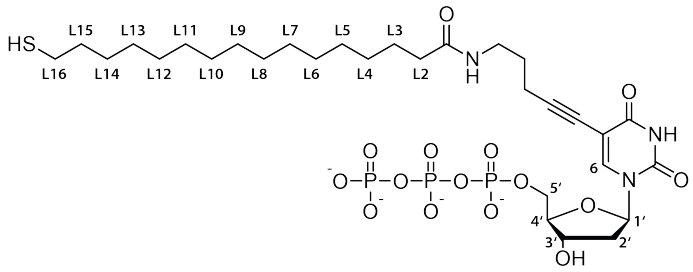

^{1}H NMR: (400 MHz, MeOD)

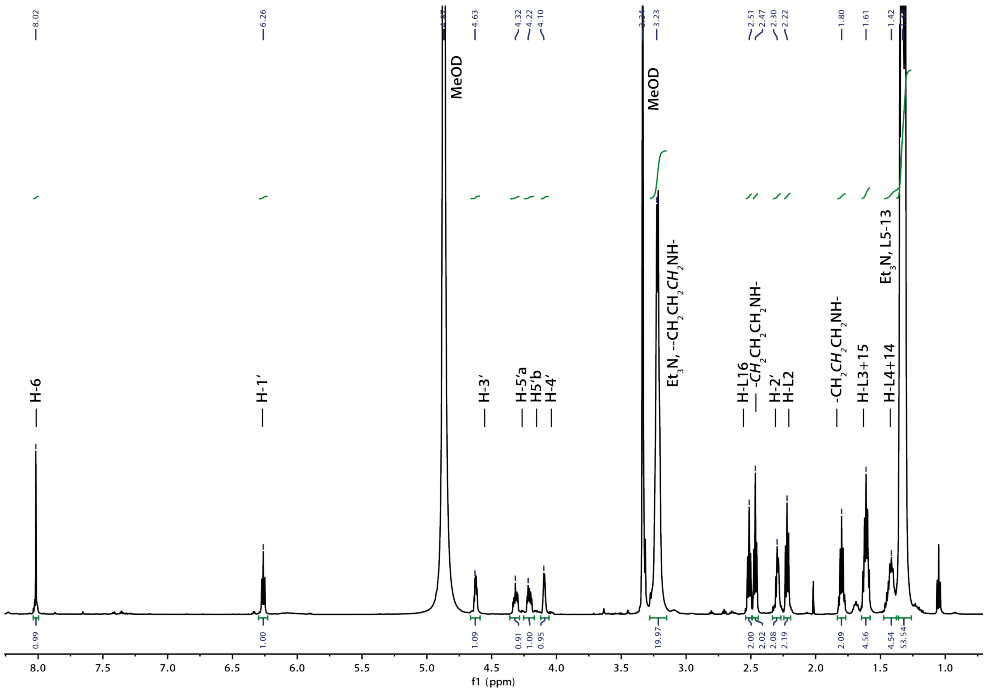

^{31}P NMR: (162 MHz, MeOD)

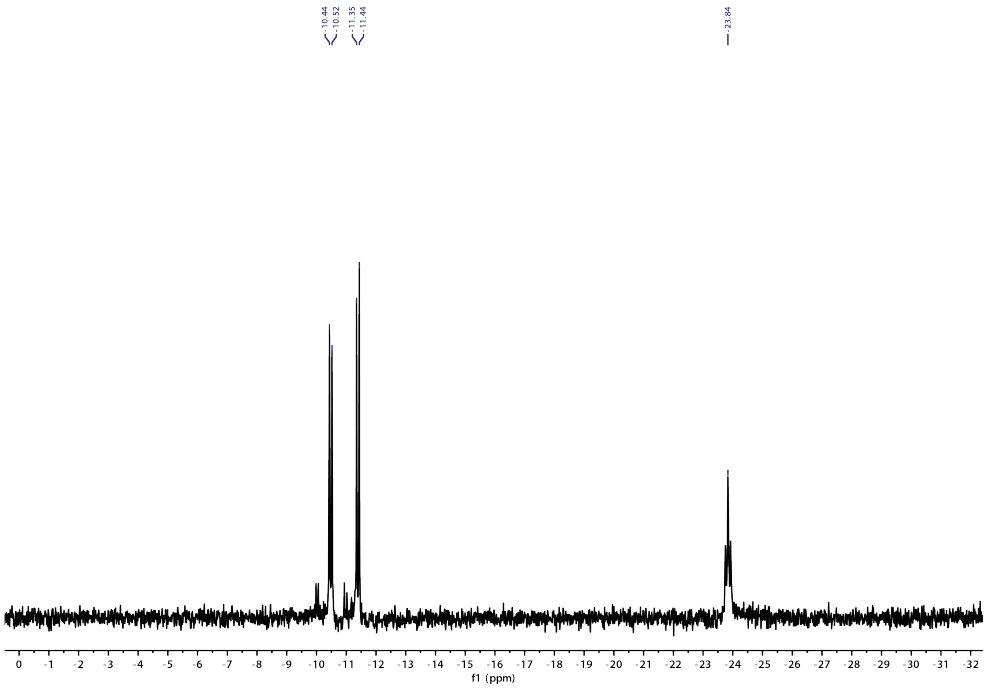

Compound 7

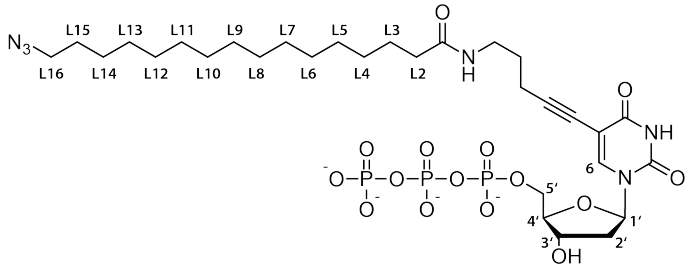

^{1}H NMR: (400 MHz, MeOD)

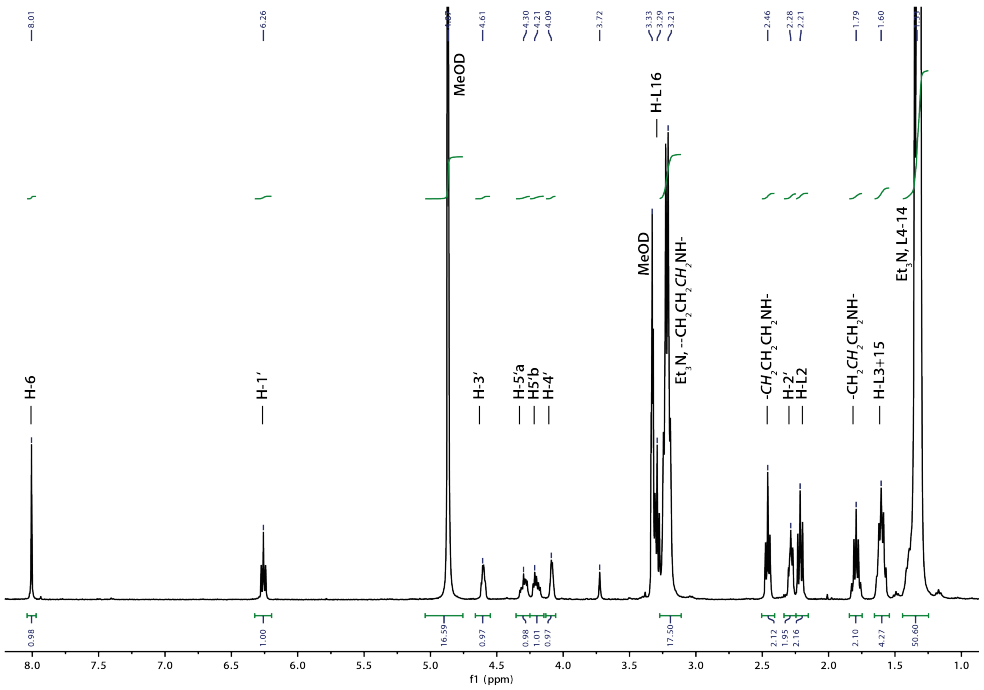

^{31}P NMR: (162 MHz, MeOD)

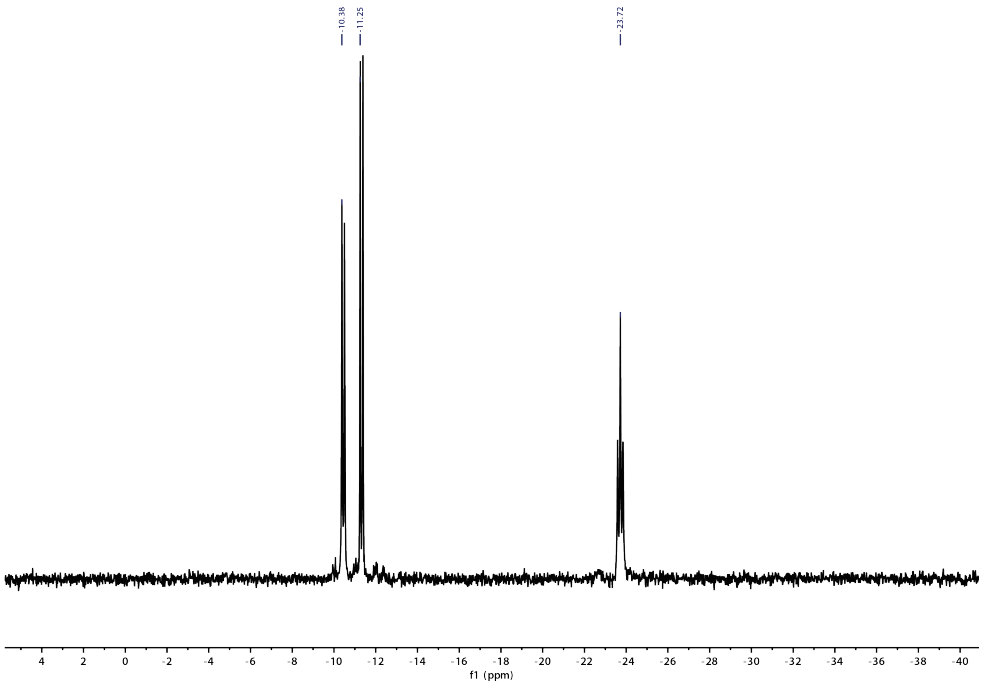

8 - Appendix

ESI-MS measurements of conjugates